1990

Mechanistic studies on reactivities of organometallic macrocyclic complexes of chromium and cobalt

Shu Shi
Iowa State University

INFORMATION TO USERS

The most advanced technology has been used to photograph and reproduce this manuscript from the microfilm master. UMI films the text directly from the original or copy submitted. Thus, some thesis and dissertation copies are in typewriter face, while others may be from any type of computer printer.

The quality of this reproduction is dependent upon the quality of the copy submitted. Broken or indistinct print, colored or poor quality illustrations and photographs, print bleedthrough, substandard margins, and improper alignment can adversely affect reproduction.

In the unlikely event that the author did not send UMI a complete manuscript and there are missing pages, these will be noted. Also, if unauthorized copyright material had to be removed, a note will indicate the deletion.

Oversize materials (e.g., maps, drawings, charts) are reproduced by sectioning the original, beginning at the upper left-hand corner and continuing from left to right in equal sections with small overlaps. Each original is also photographed in one exposure and is included in reduced form at the back of the book.

Photographs included in the original manuscript have been reproduced xerographically in this copy. Higher quality 6" x 9" black and white photographic prints are available for any photographs or illustrations appearing in this copy for an additional charge. Contact UMI directly to order.

U·M·I

University Microfilms International
A Bell & Howell Information Company
300 North Zeeb Road, Ann Arbor, MI 48106-1346 USA
313/761-4700 800/521-0600

Order Number 9110565

Mechanistic studies on reactivities of organometallic macrocyclic complexes of chromium and cobalt

Shi, Shu, Ph.D.

Iowa State University, 1990

U·M·I
300 N. Zeeb Rd.
Ann Arbor, MI 48106

Mechanistic studies on reactivities of organometallic macrocyclic complexes of chromium and cobalt

by

Shu Shi

A Dissertation Submitted to the
Graduate Faculty in Partial Fulfillment of the
Requirements for the Degree of
DOCTOR OF PHILOSOPHY

Department: Chemistry
Major: Inorganic Chemistry

Approved:

Signature was redacted for privacy.

In Charge of Major Work

Signature was redacted for privacy.

For the Major Department

Signature was redacted for privacy.

For the Graduate College

Iowa State University
Ames, Iowa

1990

TABLE OF CONTENTS

GENERAL INTRODUCTION

Part I: Organochromium(III) Macrocycles. Controlled Homolytic vs. Heterolytic Scission of the Cr(III)-C Bond.

Reason to Study: Little is known about the factors that alternate pathways of the cleavage of a metal-carbon bond (homolysis vs. heterolysis) in dark reactions. A full understanding of these factors could lead to new means to control the release of free radicals from their precursors in many chemical processes.

Conclusion: Factors that make a M-C bond more polar tend to inhibit homolysis and enhance heterolysis. Alternation of the pathways can be achieved by modification of the R group, equatorial ligand L, and trans group A (of $RML(A)^{n+}$). According to this understanding, a molecular "switch" has been successfully built into an organochromium complex for the first time to control the pathway of the scission of a Cr-C bond. (A water molecule was put at the position trans to a Cr-C bond as in $RCrL(H_2O)^{2+}$ complexes, and its deprotonation (to $RCrL(OH)^{+}$) and reprotonation was used to "switch" off and on the homolysis and heterolysis of the Cr-C bond, i.e., $RCrL(H_2O)^{2+} + H_2O \rightarrow R\cdot + CrL(H_2O)_2^{2+}$; $RCrL(OH)^{+} + H_2O \rightarrow RH + CrL(OH)_2$). Replacement of the macrocyclic ligand L by H_2O at equatorial positions (i.e., $RCr(H_2O)_5^{2+}$ vs. $RCrL(H_2O)^{2+}$) decreases Cr-C bond polarity and thus largely enhances the homolysis of the Cr-C bond (both in terms of rate constant, k_h, and

in terms of Hammett coefficient, ρ). The parallel relationship between bond polarity and the change of decomposition pathway can be understood in terms of orbital energy difference $\Delta E = E[e_g^*(Cr)] - E[\sigma(R)]$ since ΔE controls the Cr-C bond polarity and the susceptibility of the internal electron transfer (from a formal carbanion to a formal chromium(III) as shown in eq (1)) which accompanies the homolysis.

The reaction scheme is shown in eqs (1) and (2),

$$RCr^{III}L(H_2O)^{2+} + H_2O \xrightarrow{k_1} \begin{cases} \xrightarrow{HTMPO} R\text{-HTMPO} \\ R\cdot + Cr^{II}L(H_2O)_2^{2+} \\ \xrightarrow[(NH_3)_5CoBr^{2+}]{} RBr + Co(aq.)^{2+} + 5NH_3 \end{cases} \quad (1)$$

$$RCr^{III}L(OH)^{+} + H_2O \xrightarrow{k_2} RH + Cr^{III}L(OH)_2 \quad (2)$$

(where R = CH_3, C_2H_5, 1-C_3H_7, 1-C_4H_9, 2-C_3H_7, 2-C_4H_9, 4-$CH_3C_6H_4CH_2$, $C_6H_5CH_2$, 4-$BrC_6H_4CH_2$).

$RCrL(H_2O)^{2+}$ was prepared by radical capture reaction,

$$RX + CrL(H_2O)_2^{2+} \rightarrow R\cdot + XCrL(H_2O)^{2+} \quad (3)$$

$$R\cdot + CrL(H_2O)_2^{2+} \rightarrow RCrL(H_2O)^{2+} + H_2O, \quad (4)$$

(L=[15]aneN$_4$ or $(H_2O)_4$) and purified by ion-exchange. Due to the existence of the back reaction of eq (1) radical scavengers (HTMPO$\cdot$ or $BrCo(NH_3)_5^{2+}$) were used to draw the homolysis to completion. The k_1 step is rate limiting. Reactions were monitored by ESR and spectrophotometry.

Products were detected by GC and UV-vis spectra. The heterolysis rate is independent of $[OH^-]$ and $[H_3O^+]$, and has no D/H isotope effect, confirming that k_2 step is unimolecular. So both $\Delta H^{\ddagger}_1$ and $\Delta H^{\ddagger}_2$ represent fairly good estimations of the Cr(III)-C bond enthalpies toward homolysis and heterolysis respectively. k_i (i=1,2) of various $RCrL(H_2O)^{2+}$ and $RCrL(OH)^+$ were measured at 25 ^0C, and $\Delta H^{\ddagger}_i$, $\Delta S^{\ddagger}_i$ were obtained by temperature dependence of kinetic measurements leading to the above conclusions.

Part II: Mechanistic Study of the Organochromium Macrocyclic Complexes/I_2 Reactions.

Reason to study: Little is known about chain reactions in which an oxidation-induced M-C bond homolysis is involved to sustain the chain. Fundamental knowledge of such reactions is badly needed to understand reactivities of M-C bonds fully.

Conclusion: The first example that an oxidation induced M-C bond homolysis serves to sustain a chain reaction was demonstrated by this study. The overall rate law is,

$$-d[RCrL(H_2O)^{2+}]/dt = k_{ch}[I_2]^{1/2}[RCrL(H_2O)^{2+}]^{3/2} + k_{el}[I_2][RCrL(H_2O)^{2+}]$$

Where the first term represents the chain reaction and the second represents simple electrophilic substitution. Different $RCrL(H_2O)^{2+}$ complexes react differently towards the same external reagent, I_2. When R = 2^o-alkyl or aralkyl, chain reaction dominates; when R = 1^o-alkyl, electrophilic substitution dominates. $RCrL(H_2O)^{3+}$, $I_2^{-\cdot}$, and $R^{\cdot}$ are the

chain carriers. It was found that in the electrophilic substitution reactions, only I_2, not I_3^-, is reactive regardless of I^- concentration and the fact that I_2 and I_3^- are inter-convertible ($I_2 + I^- == I_3^-$) and have similar redox potentials.

The chain reaction proceeds as follows,

Initiation	$RCrL(H_2O)^{2+} + I_2 \rightarrow RCrL(H_2O)^{3+} + I_2^{-\cdot}$	(5)
Propagation	$RCrL(H_2O)^{3+} \rightarrow R\cdot + CrL(H_2O)^{2+}$	(6)
	$R\cdot + I_2 + I^- \rightarrow RI + I_2^{-\cdot}$	(7)
	$I_2^{-\cdot} + RCrL(H_2O)^{2+} \rightarrow RCrL(H_2O)^{3+} + 2I^-$	(8)
termination	$2I_2^{-\cdot} \rightarrow I_3^- + I^-$	(9)

The involvement of $R\cdot$ in the chain propagation step is confirmed by O_2 and Cu^{2+} inhibition effect.

$$R. + O_2 \rightarrow RO_2\cdot \quad (10)$$

$$2RO_2\cdot \rightarrow ROH + RHO + O_2 \quad (11)$$

$$Cu^{2+} + R\cdot + H_2O \rightarrow Cu^+ + ROH + H^+ \quad (12)$$

Small amounts of O_2 or Cu^{2+} change the fractional-order kinetic profile (which appears when the chain mechanism dominates) back to a normal pseudo-first order profile and the fast chain reaction rate back to the slow electrophilic substitution rate. Involvement of $I_2^{-\cdot}$ in a chain propagation step is confirmed by Fe^{2+} inhibition effect,

$$I_2^{-\cdot} + Fe^{2+} \rightarrow 2I^- + Fe^{3+} \quad (13)$$

The chain reaction scheme is also supported by kinetic profile analysis, product analysis and stoichiometric determinations. Various $RCrL(H_2O)^{2+}$ (R = CH_3, C_2H_5, 1-C_3H_7, 1-C_4H_9, 2-C_3H_7, 2-C_4H_9, 4-$CH_3C_6H_4CH_2$, $C_6H_5CH_2$, 4-$BrC_6H_4CH_2$) were studied. k_{ch} and k_{el} were measured. The crystal structure of $BrC_6H_4CH_2CrL(H_2O)^{2+}$ was determined by x-ray crystallography.

Part III: Reactivities of Organochromium Complexes toward Inorganic Radicals. A Pulse Radiolysis Study.

Reason to Study: The reaction between $RCrL(H_2O)^{2+}$ and $X_2^{-\cdot}$ is to be explored, and independent evidence of reaction (8) is to be sought.

Conclusion: Quick generation of reactive radical anions X_2^- was realized by pulse radiolysis and follow-up radical conversions.

$$e(aq)^- + N_2O + H_2O \rightarrow HO\cdot + HO^- + N_2 \qquad (14)$$

$$HO\cdot + 2X^- \rightarrow HO^- + X_2^{-\cdot} \qquad (15)$$

The kinetics of the reaction

$$X_2^{-\cdot} + RCrL(H_2O)^{2+} \rightarrow 2X^- + RCrL(H_2O)^{3+} \qquad (16)$$

was studied spectrophotometrically with R = 1-C_3H_7, 2-C_3H_7, 4-$BrC_6H_4CH_2$, 4-$CH_3C_6H_4CH_2$, and X = I, Br, SCN. Reaction (16) proceeds very fast ($t_{1/2}$ ~ 10 μs) consistent with the role it plays in the chain reaction (eqs (5) to (9)). Kinetic analysis suggests the formation of a loosely bound

precursor, $\{X_2^{-\cdot}, RCrL(H_2O)^{2+}\}$, prior to the electron transfer step. The reactivity trend is also discussed.

Part IV: Electron Transfer Reactions of Organochromium (IV/III) Macrocyclic Complexes and Oxidation Induced Homolysis.

Reason to Study: $RCr^{IV}(H_2O)_5^{3+}$ has been proposed as a transient before, but not confirmed. Little is known about the organochromium (IV/III) redox potential and self-exchange rate presumably due to the short life-time of RCr(IV) species. It is important to find out the redox mechanism of these organochromium complexes and their redox potentials and self-exchange rates to establish guidelines for further reactivity investigations and applications.

Conclusion: $RCr^{III}L(H_2O)^{2+}$ can be relatively easily oxidized to $RCr^{IV}L(H_2O)^{3+}$ which further decomposes to R· and $Cr^{III}L(H_2O)^{3+}$. The oxidation occurs via an outer-sphere electron transfer pathway. The outer-sphere electron transfer mechanism is also supported by the observed linear relationship predicted by Marcus' equation (with oxidants, ox = $IrCl_6^{2-}$, Fe^{3+}, and $ABTS^{-\cdot}$) and the reactivity trend of the oxidation of $RCrL(H_2O)^{2+}$ by $IrCl_6^{2-}$ (R = CH_3, C_2H_5, 1-C_3H_7, 1-C_4H_9, 2-C_3H_7, 2-C_4H_9, 4-$CH_3C_6H_4CH_2$, $C_6H_5CH_2$, 4-$BrC_6H_4CH_2$). k_1 values of all these $RCr(H_2O)^{2+}$ were measured.

The reaction scheme is shown in eqs (17) to (19),

$$RCrL(H_2O)^{2+} + ox \rightarrow RCrL(H_2O)^{3+} + red \qquad k_1 \qquad (17)$$

$$RCrL(H_2O)^{3+} \longrightarrow R^{\cdot} + CrL(H_2O)^{3+} \qquad k_2 \qquad (18)$$

$$R^{\cdot} + ox \longrightarrow P \qquad \text{fast} \qquad (19)$$

The nature of the product, P, depends on ox (e.g., P = RCl when ox = $IrCl_6^{2-}$; P = R-ABTS$^-$ when ox = ABTS$^{\cdot}$). Results of product analysis, stoichiometric determination, and kinetic study are consistent with the notion that homolysis is the major decomposition pathway of $RCrL(H_2O)^{3+}$. The reactions were followed by stopped-flow and conventional kinetic methods. The products were analyzed by GC and UV-vis spectra.

For the first time we developed a simple kinetic method to estimate a redox potential of an unstable couple (like $RCr^{IV}L(H_2O)^{3+}$ / $RCr^{III}L(H_2O)^{2+}$) along with its self-exchange rate. This kinetic method complements the existing electrochemical techniques for potential measurement. It applies to redox couples containing an unstable species (generated by an electron transfer and destroyed by a follow up chemical reaction). Contrary to cases of traditional electrochemical measurements, the faster is the follow-up reaction, the more accurate is the estimation of the potential by the kinetic method. The self-exchange rate, k_{11}, can be calculated by Marcus' equation using the estimated E^o value. Our estimated values (e.g., E^o = 0.76 + 0.13 V and k_{11} = 4.2 $M^{-1}s^{-1}$ for $4\text{-}BrC_6H_4CH_2CrL(H_2O)^{3+}/4\text{-}BrC_6H_4CH_2CrL(H_2O)^{2+}$ couple) are certainly within reasonable range.

The kinetic retardation effect of [red] = [$ABTS^{2-}$] confirms that a $RCrL(H_2O)^{3+}$ has a finite life time. The estimated life time is c.a. 1 ms.

Part V: Reduction Induced Cleavage of Cobalt-Carbon Bond in Organocobalt Macrocyclic Complexes.

Reason to Study: The fate of reduced organocobalts is a center of many debates because of its biological importance and "contradictory"

observations made in different laboratories, probably due to the lack of the knowledge about the shortly-lived reaction intermediates.

Conclusion: We demonstrated that both 1e and 2e reductions of $RCo^{III}L$ can be achieved chemically and electrochemically to yield $RCo^{II}L^{1-}$ and $RCo^{I}L^{2-}$. For the first time we found that β-elimination is the major decomposition pathway of 1°- and 2°-alkylcobalt(II) complexes, $RCo^{II}L^{1-}$. Hydrolysis of $RCo^{II}L^{1-}$, affording RH and $Co^{II}L$, becomes important only in the presence of water. The R(-H) and RH presented in the product mixture were actually produced directly from $RCo^{II}L^{1-}$ by separate pathways, rather than from disproportionation of R· (generated by homolysis, $RCo^{II}L^{1-} \rightarrow R\cdot + Co^{I}L^{1-}$) as suspected in literature. The explanation of the generation of oxidized product R(-H) from reduced organochromium, $RCo(II)L^{1-}$, involves participation of equatorial ligand L to yield LH. We also discovered that when β-H is absent in R, the R group migration from cobalt to the equatorial ligand L becomes an important reaction pathway. RH is the major decomposition product of $RCo^{I}L^{2-}$. The general reaction scheme is shown below,

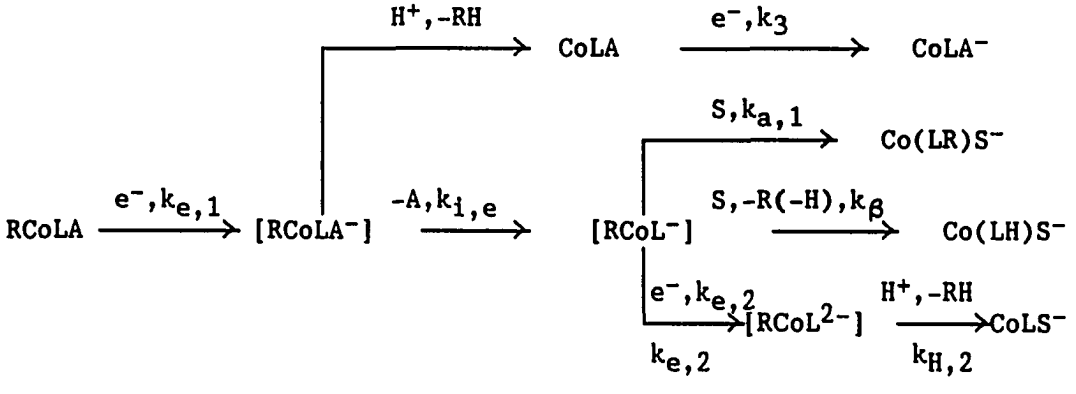

where R = CH_3, C_2H_5, 1-C_3H_7, 2-C_3H_7, 4-$CH_3C_6H_4CH_2$, $C_6H_5CH_2$, 4-$BrC_6H_4CH_2$; L = $(dmgBF_2)_2$; and with trans group A, A = H_2O, OH^-, and py. The

starting complexes, $RCo^{III}L$, were prepared by nucleophilic substitution between $Co^{I}L^{-}$ and RX. Rate constants, $k_{e,1}$ and $k_{e,2}$, of these complexes were measured by using $Ni^{I}(tmc)^{+}$ as the reductant. The reactivity trend agrees with the above scheme.

The reductions were studied both electrochemically and chemically. The reduction intermediate and products were detected by ESR, fast mixing and fast scan techniques, GC, UV-vis, NMR, and electrochemical methods. The proposed reaction scheme was based on results from intermediate trapping, change of product distribution with conditions, as well as kinetic profiles, rates and reactivity trend. $RCo^{II}L^{1-}$ with $(t)^{6}(d_{x}2_{-y}2)^{1}$ configuration provides the first example of $g > g$ in d^{7} cobalt(II) complexes, implying a flattened pseudo-Oh ligand field. This configuration explains the fact that homolysis does not occur immediately at the $RCo^{II}L^{1-}$ stage (the odd electron is not in the Co-C antibonding orbital) and instead the internal electron transfer occurs yielding $RCo^{II}L'^{1-}$ which assists the follow-up β-elimination.

Part VI: Molecular Structure of a Cobalt(I) Complex Lacking a Carbonyl Ligand. An Unique Example of C-N Bond Shortening upon Reduction.
Reason to Study: Synthesis and structural determination of cobalt(I) macrocyclic complexes have been challenges to chemists who want to study reactions catalyzed by vitamin B_{12} coenzymes. Efforts along this direction were often frustrated by the extreme instability of the cobalt(I) macrocycles. Only a few attempts were fruitful by letting electron withdrawing CO ligand coordinate to cobalt. But carbonyl cobalt macrocycles are not relavent to vitamin B_{12} systems.

Conclusion: Successful synthesis and crystallization of a cobalt(I) macrocyclic complex was accomplished by an electrolysis induced hydrolysis of an alkylcobalt(III) complex. The molecular structure of the novel cobalt(I) macrocyclic complex $Co^{I}(dmgBF_2)_2py^-$ is characterized by x-ray diffraction. The diamagnetism of the complex as reflected by ESR silence and well defined ^{1}H-NMR spectrum strongly supports the assignment of the low spin d^8 electron configuration $(t)^6(d_z2)^2$ to the complex.

A rather unexpected shortening of the Co-N (of the equatorial ligand) bonds upon reduction (as compared to those of $Co^{II}(dmgBF_2)_2$) was discovered with this complex. This discovery challenges the commonly accepted thinking: an atomic (or ionic) radius increases as the atom (or ion) is reduced, so does the bond distance related to the atom (or ion). We explain this unusual shortening upon reduction in light of orbital interaction (between $Co(d_z2)$ and $(dmgBF_2)_2(\pi^*)$), which changes from symmetry forbidden to symmetry allowed. The change of the orbital interaction is also evidenced by the changes of the bond distances within the equatorial ligand.

PART I. ORGANOCHROMIUM(III) MACROCYCLIC COMPLEXES. FACTORS CONTROLLING HOMOLYTIC VS. HETEROLYTIC CLEAVAGE OF THE CHROMIUM-CARBON BOND

INTRODUCTION

Conventional ligand substitution reactions of inorganic and organometallic complexes are two-electron processes. They are relatively well understood in terms of the electronic and structural factors that control the rate.[1-3] In contrast, much less is known about the factors controlling the rates of unimolecular bond homolysis reactions, $L_5M^{n}-R \rightarrow L_5M^{n-1} + R\cdot$ (R = alkyl, aralkyl). The data available for complexes such as $(H_2O)_5CrR^{2+}$ [4,5] and macrocyclic organocobalt complexes[6] suggest that both steric and electronic factors must be considered.

We consider here a family of organochromium(III) macrocycles, $RCrL(H_2O)^{2+}$ (L = [15]aneN$_4$ = 1,4,8,12-tetraazacyclopentadecane) in aqueous solution. With a trans ligand A (A = H_2O and OH^-), we consider the possibilities of homolysis (eq I-1) and heterolysis (eq I-2). Neither reaction type has been examined previously for these complexes.

$$RCr^{III}L(A)^{n+} \longrightarrow Cr^{II}L(A)^{n+} + R\cdot \qquad (I\text{-}1)$$

$$RCr^{III}L(A)^{n+} + H_2O \longrightarrow HOCr^{III}L(A)^{n+} + RH \qquad (I\text{-}2)$$

The presence of the macrocyclic ligand offers certain advantages in studying the reactivity of the metal-carbon bond. Most significantly, the macrocycle permits variation of the pH over a wide range, in contrast to the complexes $(H_2O)_5CrR^{2+}$ that rapidly decompose above pH ~ 4. This allows examination of the species with A = OH^-. In this article we present data showing that variation of A changes the mechanism of the Cr-

C bond cleavage from homolytic to heterolytic. We explain this finding by the stabilizing effect of the strongly electron-donating OH^- group on the 3+ oxidation state of chromium. The same phenomenon helps in the understanding of the reactivity order when the R group is changed.

EXPERIMENTAL SECTION

Materials. The complexes $RCrL(H_2O)^{2+}$ were prepared by the known reaction of RBr or RI with $(H_2O)_2CrL^{2+}$, and separated by ion exchange chromatography on Sephadex C25.[7] The electronic spectra matched the reported values.[7] Radical scavengers were $[Co(NH_3)_5Br](ClO_4)_2$ [8] and HTMPO[9] (Aldrich). The ESR and UV-visible spectrum of HTMPO matched the literature values.[10]

Techniques. ESR spectra were recorded on aqueous solutions with an IBM-Bruker ER-200 spectrometer. Since the activation energies of metal-alkyl homolysis are in general rather large,[4-6] homolysis can be promoted at elevated temperature. This approach was used to conduct the ESR study. Samples of the complex $RCrL(A)^{n+}$ in the presence of a three-fold excess of HTMPO were immersed in a water bath at 40 °C to initiate decomposition. At a fixed time, decomposition was quenched by immersing the sample in an ice-water bath. The sample was then warmed back to 15 °C and the ESR spectrum recorded. With bath temperature and timing controlled, the method was reproducible.

Organic products were identified with a Hewlett-Packard Model 5790 gas chromatograph, with a 6′ x 1/8" column packed with OV-101 or VZ-10. The gas chromatograph was calibrated with standard organic halides and hydrocarbons. Electronic spectra were recorded with a Perkin-Elmer Lambda Array 3840 diode array spectrophotometer.

Kinetic Measurements. The homolytic decomposition of the organochromium macrocycles $RCrL(H_2O)^{2+}$ was monitored spectrophotometrically at their absorption maxima: λ 287 and 400 nm for R = i-Pr, 359 nm for p-$CH_3C_6H_4CH_2$, 353 nm for $C_6H_5CH_2$, and 360 nm for p-$BrC_6H_4CH_2$. These measurements were carried out in an argon atmosphere on solutions containing 0.010 M $HClO_4$ and 0.20 M $NaClO_4$. The heterolytic decomposition in basic solutions was monitored at 274 nm (R = i-Pr) and 260 nm (n-Pr) at $[OH^-]$ = 7.2 - 160 mM, μ = 0.20 M. Some experiments, including the temperature dependence, were done at $[OH^-] = \mu$ = 0.82 M. In every case temperature was precisely controlled by immersing the quartz cuvette in a water bath positioned in the light beam of the spectrophotometer; thermostated water was circulated through the jacket of the water bath. Organochromium macrocycles were used as limiting reagents in both homolysis and heterolysis studies. The kinetic data were obtained by means of a Cary Model 14 spectrophotometer that had been converted to a computer-controlled instrument by On Line Instrument Systems. The OLIS data station also provided the least squares program for the analysis of the absorbance-time data according to the first-order equation $A_t = A_\infty + (A_0 - A_\infty)e^{-kt}$.

RESULTS

Bond Homolysis. Unimolecular homolysis of the chromium-carbon bond was observed for secondary alkyl and aralkyl chromium complexes $RCrL(H_2O)^{2+}$ in slightly acidic ($[H^+] = 1.0 \times 10^{-2}$ M) solutions in the presence of free radical scavengers. For example, some experiments were conducted in the presence of the persistent free radical HTMPO,[9] which is known[11] to capture in situ generated free radicals, eq I-3. We found that HTMPO also reacts rapidly with $(H_2O)_2CrL^{2+}$, eq I-4. The ESR technique was employed in this study to estimate the rate of homolysis. The intensity of the ESR signal of HTMPO decreased as the homolysis of the i-propylchromium complex proceeded, **Figure I-1.**

$$R\cdot + HTMPO \longrightarrow R\text{-}HTMPO \qquad (I\text{-}3)$$

$$(H_2O)_2CrL^{2+} + HTMPO \longrightarrow (H_2O)_2CrL^{3+} + HTMPO^- \qquad (I\text{-}4)$$

Another scavenger is $(NH_3)_5CoBr^{2+}$, which reacts with free radicals[12] (eq I-5) and with the chromium(II) macrocycle[13] (eq I-6). Because of their dual functions both HTMPO and $(NH_3)_5CoBr^{2+}$ are effective scavengers in this system.

$$(NH_3)_5CoBr^{2+} + R\cdot \xrightarrow{H_3O^+} RBr + Co_{aq}^{2+} + 5NH_4^+ \qquad (I\text{-}5)$$

$$(NH_3)_5CoBr^{2+} + (H_2O)_2CrL^{2+} \xrightarrow{H_3O^+} BrCrL(H_2O)^{2+} + Co_{aq}^{2+} + 5NH_4^+ \qquad (I\text{-}6)$$

The analysis of organic products by GC confirmed that homolysis is the only reactivity mode in acidic solutions for all the complexes examined. For example, the reaction of (2-Pr)Cr([15]aneN$_4$)$^{2+}$ in the presence of $(NH_3)_5CoBr^{2+}$ yielded 2-PrBr as the exclusive organic product, consistent with the sequence of reactions I-1 and I-5.[12] No propane was detected, which effectively rules out any heterolysis under these conditions.

Quantitative kinetic studies of the homolysis were conducted spectrophotometrically in the presence of either HTMPO or $(NH_3)_5CoBr^{2+}$. The reactions (eq I-7) are first-order with respect to the concentration of the organochromium macrocycle and zero order with respect to the scavenger concentration (eq I-8). The concentration conditions and rate constants are summarized in Table I-1.

$$RCrL(H_2O)^{2+} \xrightarrow{H_2O} R\cdot + CrL(H_2O)_2^{2+} \qquad \text{(I-7)}$$

$$-d[RCrL(H_2O)^{2+}]/dt = k_7[RCrL(H_2O)^{2+}] \qquad \text{(I-8)}$$

No homolytic cleavage of the Cr-C bond was observed for $RCrL(H_2O)^{2+}$ when R was a primary alkyl group, as tested for R = C_2H_5, n-C_3H_7, and n-C_4H_9. Indeed, in the absence of a scavenger even the secondary alkyl and aralkyl complexes do not undergo net homolysis because the reverse of reaction I-7 occurs rapidly. Thus these organochromium macrocycles can be stored for weeks when kept in a refrigerator under nitrogen or argon.

Trans Effects on Homolysis of the Hydroxo Complexes. A change of pH from 4 to 6 of a solution of $RCrL(H_2O)^{2+}$ causes an instantaneous color change from yellow to red. The associated spectral changes are shown in **Figure I-2.** When the solution is re-acidified, the yellow color is restored and the spectrum of $RCrL(H_2O)^{2+}$ reappears. The reversibility of the spectral changes indicates that the chromium-carbon bond remains intact; reversible deprotonation of the trans water molecule yields $RCrL(OH)^{+}$.[14,15]

The progress of the homolysis was monitored by the ESR signal of the scavenger HTMPO. As shown in **Figure I-1A**, the intensity of the ESR spectrum of HTMPO in the presence of $i\text{-}C_3H_7CrL(OH)^{+}$ remains virtually unchanged after 15 min at 40 °C. In contrast, the decreasing ESR signal, **Figure I-1B**, shows a significant loss of HTMPO during the homolysis of $i\text{-}C_3H_7CrL(H_2O)^{2+}$ in ~12 min at 40 °C. This establishes that the homolysis rate of the hydroxo complex is negligibly small compared to that of the aqua complex.

Temperature Dependence of Homolysis Rate Constants. The value of k_7 was determined over a range of temperatures for each of the complexes $RCrL(H_2O)^{2+}$ with either $(NH_3)_5CoBr^{2+}$ or HTMPO used to draw the reaction to completion. The groups R and the temperature range for each are: $i\text{-}C_3H_7$, 286-333 K; $p\text{-}CH_3C_6H_4CH_2$, 295-332 K; $C_6H_5CH_2$, 298-333 K; $p\text{-}BrC_6H_4CH_2$, 298-344 K, as shown in **Figure I-3.** The values of $\Delta H^{\ddagger}$ and $\Delta S^{\ddagger}$ were determined from a fit of the data to the Eyring equation, to which they nicely conformed. The values of $\Delta H^{\ddagger}$ and $\Delta S^{\ddagger}$ are summarized in **Table I-2.**

Heterolytic Cleavage of the Cr-C Bond. Although the trans aqua organochromium macrocyclic cations do not undergo acidolysis in acidic solutions (at least not in comparison with the dominant homolysis reaction), the situation is different for the hydroxo complexes $RCrL(OH)^+$ at pH 12-14. Here, the complexes with R = i-C_3H_7 and n-C_3H_7 both undergo slow hydrolysis, eq I-9, to yield propane as the only organic product detected gas chromatographically. Both the kinetics and the organic products are unaffected by the presence of HTMPO and $(NH_3)_5CoBr^{2+}$. This clearly rules out any contribution from a homolytic pathway. The nature of the chromium product in eq I-9 was assumed but not verified. No decomposition of the aralkyl chromium complexes was observed in basic solutions.

$$RCrL(OH)^+ + H_2O \longrightarrow RH + CrL(OH)_2^+ \qquad (I\text{-}9)$$

The rate of reaction I-9 follows first-order kinetics, with k_9 = $(2.3 \pm 0.2) \times 10^{-4}$ s^{-1} for R = i-C_3H_7, and $(6.6 \pm 0.3) \times 10^{-5}$ s^{-1} for R = n-C_3H_7 at 25 °C. The values of k_9 are independent of $[OH^-]$ in the range 7.2 - 160 mM at μ = 0.20 M and in the range 0.16 - 1.0 M at nonconstant ionic strength. The variation of temperature (298 - 338 K) gave the activation parameters: $\Delta H^{\ddagger}$ = 78 ± 1 kJ mol^{-1}, $\Delta S^{\ddagger}$ = -53 ± 2 J mol^{-1} K^{-1} for R = i-C_3H_7, and $\Delta H^{\ddagger}$ = 83 ± 3 kJ mol^{-1}, $\Delta S^{\ddagger}$ = -46 ± 9 J mol^{-1} K^{-1} for R = n-C_3H_7 as shown in Table I-2. The rate constant for n-$C_3H_7CrL(OD)^+$ in D_2O was also measured, with $k_9 = 6.2 \times 10^{-5}$ s^{-1} at 25.0 °C.

DISCUSSION

The instantaneous and reversible optical change, **Figure I-2**, in the pH range 4-6 has been assigned to the conversion of $RCrL(H_2O)^{2+}$ to $RCrL(OH)^{+}$. The lowest energy charge transfer (R→Cr) band shifts to higher energy in basic solution, consistent with the π-donor ability of OH^- which increases the energy of the "t_{2g}" orbitals resulting in a higher energy for the R→Cr charge transfer transition. Put differently, $RCrL(OH)^{+}$ is a weaker oxidant than $RCrL(H_2O)^{2+}$.

The existence of both aqua and hydroxo complexes allows the study of the homolysis of both species. For the secondary alkyl and aralkyl aqua complexes the reaction is indeed homolysis based on the following evidence: (a) the reaction proceeds in the presence of scavengers for both R· and $(H_2O)_2CrL^{2+}$; (b) the rate constant remains independent of the scavenger concentration; (c) the rate constant is independent of which scavenger was used, but varies with the group R. The primary alkyl complexes do not undergo homolysis even over very long times. This is consistent with the lower thermodynamic stability of primary alkyl radicals as compared to secondary and aralkyl radicals.

Under the same concentration and temperature conditions none of the hydroxo complexes, $RCrL(OH)^{+}$, undergoes homolysis. This is again related to the electron donating effect of OH^-, which stabilizes the Cr(III) state and thus makes it less susceptible to internal electron transfer that accompanies homolysis of eq I-7.

The activation parameters for bond homolysis are listed in

Table I-2. The large values of $\Delta H^{\ddagger}$ reflect the large chromium-carbon bond strengths of these complexes. Indeed, they can be taken as an approximate measure of the bond dissociation enthalpy, once allowance is made for the relatively small value of $\Delta H^{\ddagger}_{-7}$ for the radical recombination reaction.[6,16] The value of $\Delta H^{\ddagger}$ for $(H_2O)_5CrCH_2Ph^{2+}$ (133 kJ mol^{-1}) is significantly larger than the value of 103 kJ mol^{-1} for its macrocyclic analogue. This difference in $\Delta H^{\ddagger}$ can be explained on the basis of the molecular structures, in particular the longer Cr-C bond in the macrocycle.[17] The compound $[p\text{-}BrC_6H_4CH_2CrL(H_2O)](ClO_4)_2 \cdot THF$ has a Cr-C bond length of 2.14 Å,[17] noticeably longer than the 2.06 Å distance in trans-$[CH_2ClCr(acac)_2H_2O]$.[18] No complex in the $[(H_2O)_5CrR]X_2$ series has been crystallized, although one anticipates a Cr-C bond as short or shorter than that in the acac derivative. This argument is, however, somewhat speculative, since the overall charge is different in the pentaaqua and acac series.

The observed effect of the macrocycle on the Cr-C bond strength is the net result of two opposing effects, steric and electronic. The former weakens and lengthens the bond. The electron donation from the N_4 macrocycle, on the other hand, stabilizes the Cr(III) state, and thus inhibits homolysis. The size of the electronic effect of [15]aneN_4 becomes obvious if one compares the reduction potentials for the couples $Cr([15]aneN_4)(H_2O)_2^{3+/2+}$ (-0.58 V)[7] and $Cr(H_2O)_6^{3+/2+}$ (-0.41 V). Yet despite the electronic effect favoring the Cr(III) state, the Cr-C bond is weaker in the macrocyclic series. This point illustrates just how dominant steric effects are on bond strengths, a point made already in earlier work.[19,20]

Despite the lowering of $\Delta H^{\ddagger}$ for the macrocycle, the homolysis of $(H_2O)_5CrCH_2Ph^{2+}$ ($k = 2.6 \times 10^{-3}$ s^{-1})[5] proceeds more rapidly than that of the analogous $PhCH_2CrL(H_2O)^{2+}$ (1.2×10^{-4} s^{-1}). This, of course, is due to the more-than-offsetting values of $\Delta S^{\ddagger}$. The complex $(H_2O)_5CrCH_2Ph^{2+}$ has a $\Delta S^{\ddagger}$ value of 153 J mol^{-1} K^{-1}, as compared to 28 J mol^{-1} K^{-1} for $(H_2O)Cr(L)CH_2Ph^{2+}$. This large difference seems to indicate that the second coordination sphere "loosens up" much more in reaching the transition state in the aqua series. This is not unreasonable given that $(H_2O)_5CrR^{2+}$ must be much more strongly solvated than the macrocyclic analogues and that in reaching the transition state for homolysis the bond distances approach those for Cr(II) complexes. This means that the Cr-O distances in $[(H_2O)_5Cr\text{---}R^{2+}]^{\ddagger}$ stretch significantly, whereas the Cr-N bond lengths in $[([15]aneN_4)(H_2O)Cr\text{---}R^{2+}]^{\ddagger}$ remain virtually the same. Thus the effect on the second coordination sphere must be quite dramatic for $(H_2O)_5CrR^{2+}$, but negligible in the macrocyclic series. In addition, there is a contribution from the rotational entropy changes of the coordinated molecules of water in $(H_2O)_5CrR^{2+}$, a gain that has no counterpart in the macrocyclic series.

The rate constants for homolysis of $ArCH_2CrL(H_2O)^{2+}$ vary little as the substituent on the benzene ring changes from p-CH_3 to H to p-Br. This is different from the behavior of the corresponding pentaaqua series, p-X-$C_6H_4CH_2Cr(H_2O)_5^{2+}$, where the Hammett correlation yields the reaction constant $\rho = -1.01$.[5] The greater sensitivity to substituents in the pentaaqua complexes is qualitatively consistent with the Cr-C bond being stronger for them. A greater degree of charge transfer in the

transition state is required for homolysis of $(H_2O)_5CrCH_2Ar^{2+}$ as compared to $ArCH_2Cr(L)H_2O^{2+}$.

Turning to the pathway for the heterolytic solvolysis reaction, we note that $RCrL(OH)^+$ is not attacked by external OH^-; i.e., the rate is independent of $[OH^-]$. This compares with the behavior of $(H_2O)_5CrR^{2+}$ complexes, where inverse $[H^+]$ terms signal a conjugate base pathway that is significant enough to provide the major decomposition route at pH 4-7.[21,22] With the macrocycles we find that only the hydroxo complexes, but not the aqua, are subject to heterolytic decomposition. It is significant that a reaction of the aqua complex with H_3O^+ is not important. Even though H_3O^+ itself might function as an electrophile, there is no kinetically significant term with a direct dependence on $[H_3O^+]$, unlike the pentaaqua series where a term $k_A[(H_2O)_5CrR^{2+}][H_3O^+]$ provides, for most R groups, a major pathway.[4] This means that proton transfer to an incipient carbanion is not important for chromium-carbon bond heterolysis of $RCrL(OH)^+$ complexes.

How is the rate law, which has the form $k_9[RCrL(OH)^+]$, to be interpreted? One can hardly attribute it to a path in which an external H_2O molecule acts as a kinetically active electrophile, given the inactivity of the more powerful electrophile H_3O^+ towards the aquo complex. Moreover we find no kinetic isotope effect in D_2O: the complex $[n\text{-}PrCrL(OD)^+]$ has $k_9 = 6.2 \times 10^{-5}\ s^{-1}$ (25 °C, pD = 12 in D_2O), compared to $k_9 = (6.6 \pm 0.3) \times 10^{-5}\ s^{-1}$ for the reaction of $[n\text{-}PrCrL(OH)^+]$ in H_2O. Thus proton transfer from H_2O to R is not significantly advanced in the transition state.

The heterolytic reactions are accompanied by substantial and negative activation entropies as shown in Table I-2. This suggests a transition state with larger charge separation as compared to that of reactant. Hence, the interpretation we offer is that the rate-limiting step is intramolecular charge transfer to form an incipient carbanion, and the transition state might be represented as $[HOCr^{\delta+}(L)R^{\delta-}\cdots H\text{-}OH^{+}]^{\ddagger}$. We further note that heterolysis applies only to the complex in which the trans ligand is OH^{-}, not H_2O. The evident role for coordinated OH^{-} is to act as a strong electron donor, which improves the energetics of carbanion formation.

The aralkyl complexes are not subject to heterolytic solvolysis, even in the case of the trans-hydroxo species. This contrasts with the very slow but easily observed decomposition of $(H_2O)_5CrCH_2Ph^{2+}$.[23]

Table I-1. Rate Constants for the Homolysis of $RCr([15]aneN_4)(H_2O)^{2+}$ Complexes in Aqueous Solutions[a]

R	Scavenger, concentration/mM	$10^4\ k_6/s^{-1}$
$i\text{-}C_3H_7$	$(NH_3)_5CoBr^{2+}$, 0.63 - 4.65	5.0 ± 0.3
$i\text{-}C_3H_7$	HTMPO, 0.20 - 1.60	5.0 ± 0.4
$p\text{-}CH_3C_6H_4CH_2$	HTMPO, 0.31 - 1.67	1.36 ± 0.01
$C_6H_5CH_2$	HTMPO, 0.76 - 2.00	1.24 ± 0.04
$p\text{-}BrC_6H_4CH_2$	HTMPO, 0.23 - 1.00	1.15 ± 0.01

[a]At 25.0 °C with $[H^+] = 1.0 \times 10^{-2}$ M, $\mu = 0.20$ M, $[RCr([15]aneN_4)(H_2O)^{2+}]_0 = 0.02 - 0.35$ mM, used always as a limiting reagent.

Table I-2. Activation Parameters for the Homolysis and Heterolysis of Organochromium Cations[a]

Complex	Reaction	$\Delta H^{\ddagger}$/kJ mol^{-1}	$\Delta S^{\ddagger}$/J mol^{-1} K^{-1}
i-$C_3H_7CrL(H_2O)^{2+}$ [b]	homolysis	110 ± 3	62 ± 6
p-$CH_3C_6H_4CH_2CrL(H_2O)^{2+}$ [b]	homolysis	111 ± 2	54 ± 6
$C_6H_5CH_2CrL(H_2O)^{2+}$ [b]	homolysis	103 ± 2	28 ± 5
p-$BrC_6H_4CH_2CrL(H_2O)^{2+}$ [b]	homolysis	101 ± 3	22 ± 9
$(H_2O)_5CrCH_2C_6H_5^{2+}$ [c]	homolysis	133	153
i-$C_3H_7CrL(OH)^{+}$ [d]	heterolysis	78 ± 1	-53 ± 2
n-$C_3H_7CrL(OH)^{+}$ [d]	heterolysis	83 ± 3	-42 ± 9

[a] L = [15]aneN_4.

[b] In aqueous solution with 1.0 x 10^{-2} M H^+ at μ = 0.20 M.

[c] Ref. 5.

[d] [NaOH] = μ = 0.82 M.

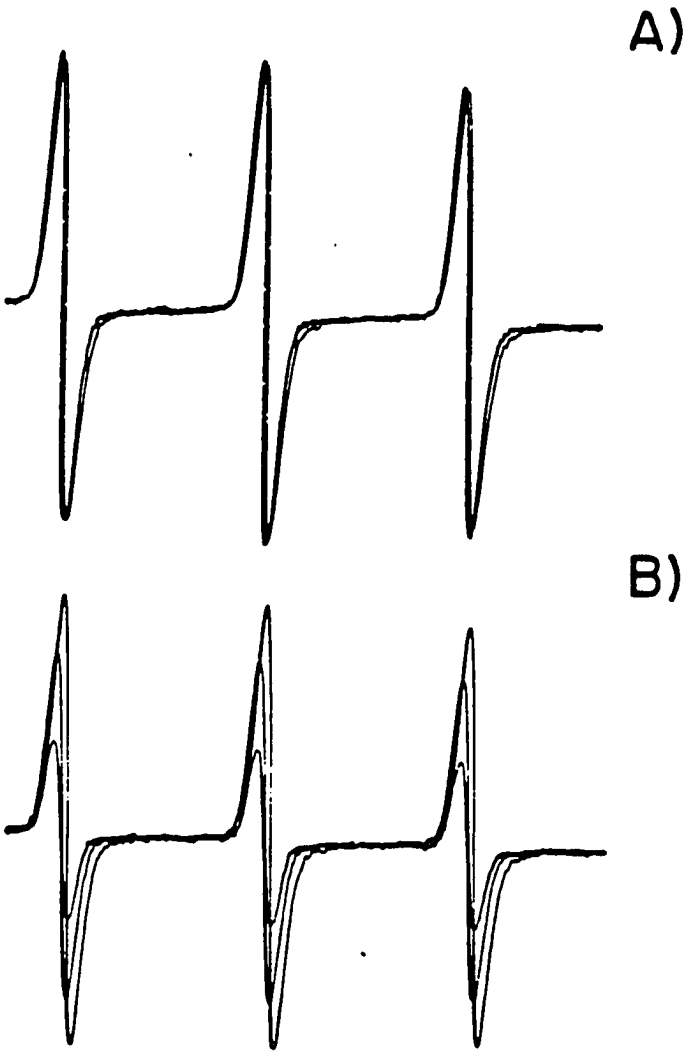

Figure I-1. Changes in the ESR spectrum of the radical scavenger HTMPO in the presence of $i\text{-}C_3H_7CrL(OH)^+$ (A) and $i\text{-}C_3H_7CrL(H_2O)^{2+}$ (B), L = [15]aneN$_4$. The spectra were recorded on reaction solutions that were kept at 40 °C for 0 and 15 min (A) and 0, 2, and 12 min (B). The ESR spectra were recorded at 15 °C, with a sweep width of 50 G. Small fluctuation of frequency with time causes small shifts of central field around 3475 G

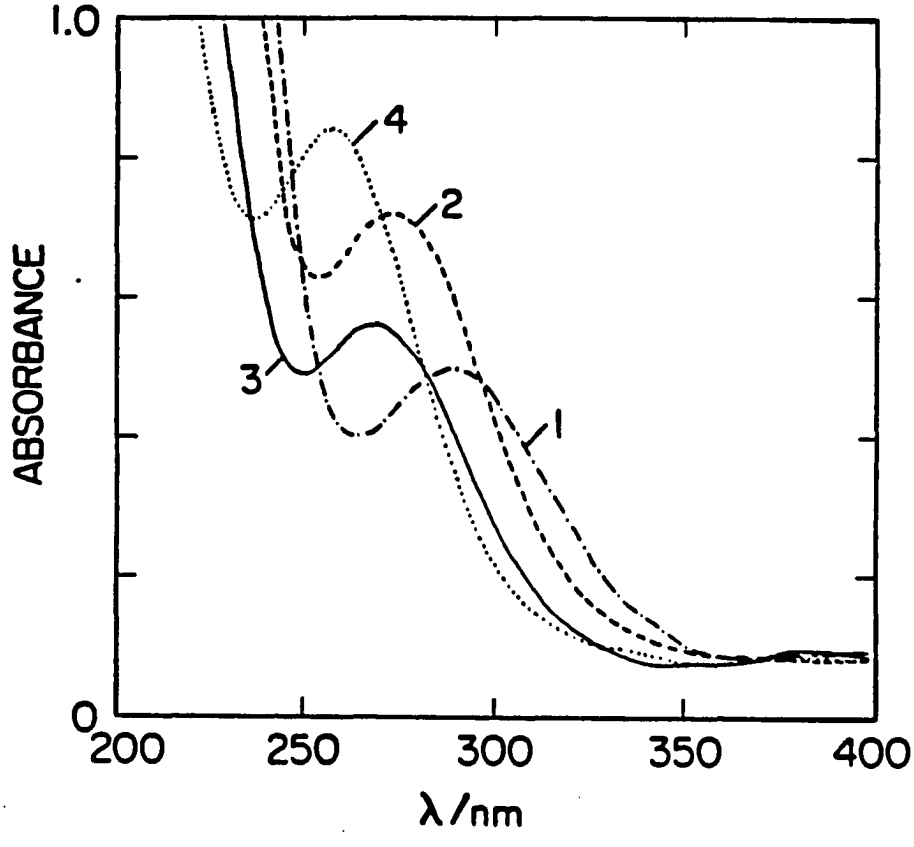

Figure I-2. Electronic spectra of $RCrL(A)^{n+1}$ complexes, L = [15]aneN$_4$. Optical pathlength 1 mm. (1) 1.5 mM i-$C_3H_7CrL(H_2O)^{2+}$ at pH 4; (2) 1.5 mM i-$C_3H_7CrL(OH)^{+}$ at pH 7; (3) 2.2 mM n-$C_3H_7CrL(H_2O)^{2+}$ at pH 4; (4) 2.2 mM n-$C_3H_7CrL(OH)^{+}$ at pH 7

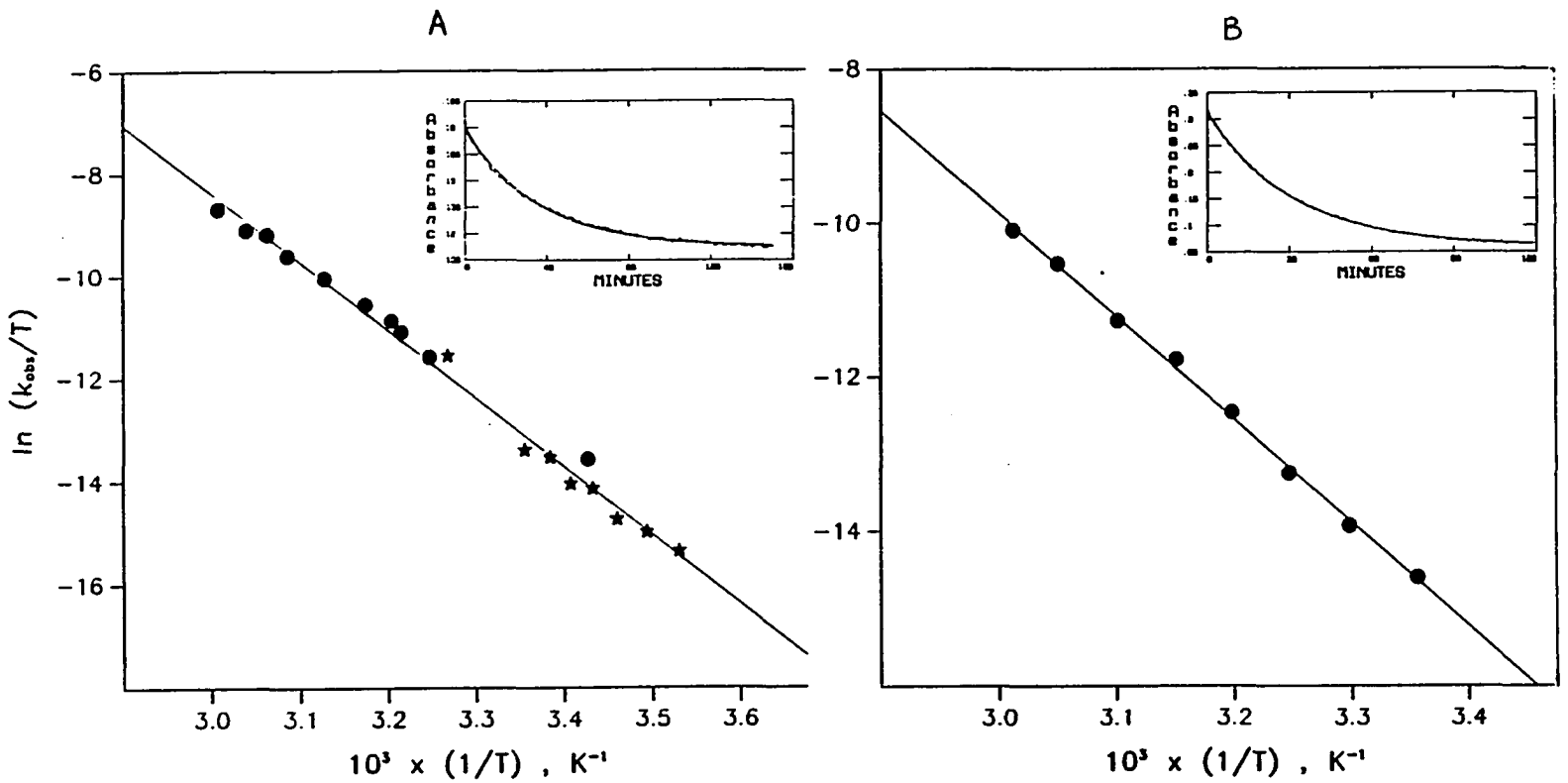

Figure I-3. Temperature dependence of homolysis rate of (A) $i\text{-}C_3H_7CrL(H_2O)^{2+}$; (B) $p\text{-}CH_3C_6H_4CH_2CrL(H_2O)^{2+}$; (C) $C_6H_5CH_2CrL(H_2O)^{2+}$; (D) $p\text{-}BrC_6H_4CH_2CrL(H_2O)^{2+}$, L = [15]ane$N_4$. Insets show observed kinetic profiles along with fitted pseudo-first-order curves: (A) at 298.0 K; (B) 317.4 K; (C) 303.7 K; (D) 311.1 K

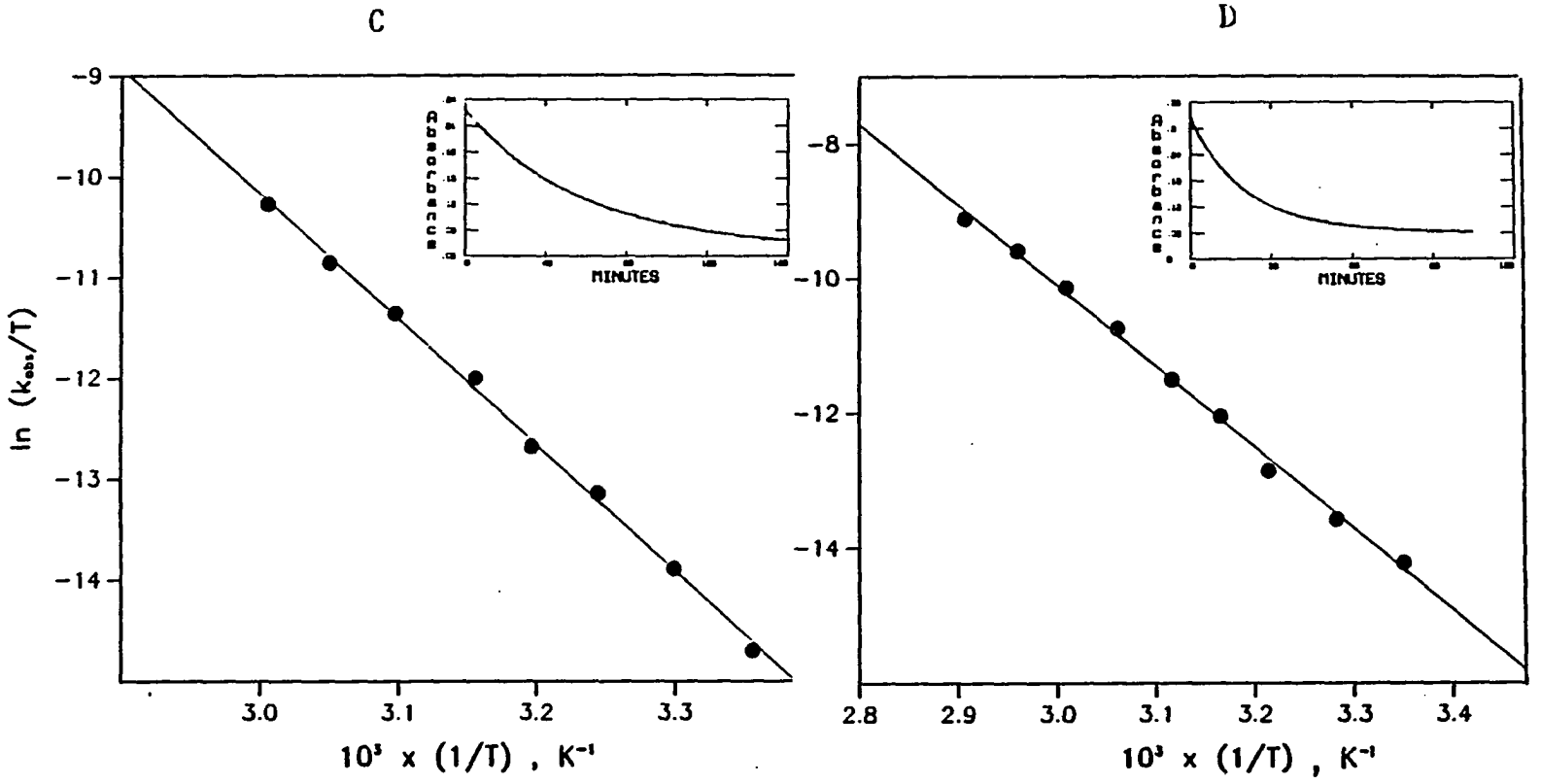

Figure I-3. (continued)

REFERENCES

(1) Kochi, J. K. "Organometallic Mechanisms and Catalysis", Academic Press, New York, 1978, p 190.

(2) Green, M. in "Mechanisms of Inorganic and Organometallic Reactions", Twigg, M. V., Ed., Plenum Press, New York, 1983, Vol. 1, p 221.

(3) Johnson, M. D.; Winterton, N. J. Chem. Soc. (A) 1970, 511.

(4) (a) Espenson, J. H. Adv. Inorg. Bioinorg. Mech. 1982, 1, 1-62; (b) Prog. Inorg. Chem. 1983, 30, 189-212.

(5) Nohr, R. S.; Espenson, J. H. J. Am. Chem. Soc. 1975, 97, 3392.

(6) Halpern, J. Acc. Chem. Res. 1982, 15, 238.

(7) Samuels, G. J.; Espenson, J. H. Inorg. Chem. 1979, 18, 2587.

(8) Diehl, H.; Clark, H.; Willard, H. H. Inorg. Synth. 1939, 1, 186.

(9) HTMPO = 4-hydroxy-2,2,6,6-tetramethylpiperidinyloxyl.

(10) Mossoba, M. M.; Makino, K.; Riesz, P. J. Phys. Chem. 1984, 88, 4717.

(12) Kelley, D. G.; Bakac,A.; Espenson, J. H., submitted for publication. Chemistry Department, Iowa State University.

(13) Qualitative tests showed a very rapid reaction between $(H_2O)_2CrL^{2+}$ and $(NH_3)_5CoBr^{2+}$. The cobalt(III) complex is also reduced very rapidly by $Cr(H_2O)_6^{2+}$. (Candlin, J. P.; Halpern, J.; Trimm, D. L. J. Am. Chem. Soc. 1964, 86, 1019).

(14) The protonation and deprotonation of a nitrogen of L can probably be ruled out at this pH. Also, the deprotonation of a coordinated

molecule of H_2O in $(H_2O)_2CrL^{3+}$ is known to have a pKa of 2.9 (see ref. 15).

(15) Richens, D. T.; Adzamli, I. K.; Leupin, P.; Sykes, A. G. Inorg. Chem. 1984, 23, 3065.

(16) Koenig, T. W.; Hay, B. P.; Finke, R. G. Polyhedron 1988, 7, 1499.

(17) Shi, S.; Espenson, J. H.; Bakac, A. J. Am. Chem. Soc. 1990, 112, 1841.

(18) Ogino, H.; Shoji, M.; Abe, Y.; Shimura, M.; Shimoi, M. Inorg. Chem. 1987, 26, 2542.

(19) (a) Kirker, G. W.; Bakac, A.; Espenson, J. H. J. Am. Chem. Soc. 1982, 104, 1249; (b) Bakac, A.; Espenson, J. H. J. Am. Chem. Soc. 1990, 112, 2273.

(20) Rüchardt, C. Top. Curr. Chem. 1980, 88, 1.

(21) Cohen, H.; Meyerstein, D. Inorg. Chem. 1984, 23, 84.

(22) Rotman, A.; Cohen, H.; Meyerstein, D. Inorg. Chem. 1985, 24, 4158.

(23) Kita, P.; Jordan, R. B. Inorg. Chem. 1989, 28, 3489.

PART II. STRUCTURE AND REACTIVITY OF ORGANOCHROMIUM MACROCYCLES WITH IODINE BY CHAIN AND ELECTROPHILIC MECHANISMS

INTRODUCTION

The cleavage of metal-carbon bonds by halogens has been fairly widely studied.[1] Generally, two mechanisms are operative. One is electrophilic substitution, often an S_E2 process, that cleanly converts reactants to products. This is usually accompanied by inversion of stereochemistry at the α-carbon atom if the substrate is a transition metal complex with a high coordination number. The S_E2 mechanism is a two-electron process that occurs without the intervention of reaction intermediates. The second mechanism is a one-electron transfer process, in which the initial step is the formation of a caged radical pair, $\{RM^+, X_2^{\cdot -}\}$. The electron transfer step may initiate a chain sequence for halogenolysis.

The literature in the field includes extensive studies on a series of organochromium complexes, $(H_2O)_5CrR^{2+}$,[2] and macrocyclic complexes of cobalt, including the cobaloximes, $RCo(dmgH)_2B$ (B = H_2O, pyridine, etc.).[3-6] The former complexes adopt an S_E2 mechanism for halogenolysis, whereas the mechanism for the cobaloximes includes an electron transfer step. The participation of inorganic transition metal complexes in photoinduced chain reactions was also noticed before.[7]

We have turned our attention to iodinolysis reactions of a different group of organometallic complexes. This is a series of alkyl and aralkyl derivatives of a chromium macrocycle, $RCr([15]aneN_4)H_2O^{2+}$.[8] Cleavage of the carbon-chromium bond in such complexes by electrophilic mercury(II) ions occurs strictly by an S_E2 mechanism.[9] Halogenolysis reactions have

not been previously investigated for these complexes. Rather to our surprise, we find that the mechanism for the reaction of $RCr([15]aneN_4)H_2O^{2+}$ with I_2 changes along the series of R groups and both electrophilic and oxidative mechanisms have to be considered. We present the results of kinetic investigations in this paper.

No crystal structure data were available for the complexes $RCr([15]aneN_4)H_2O^{2+}$ until now. In this work we have determined by X-ray diffraction the structure of the perchlorate salt of the complex with R = 4-bromobenzyl. Among other factors, we were interested in establishing the identity of the compound on more secure grounds, in the extent of steric hindrance at the chromium-carbon bond, and in the ground-state steric influence, as measured by the extent of the elongation of the bond to the trans water molecule.

EXPERIMENTAL SECTION

Materials. The chromium(II) complex, CrL^{2+} (L = [15]aneN$_4$) was prepared by mixing stoichiometric amounts of $CrCl_2 \cdot 4H_2O$[10] and ligand L (Strem Chemical Co.) in aqueous solution.[8] The organochromium complexes, $RCrL(H_2O)^{2+}$, (R = CH_3, C_2H_5, 1-C_3H_7, and 1-C_4H_9) were prepared from CrL^{2+} and the corresponding organic bromide following the published procedure.[8] Similarly, sec-alkyl and aralkyl complexes were prepared from the organic halides. All organochromium macrocycles were separated and purified by ion exchange on Sephadex C-25. Iodine solutions were prepared by dissolving the AR grade reagent in 0.01 M perchloric acid.

Iodine and triodide ion concentrations were determined spectrophotometrically at 467 nm (ε 733 M^{-1} cm^{-1} for I_2) and 352 nm (2.46 x 10^4 M^{-1} cm^{-1} for I_3^-).[11] The extinction coefficients for $RCrL(H_2O)^{2+}$ were taken from the literature.[8] For R = CH_3, λ_{max}/nm (ε/M^{-1} cm^{-1}) are 258 (3.30 x 10^3) and 375 (2.27 x 10^2); C_2H_5, 264 (3.10 x 10^3) and 383 (3.87 x 10^2); 1-C_3H_7, 265 (3.44 x 10^3) and 383 (4.65 x 10^2); and 1-C_4H_9, 268 (3.30 x 10^3) and 383 (4.59 x 10^2). The molar absorptivities listed were used to determine the concentrations of the organochromium ions. The new complex prepared in this work, 4-$BrC_6H_4CH_2CrL(H_2O)^{2+}$, has maxima at 245 nm ($\varepsilon$ 1.07 x 10^4 M^{-1} cm^{-1}), 281 (9.82 x 10^3), 303 (8.83 x 10^3), and 361 (2.40 x 10^3).

Kinetics. The kinetics of the reaction of $CrL(H_2O)^{2+}$ with $4\text{-}BrC_6H_4CH_2Br$ were followed at room temperature at 305 nm with a Durrum-Dionex stopped-flow spectrophotometer. Anaerobic conditions were required by the extreme sensitivity of the chromium(II) complex towards oxygen.

The kinetic study of the chain reaction between I_2 and $4\text{-}BrC_6H_4CH_2CrL(H_2O)^{2+}$ was conducted with the chromium complex in excess over iodine in solutions containing free iodide. The progress of the reaction was monitored by following the disappearance of I_3^- at λ 352 nm. The kinetics of the electrophilic reactions of the primary alkyl complexes were studied under pseudo-first-order conditions with $RCrL^{2+}$ in excess (R = CH_3, C_2H_5, $1\text{-}C_3H_7$, $1\text{-}C_4H_9$). For the case of R = $1\text{-}C_3H_7$ the results were also checked with I_2 in excess. All reactions with I_2 were conducted at 25.0 ± 0.1 °C at a constant ionic strength of 0.20 M controlled by $NaClO_4$ and a constant pH of 2.00, controlled by perchloric acid.

Crystal Growth. Orange crystals of $[4\text{-}BrC_6H_4CH_2CrL(H_2O)](ClO_4)_2\cdot THF$ were grown from a sample of the purified organochromium cation in a mixture of THF and water in an ESR tube encapsulated within a sealed test tube. This system was employed to slow the temperature change as the solution was being cooled. This procedure afforded crystals suitable for X-ray diffraction.

X-Ray Data and Structure. A crystal of approximate dimensions 0.30 x 0.14 x 0.13 mm was used to collect X-ray diffraction data with an Enraf-Nonius CAD-4 diffractometer. The cell constants were determined from reflections found by an automated search routine. An empirical absorption correction was based on a series of psi-scans. Pertinent results are given in **Table II-1.**

The positions of Cr, Br, and Cl atoms were taken from an E-map produced by direct methods. Trial positions of other atoms were determined by a difference Fourier map and subsequent least-squares refinement. Because of the disorder in perchlorate anions and THF molecules, as well as a relatively low observation to parameter ratio, the phenyl group was subsequently refined as a rigid hexagon with C-C bond lengths of 1.395 Å and the perchlorate ions as rigid tetrahedra with Cl-O bond lengths of 1.50 Å. Based on the difference map, two orientations were assigned to each of the two independent perchlorate groups, with occupancy factors of 0.46:0.54 and 0.81:0.19. Hydrogen atoms were not included in the refinement but were used for the determination of F_{calc}. Final R and R_w values are shown in **Table II-1.** All calculations were performed on a Digital Equipment Corp. Micro Vax II computer. The refinement was carried out with the SHELX-76 package.

Spectrum and Product Analysis. The UV-visible spectra were taken with a Perkin-Elmer Lambda Array 3840 UV/vis spectrophotometer. The I_3^- ion was identified spectrophotometrically. The organic products were identified with a Hewlett-Packard Model 5790 gas chromatograph with a 6′

column packed with OV-101 stationary phase. The instrument was calibrated by use of standard organic halides.

RESULTS AND DISCUSSION

Formation of $4\text{-BrC}_6\text{H}_4\text{CH}_2\text{CrL}(\text{H}_2\text{O})^{2+}$. The reaction between the $4\text{-BrC}_6\text{H}_4\text{CH}_2\text{Br}$ (RBr) and CrL^{2+} was studied in 10% ethanol-water, since the bromide is insoluble in strictly aqueous solution. CrL^{2+} was used in at least ten-fold excess over RBr. The reaction followed pseudo-first-order kinetics in each run, and the plot of k_{obsd} vs $[\text{CrL}^{2+}]$ was linear, as depicted in **Figure II-1.** The second-order rate constant obtained is 3.73 x 10^4 M^{-1} s^{-1}.

The reaction produces the indicated organochromium(III) cation, as shown by its UV/visible spectrum (after separation by ion exchange chromatography) and by X-ray crystallography. The rate constant of 3.7 x 10^4 M^{-1} cm^{-1} is slightly higher than the value for PhCH_2Br, k = 1.9 x 10^4 M^{-1} s^{-1}.[8] This small difference is consistent with the proposed free radical mechanism for such reactions:

$$\text{CrL}(\text{H}_2\text{O})_2^{2+} + \text{RBr} \longrightarrow \text{BrCrL}(\text{H}_2\text{O})^{2+} + \text{R}^{\cdot} + \text{H}_2\text{O} \qquad k_1 \qquad \text{(II-1)}$$

$$\text{CrL}(\text{H}_2\text{O})_2^{2+} + \text{R}^{\cdot} \longrightarrow \text{RCrL}(\text{H}_2\text{O})^{2+} + \text{H}_2\text{O} \qquad k_2 \text{ (fast)} \qquad \text{(II-2)}$$

According to this scheme, $-d[\text{RBr}]/dt = k_1[\text{CrL}^{2+}][\text{RBr}]$. Thus the values of the rate constants cited above represent k_1. The 4-Br derivative is expected to react more rapidly than the unsubstituted benzyl complex owing to the electron-withdrawing properties of bromine and resonance stabilization of the alkyl radical by the para-bromine.

The complex $4\text{-}BrC_6H_4CH_2CrL(H_2O)^{2+}$ is more stable toward air than $PhCH_2CrL(H_2O)^{2+}$ is. In both cases the reaction proceeds by unimolecular homolysis.[12] The electron withdrawing effect of the para bromine makes the Cr-C bond more polar thereby retarding the homolysis. The complex $4\text{-}BrC_6H_4CH_2CrL(H_2O)^{2+}$ is quite stable toward acid; it can be stored in solution at pH 2 and 0 °C for weeks.

The crystal structure of $[p\text{-}BrC_6H_4CH_2CrL(H_2O)](ClO_4)_2\cdot THF$ is shown in **Figure II-2.** The cation adopts a distorted octahedral structure with a molecule of water trans to the Cr-C bond. The relevant bond lengths and bond angles are summarized in **Table II-2** and **Table II-3.** The Cr-C bond length (2.14 Å) in this cation is slightly longer than the reported values of other stable organochromium complexes (2.06 Å in trans-$[(CH_2Cl)Cr(acac)_2\cdot H_2O]$ and 2.077 - 2.129 Å in trans-$RCr(acac)_2py$, for R = $CHCl_2$ and CH_2Cl, respectively).[13,14] The Cr-C(1)-C(2) angle of 123° is also larger than that for a typical sp^3 carbon. All of these deviations are due to the steric repulsion between the para-bromobenzyl group and the bulky macrocyclic ligand. Similar distortions have been observed before.[13,14] We also note the large Cr-C-Si bond angle (127.9° - 128.3°) in the compound cis-$[Me_3SiCH_2Cr(bipy)]I$.[15]

It is noted from **Figure II-2** that the coordinated nitrogens adopt a configuration with three of the four N-H bonds pointing upward and one downward. This asymmetric configuration makes the two sides of the CrN_4 plane different (designated as side A and side B, respectively, in **Figure II-2**). A space filling model shows that this asymmetric binding of [15]aneN_4 to chromium(III) results in the A side being less crowded than

the B side. It is therefore not too surprising that the 4-bromobenzyl group binds preferentially to the A side even though the CrN_4 plane is quite flat.

A comparison between the Cr(III)-OH_2 bond length in trans-4-$BrC_6H_4CH_2CrL(H_2O)^{2+}$ (2.13 Å) and that in trans-$ClCrL(H_2O)^{2+}$ (2.04 Å)[16] can also be made. The reported crystal structure of the chloro complex has the H_2O molecule bound to the more open A side, rather than the B side as in the case of the organometallic complex. Hence both the trans influence of the Cr(III)-C bond and the steric crowdedness of the B side might contribute to the elongation of the Cr(III)-OH_2 bond in the 4-bromobenzyl complex.

Electrophilic Substitution Reactions with Iodine. All the primary alkyl chromium complexes, $RCrL(H_2O)^{2+}$, are quite stable toward O_2. No reaction was observed in 60 min in oxygen-saturated solutions, $[RCrL(H_2O)^{2+}] \sim 3 \times 10^{-4}$ M. These solutions are also stable toward acidolysis. No significant reaction was observed in 60 min in solutions of $RCrL(H_2O)^{2+}$ containing 0.01 - 0.4 M $HClO_4$ at room temperature.

The Cr-C bond in $RCrL(H_2O)^{2+}$ can be easily cleaved heterolytically by I_2. Advantage was taken of the strong light absorption of I_3^- at 352 nm to monitor the reaction which proceeds according to the net equation II-3. All the experiments were done in the presence of excess I^- to

$$I_2 + RCrL(H_2O)^{2+} + H_2O \longrightarrow I^- + RI + (H_2O)_2CrL^{3+} \qquad \text{(II-3)}$$

create the I_3^- chromophore. The reaction rate is first-order with respect to both iodine and alkyl chromium concentrations, regardless of which one was used as the limiting reagent.

Since I_2 and I_3^- have almost identical reduction potentials, both should be considered as possible electrophiles. To distinguish between them, consider the rate laws in experiments with I_2/I_3^- as the limiting reagent. We consider three cases, in which K_f represents the formation constant of I_3^-, and k_{obsd} the value of $-d\ln[I_2]/dt$:

(1) I_3^- is the only active electrophile:

$$k_{obsd} = \frac{\{k_{I_3} K_f[I^-]\}[RCrL(H_2O)^{2+}]}{1 + K_f[I^-]} \qquad \text{(II-4)}$$

(2) I_2 is the only active electrophile:

$$k_{obsd} = \frac{k_{I_2}[RCrL(H_2O)^{2+}]}{1 + K_f[I^-]} \qquad \text{(II-5)}$$

(3) Both I_3^- and I_2 are active electrophiles:

$$k_{obsd} = \frac{\{k_{I_3} K_f[I^-] + k_{I_2}\}[RCrL(H_2O)^{2+}]}{1 + K_f[I^-]} \qquad \text{(II-6)}$$

The distinction between these cases clearly lies in the form of the

dependence of k_{obsd} upon $[I^-]$. For all the primary alkyl chromium complexes studied, the pseudo-first-order rate constant decreases as the free iodide concentration increases, as shown in **Figure II-3**. The clear linearity in the plots of k_{obsd} versus $[RCrL(H_2O)^{2+}]/(1 + K_f[I^-])$ shows that only I_2 is the active electrophile and the rate law of eq II-5 applies. Thus I_3^- serves only as a chromophore useful in following the progress of the reaction, and is in instantaneous equilibrium with I_2 ($I_3^- \rightleftharpoons I^- + I_2$). Consistent with that, the kinetics were unaffected by the variation of ionic strength in the range 5×10^{-3} to 0.8 M.

The only organic product of the reaction was identified by gas chromatography as the alkyl iodide. As an independent test for the formation of RI, we conducted a two stage reaction. In the first stage of this process, the reaction between I_2 and the organochromium macrocycle $RCrL(H_2O)^{2+}$ (here R = C_2H_5, 1-C_3H_7, and 4-$BrC_6H_4CH_2$) was carried out with a slight excess of the latter. Then a solution of $(H_2O)_2CrL^{2+}$ was added to react with any RI formed. Upon this addition the spectrum of $RCrL(H_2O)^{2+}$ quantitatively reappeared. This confirms the quantitative production of RI in the initial reaction with iodine as given in eq II-3.

Other lines of evidence supporting the mechanism were obtained from stoichiometric relationships. A spectrophotometric titration (**Figure II-4**) shows the stoichiometric ratio of I_2:$EtCrL(H_2O)^{2+}$ to be 1:1. The absorbance changes with either I_2 in excess (no free I^- added) or $RCrL(H_2O)^{2+}$ in excess (free I^- added) are consistent with the 1:1 stoichiometry. In the case of 1-$C_3H_7CrL(H_2O)^{2+}$, a kinetic

study was also conducted with I_2 in excess (no free I^- added) affording the same second-order rate constant as shown in **Table II-3.**

The slopes in **Figure II-3** give the second-order rate constants for the bimolecular reaction between I_2 and $RCrL(H_2O)^{2+}$ (eq II-3), as shown in the applicable rate law, eq II-5. The second-order rate constants are summarized in **Table II-4.** The decrease in rate constant from R = Me ($k = 4.7 \times 10^3$ M^{-1} s^{-1}) to n-Bu (8.9 M^{-1} s^{-1}) is to be noted. In particular, this trend points to an S_E2 mechanism proceeding with inversion of configuration at carbon. The values reflect a trend in which the rate constant declines as the alkyl group gets bulkier because of increasing steric hindrance on the alpha carbon from methyl to 1-butyl.[2]

Chain Reaction between $4\text{-}BrC_6H_4CH_2CrL(H_2O)^{2+}$ and Iodine. When the chromium complex is present in excess (~ 10^{-4} M), the reaction is half-order with respect to the iodine concentration, as illustrated in **Figures II-5** and **II-6.** Under those conditions, the presence of O_2 results in a much slower reaction and a pseudo-first-order kinetic profile. A decrease in the concentration of the chromium complex to ~10^{-5} M, while keeping the I_2 in excess, also results in a pseudo-first-order trace even under strictly anaerobic conditions. The reaction proceeds much more rapidly when the chromium complex is used as excess reagent (at ~10^{-4} M level) than it does when iodine is present in excess (at the same ~10^{-4} M level). These observations suggest a free radical chain pathway which requires a relatively high concentration of $4\text{-}BrC_6H_4CH_2CrL(H_2O)^{2+}$ and anaerobic conditions to proceed.

Several extraneous reagents were used to diagnose the reaction mechanism. This entailed the addition of a substance (O_2, Cu^{2+}, or Fe^{2+}) that might fulfill a chain breaking role. Blank experiments confirmed the absence of a reaction between each of these reagents and the bromobenzylchromium cation.

Addition of O_2 (< 1 mM) or $CuCl_2$ (4 mM) significantly retarded the reaction and changed the appearance of the kinetic trace. **Figure II-5** illustrates the unaffected half-order absorbance-time profile along with ones with added O_2 and Cu^{2+}. Dioxygen is well known to react rapidly with free radicals ($C_2H_5\cdot + O_2 \longrightarrow C_2H_5OO\cdot$, for example, has $k = 4.7 \times 10^9$ M^{-1} s^{-1}),[17] and presumably plays this chain-breaking role in the overall reaction scheme. The oxidation of benzyl radicals by Cu^{2+} has been established as well:[18]

$$PhCH_2^{\cdot} + Cu^{2+} + H_2O \longrightarrow PhCH_2OH + Cu^{+} + H^{+} \qquad \text{(II-7)}$$

The dramatic inhibitory effect of Cu^{2+} again points to the involvement of $4\text{-}BrC_6H_4CH_2\cdot$ radical in the chain reaction.

Addition of Fe^{2+} as $Fe(ClO_4)_2(aq)$ (0.04 - 11 mM) effectively decreases the reaction rate as shown in **Figure II-5**. The kinetic profile fits a fractional order between 0.5 and 1. The reaction

$$Fe^{2+} + I_2^{-} \longrightarrow Fe^{3+} + 2I^{-} \qquad \text{(II-8)}$$

with $k_8 = 6 \times 10^6$ M^{-1} s^{-1},[19] is believed to be the reason for the retardation by Fe^{2+}. Hence $I_2^{\cdot -}$ is suggested as another chain-carrying radical intermediate.

A more detailed analysis of the kinetics of the chain reaction is now given. A plot of the instantaneous reaction rate versus the average concentration of I_2 in the interval as a double logarithmic plot gave lines of slopes between 0.47 and 0.58. In other words, the order of the reaction with respect to $[I_2]$ appears to be 1/2. The rate law at a constant concentration of the bromobenzyl chromium complex is thus:

$$-d[I_2]/dt = k_{obsd}[I_2]^{1/2} \qquad \text{(II-9)}$$

This was tested by application of the integrated half-order equation; plots of the kinetic data as $(A_t - A_\infty)^{1/2}$ versus time give a straight line as depicted in Figure II-6. The slope of the half-order plot is a function of the concentration of the excess bromobenzyl chromium reagent. A plot of ln k_{obsd} vs ln $[4\text{-}BrC_6H_4CH_2CrL(H_2O)^{2+}]$ has a slope of 1.5, implying a kinetic order of the reaction with respect to organochromium complex concentration of 3/2. The plot of k_{obsd} vs $[4\text{-}BrC_6H_4CH_2CrL(H_2O)^{2+}]^{3/2}$, shown in Figure II-7, defines a straight line through the origin; its slope gives the second-order rate constant $k_{10} = 18.3$ M^{-1} s^{-1}, as defined by eq II-10.

$$\frac{-d[4\text{-}BrC_6H_4CH_2CrL(H_2O)^{2+}]}{dt} = k_{10}[I_2]^{1/2}[4\text{-}BrC_6H_4CH_2CrL(H_2O)^{2+}]^{3/2} \quad \text{(II-10)}$$

The chain mechanism proposed to account for the kinetic data is the following (with p-$BrC_6H_4CH_2CrL(H_2O)^{2+}$ = $RCrL^{2+}$):

$$RCrL^{2+} + I_2 \longrightarrow RCrL^{3+} + I_2^{\cdot -} \quad \text{(II-11)}$$

$$RCrL^{3+} \longrightarrow R^{\cdot} + CrL^{3+} \quad \text{(II-12)}$$

$$R^{\cdot} + I_2 + I^- \longrightarrow RI + I_2^{\cdot -} \quad \text{(II-13)}$$

$$I_2^{\cdot -} + RCrL^{2+} \longrightarrow RCrL^{3+} + 2I^- \quad \text{(II-14)}$$

$$2I_2^{\cdot -} \longrightarrow I_3^- + I^- \quad \text{(II-15)}$$

The resulting net reaction, assuming that the kinetic chain is long, is:

$$RCrL^{2+} + I_2 \longrightarrow RI + CrL^{3+} + I^- \quad \text{(II-16)}$$

With the steady-state approximation for the concentration of $I_2^{\cdot -}$ and the aralkyl radical, the rate expression associated with the mechanism given in eq II-11 to II-15 is the following:

$$-d[RCrL^{2+}]/dt = k_{14}(k_{11}/k_{15})^{1/2}\ [RCrL^{2+}]^{3/2}[I_2]^{1/2} \qquad \text{(II-17)}$$

The predominant organic product of the reaction was determined to be RI by the method herein previously described, in which the reformation of $RCrL^{2+}$ was observed upon addition of the chromium(II) macrocycle. Further confirmation came from the observed absorbance change at 352 nm, which was consistent with the formation of RI in eq II-13, and not (for example) ROH from a reaction such as $R^{\cdot} + I_2 + H_2O \longrightarrow ROH + H^+ + I_2^{\cdot -}$.

The unique aspects of the mechanism are the oxidatively induced homolysis and the consequent participation of a chromium(IV) macrocycle in a kinetic chain. To our knowledge this is the first kinetically characterized reaction of RM in which the RM^+ species is a chain-carrying intermediate and homolysis of a transition metal-carbon bond is involved in a chain propagation process. Also, it should be noted that the mild oxidant I_2 reacts just sufficiently to initiate the kinetic chain (eq II-11), and the much stronger oxidant $I_2^{\cdot -}$ is required to cause chain propagation (eq II-14).

Exploratory experiments were conducted on the reactions between iodine and other benzylchromium macrocycles and on two secondary alkyl complexes. Fractional order kinetic behavior was also observed for R = $PhCH_2$, $4\text{-}CH_3C_6H_4CH_2$, $2\text{-}C_3H_7$, and $2\text{-}C_4H_9$. We surmise that each of these reactions also proceeds by a chain mechanism, most likely as in eq II-11 to II-15. Detailed measurements were not conducted in any of these cases, however.

One notes the facility of the oxidation of $4\text{-}BrC_6H_4CH_2CrL(H_2O)^{2+}$ to the corresponding Cr(IV) complex, as shown in eq II-11. Independent studies show that $RCrL(H_2O)^{2+}$ complexes, with R = aralkyl and secondary alkyl, are readily oxidized by various kinds of weak oxidants (e.g., Fe^{3+}, $ABTS^{\cdot-}$,[20] and $Co^{III}(tetraeneN_4^+)$. These studies will be reported elsewhere.[21]

Bimolecular Electrophilic Substitution Reaction between $4\text{-}BrC_6H_4CH_2CrL(H_2O)^{2+}$ and Iodine. All indications of a chain reaction disappear when the reaction is conducted under different concentration conditions. Evidently a new pathway becomes important. This occurs when the bromobenzyl chromium complex is used as the limiting reagent at sufficiently low concentrations ($\leq 10^{-5}$ M). Under these conditions the rate law appears to be first-order with respect to each reagent. The two pathways operate in parallel, and the complete rate law is

$$-d[RCrL^{2+}]/dt = k_{I_2}[I_2][RCrL^{2+}] + k_{10}[I_2]^{1/2}[RCrL^{2+}]^{3/2} \qquad \text{(II-18)}$$

The relative importance of the two terms is governed mainly by the concentration of the organochromium complex. Experiments to evaluate the k_{I_2} term were conducted in the following concentration ranges: $[RCrL^{2+}]_o = 1.9 \times 10^{-5}$ and $[I_2] = (0.33 - 1.1) \times 10^{-3}$ M. The kinetic data fit fairly well to pseudo-first-order kinetics, but not perfectly, since the fractional-order term is not entirely negligible. The value of k_{I_2} was estimated from the iodine variation and has the value of 9.5 M^{-1}

s^{-1}. The product analysis shows that RI is the only organic product both in the absence and in the presence of O_2. This result confirms the nature of the observed bimolecular process being an electrophilic substitution. The relative importance of the k_{10} term in eq II-18 increases as the chromium concentration increases. At high ($> 10^{-4}$ M) concentrations the chain pathway becomes predominant.

It is noted that the complexes with primary alkyl groups behave differently toward iodine compared to those with aralkyl and secondary alkyl groups. This difference is related to the ease of oxidation of a given class of these complexes and by the different stabilities of the corresponding free radicals. Aralkyl and secondary alkyl groups are more electron donating than primary alkyl groups, resulting in more oxidizable organochromium complexes. Also, the greater stability of secondary and aralkyl radicals compared to primary alkyls makes the homolysis of the organochromium(IV) macrocycle (eq II-12) occur more readily. Both of these factors facilitate the chain process for the secondary alkyl and aralkyl chromium macrocycles, and disfavor that for the primary alkyl complexes.

Table II-1. Crystallographic Data for $[4\text{-}BrC_6H_4CH_2CrL(H_2O)](ClO_4)_2 \cdot THF$

Formula	$CrBrCl_2O_{10}N_4C_{22}H_{42}$
Formula weight	725.41
Space group	$P2_1/c$ (no. 14)
a, Å	11.683(3)
b, Å	8.816(3)
c, Å	29.959(8)
β, °	96.29(1)
V, $Å^3$	3067(3)
Z	4
d_{calc}, g/cm^3	1.571
Crystal size, mm	0.30 x 0.14 x 0.13
μ (MoK_α), cm^{-1}	18.84
Data collection instrument	Enraf-Nonius CAD4
Radiation (monochromated in incident beam)	MoK_α (λ = 0.71073 Å)
Orientation reflections, number, range (2Θ)	25, 14° < 2Θ < 32°
Temperature, °C	22 ± 1
Scan method	Θ - 2Θ
Data collection range, 2Θ deg	0 - 45
No. of unique data, total:	4018
with $F_o^2 > 2.5\sigma(F_o^2)$:	1293
Number of parameters refined	163
Trans. factors, max, min (psi-scans)	1.00, 0.93
R[a]	0.0806
R_w[b]	0.0943
Quality-of-fit indicator[c]	1.66
Largest shift/esd, final cycle	0.15
Largest peak, $e/Å^3$	0.69

[a] $R = \Sigma||F_o| - |F_c||/\Sigma|F_o|$.

[b] $R_w = [\Sigma w(|F_o| - |F_c|)^2/\Sigma w|F_o|^2]^{1/2}$; $w = 1/[\sigma^2(|F_o|) + 0.001|F_o|^2]$.

[c] Quality-of-fit = $[\Sigma w(|F_o| - |F_c|)^2/(N_{obs} - N_{parameters})]^{1/2}$.

Table II-2. Bond Distances (Å)

Atom 1	Atom 2	Distance	Atom 1	Atom 2	Distance
Cr	O(1)	2.13(1)	C(3)	C(4)	1.48(3)
Cr	N(1)	2.11(2)	C(5)	C(6)	1.52(3)
Cr	N(2)	2.08(2)	C(6)	C(7)	1.56(3)
Cr	N(3)	2.12(2)	C(8)	C(9)	1.44(4)
Cr	N(4)	2.08(2)	C(9)	C(10)	1.60(5)
Cr	C(1)	2.14(2)	C(11)	C(12)	1.56(4)
Br	C(24)	1.89(1)	C(21)	C(22)	1.39(2)
N(1)	C(2)	1.52(3)	C(21)	C(26)	1.39(2)
N(1)	C(12)	1.45(3)	C(22)	C(23)	1.40(1)
N(2)	C(4)	1.50(3)	C(23)	C(24)	1.39(2)
N(2)	C(5)	1.45(3)	C(24)	C(25)	1.39(2)
N(3)	C(7)	1.36(3)	C(25)	C(26)	1.39(1)
N(3)	C(8)	1.53(3)	O(10)	C(31)	1.43(3)
N(4)	C(10)	1.24(5)	O(10)	C(34)	1.45(3)
N(4)	C(11)	1.82(4)	C(31)	C(32)	1.46(4)
C(1)	C(21)	1.48(2)	C(32)	C(33)	1.43(5)
C(2)	C(3)	1.50(3)	C(33)	C(34)	1.43(5)

Numbers in parentheses are estimated standard deviations in the least significant digits.

Table II-3. Bond Angles (deg)

Atom 1	Atom 2	Atom 3	Angle	Atom 1	Atom 2	Atom 3	Angle
O(1)	Cr	N(1)	90.6(6)	Cr	N(4)	C(10)	125.(2)
O(1)	Cr	N(2)	87.7(5)	Cr	N(4)	C(11)	106.(1)
O(1)	Cr	N(3)	87.9(6)	C(10)	N(4)	C(11)	87.(2)
O(1)	Cr	N(4)	83.1(7)	Cr	C(1)	C(21)	123.(1)
O(1)	Cr	C(1)	178.0(6)	N(1)	C(2)	C(3)	112.(2)
N(1)	Cr	N(2)	95.4(7)	C(2)	C(3)	C(4)	113.(2)
N(1)	Cr	N(3)	168.9(7)	N(2)	C(4)	C(3)	117.(2)
N(1)	Cr	N(4)	82.7(7)	N(2)	C(5)	C(6)	114(2)
N(1)	Cr	C(1)	88.7(6)	C(5)	C(6)	C(7)	115(2)
N(2)	Cr	N(3)	95.5(8)	N(3)	C(7)	C(6)	111(2)
N(2)	Cr	N(4)	170.6(8)	N(3)	C(8)	C(9)	113(2)
N(2)	Cr	C(1)	90.4(8)	C(8)	C(9)	C(10)	133(3)
N(3)	Cr	N(4)	86.2(8)	N(4)	C(10)	C(9)	92(3)
N(3)	Cr	C(1)	93.1(7)	N(4)	C(11)	C(12)	96(2)
N(4)	Cr	C(1)	98.7(8)	N(1)	C(12)	C(11)	107(2)

Table II-3. (continued)

Cr	N(1)	C(2)	119(1)	C(1)	C(21)	C(22)	122(1)
Cr	N(1)	C(12)	112(1)	C(1)	C(21)	C(26)	118(1)
C(2)	N(1)	C(12)	110(2)	Br	C(24)	C(23)	120(1)
Cr	N(2)	C(4)	115(1)	Br	C(24)	C(25)	120.0(9)
Cr	N(2)	C(5)	115(1)	C(31)	O(10)	C(34)	109(2)
C(4)	N(2)	C(5)	109(2)	O(10)	C(31)	C(32)	103(2)
Cr	N(3)	C(7)	123(2)	C(31)	C(32)	C(33)	106(3)
Cr	N(3)	C(8)	112(1)	C(32)	C(33)	C(34)	109(3)
C(7)	N(3)	C(8)	109(2)	O(10)	C(34)	C(33)	105(3)

Numbers in parentheses are estimated standard deviations in the least significant digits.

Table II-4. Second-Order Rate Constants for the Electrophilic Cleavage of Chromium-Carbon Bonds of $RCr([15]aneN_4)H_2O^{2+}$ by Iodine[a]

R	$k/M^{-1}\ s^{-1}$
CH_3	4.7×10^3
C_2H_5	8.1×10^1
$n\text{-}C_3H_7$	1.2×10^1
$n\text{-}C_4H_9$	8.9×10^0
$4\text{-}BrC_6H_4CH_2$	(9.5×10^0)[b]

[a]In aqueous solution at 25.0 °C; ionic strength 0.2 M ($HClO_4$ + $NaClO_4$). $[H^+]$ = 0.010 M.

[b]Electrophilic pathway only (see text).

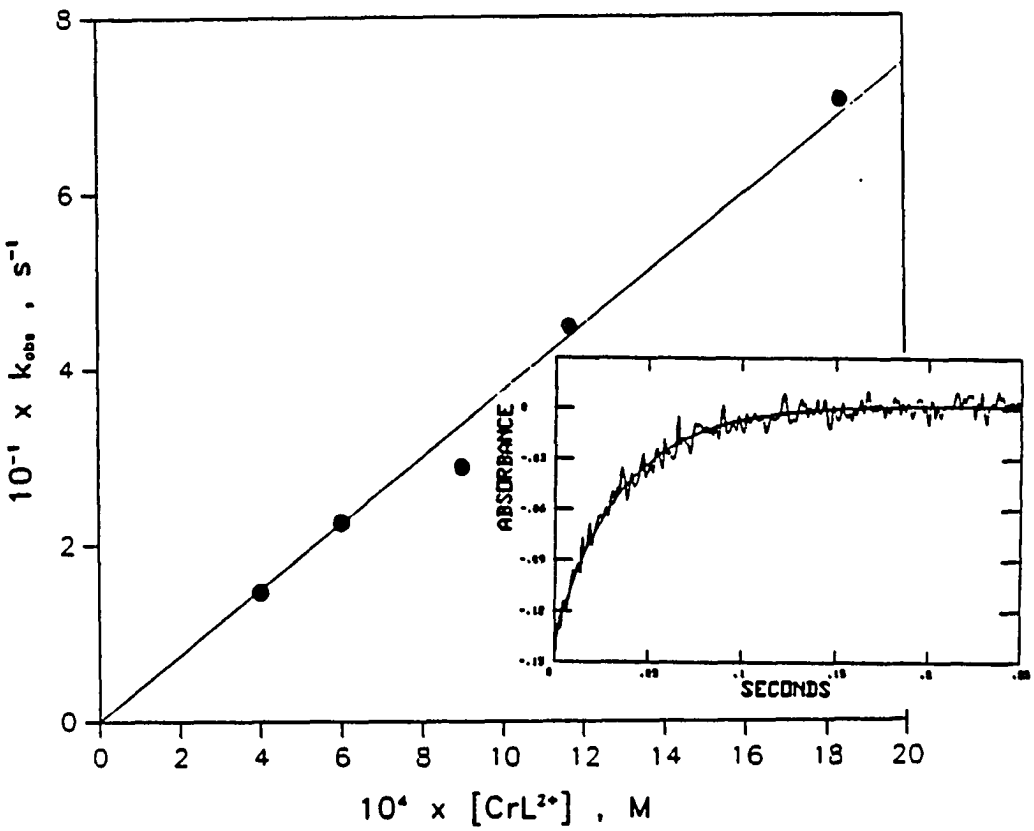

Figure II-1. Plot for the reaction of $CrL(H_2O)^{2+}$ with $4\text{-}BrC_6H_4CH_2Br$ showing the variation of the pseudo-first-order rate constant k_{obsd} with the concentration of the chromium(II) macrocycle. The inset shows a stopped-flow kinetic trace for a run with $[CrL^{2+}]_o = 9.0 \times 10^{-4}$ M and [RBr] = 8.8×10^{-6} M

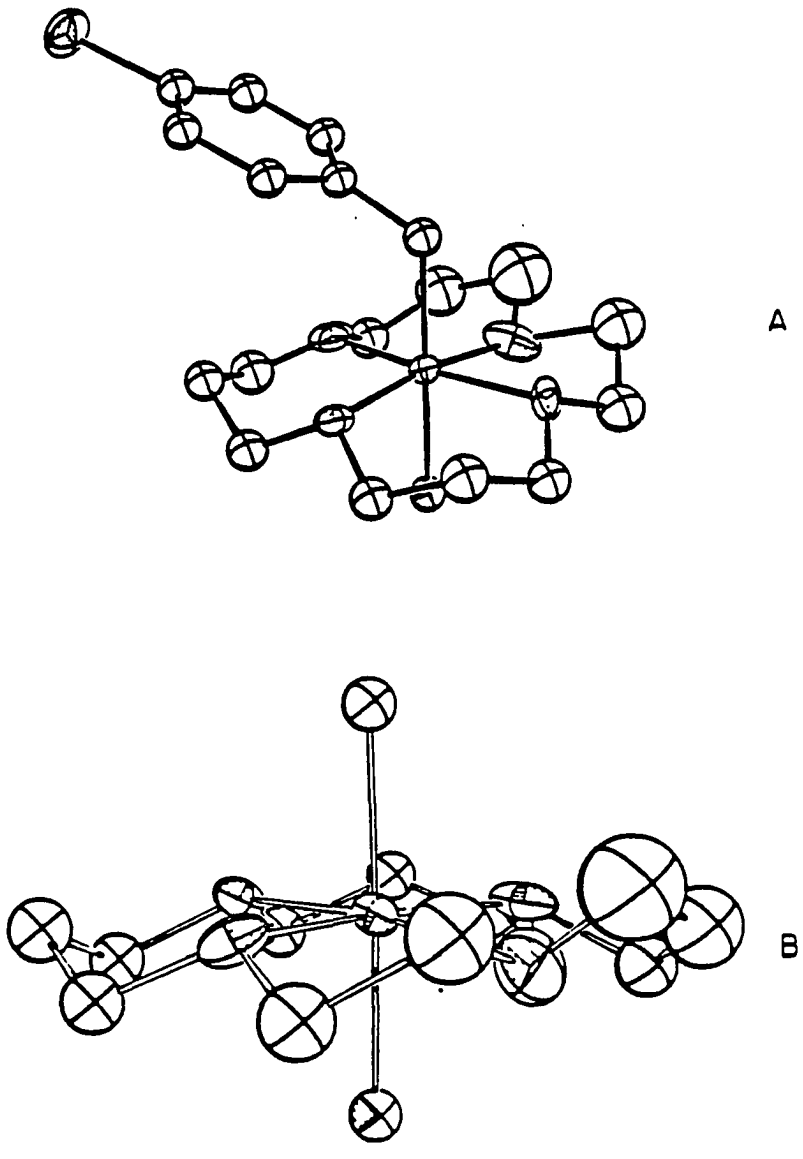

Figure II-2. ORTEP diagram of the bromobenzyl chromium macrocycle showing (a) the molecular structure of the cation and (b) the primary coordination shell of the chromium, with emphasis of the distinction between sides A (above) and B (below)

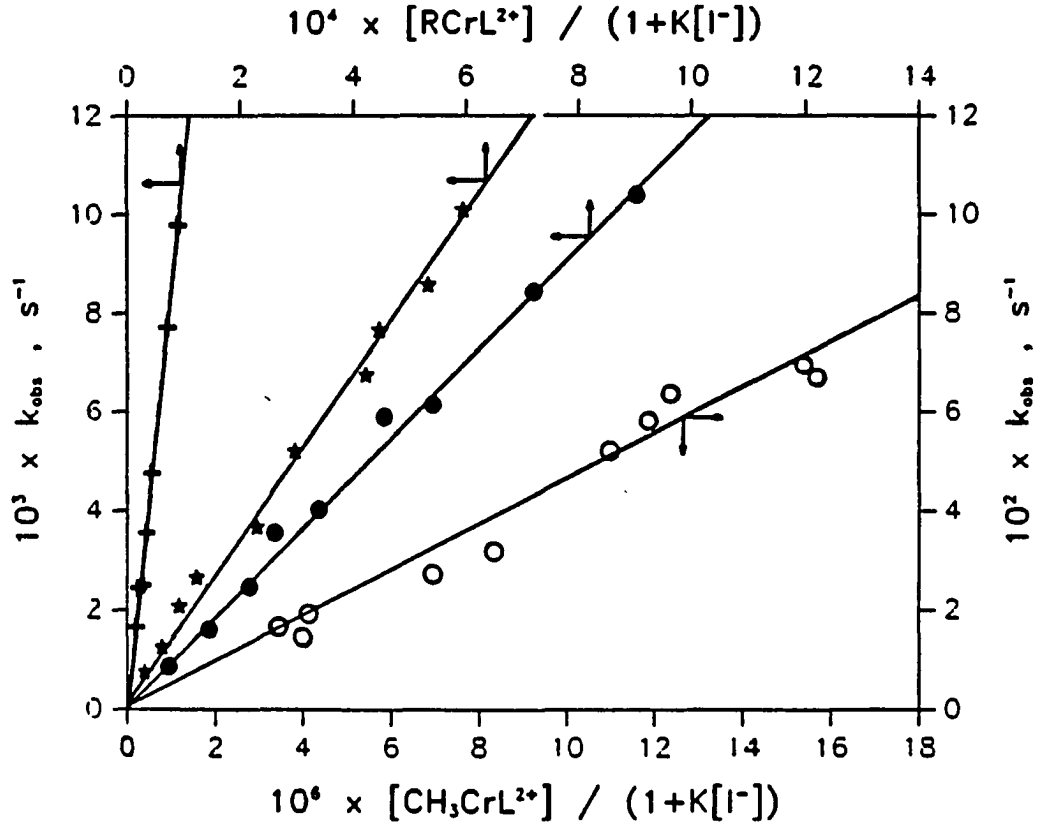

Figure II-3. Plots of kinetic data for the reaction of alkylchromium macrocycles (R = Me, 0; C_2H_5, +; 1-C_3H_7, *; 1-C_4H_9,) with iodine in acidic solution showing the effects of the variation of the alkylchromium and iodide concentrations. $[RCrL(H_2O)^{2+}]_o$ = (0.02 - 2.8) x 10^{-3} M; $[I^-]_o$ = (1.0 - 8.0) x 10^{-3} M; $[I_2]_o$ = (0.39 - 2.2) x 10^{-5} M

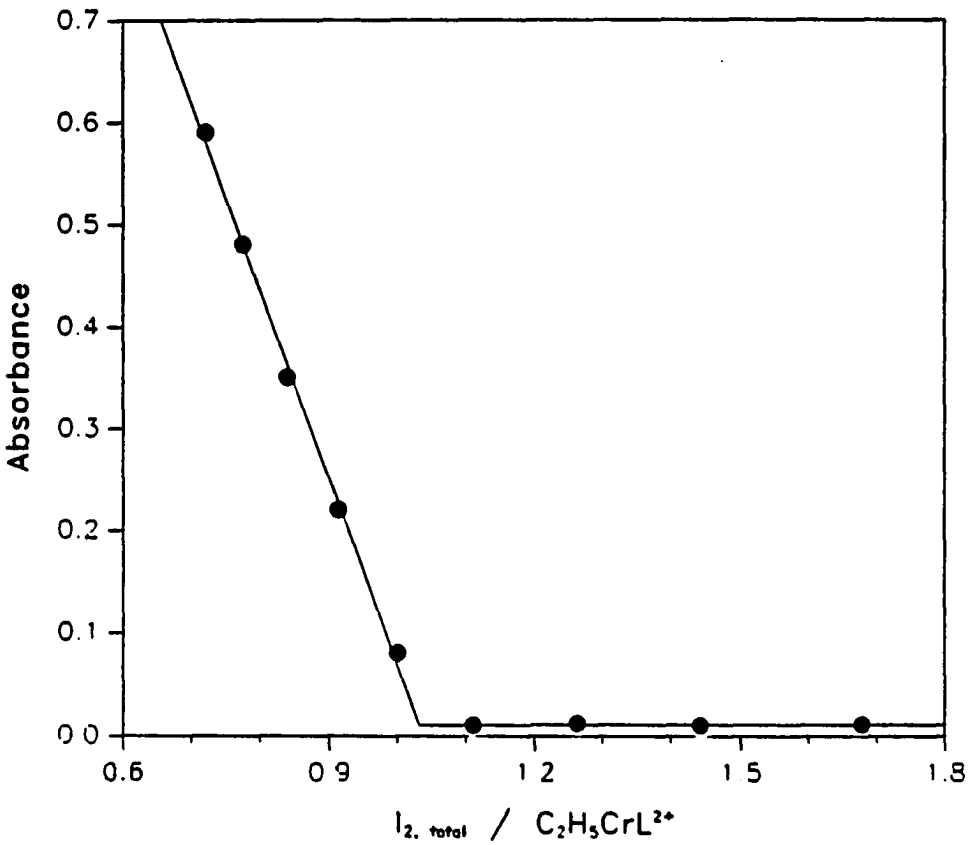

Figure II-4. The titration of the ethylchromium macrocycle with iodine showing the endpoint at a 1:1 ratio

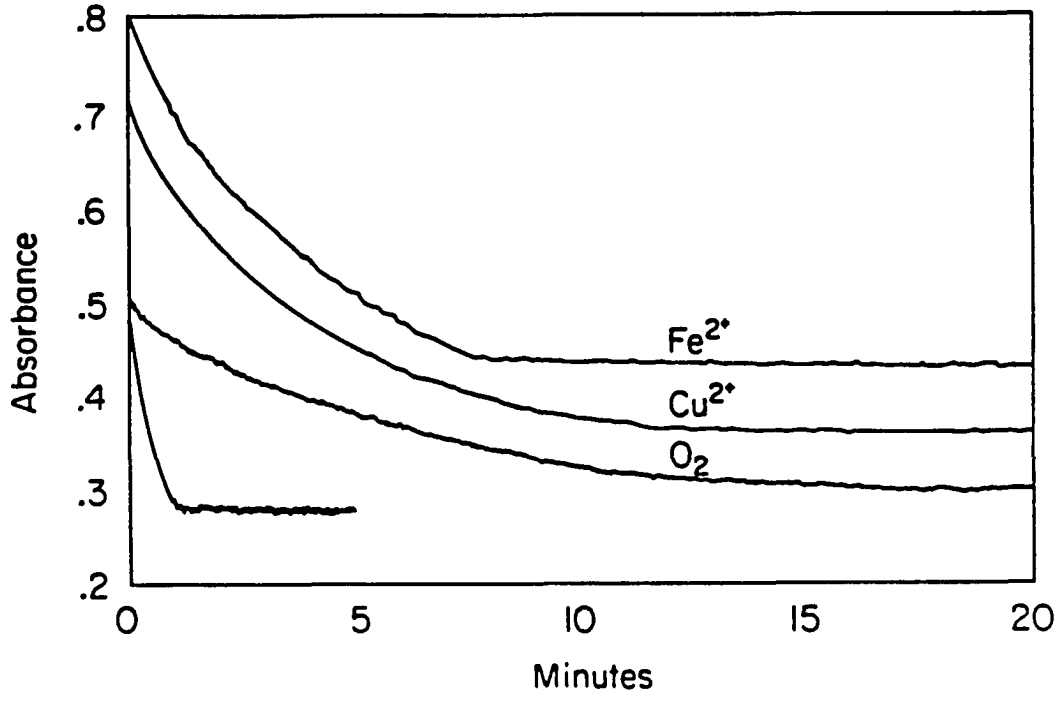

Figure II-5. Kinetic traces for the reaction of I_2 (2.0×10^{-5} M) and 4-$BrC_6H_4CH_2CrL(H_2O)^{2+}$ (1.7×10^{-4} M). The unaffected chain reaction is shown along with reactions that are inhibited by O_2 (1.3×10^{-3} M), Cu^{2+} (4.0×10^{-3} M), and Fe^{2+} (3.7×10^{-4} M). Each run contained 4.0×10^{-3} M I^-

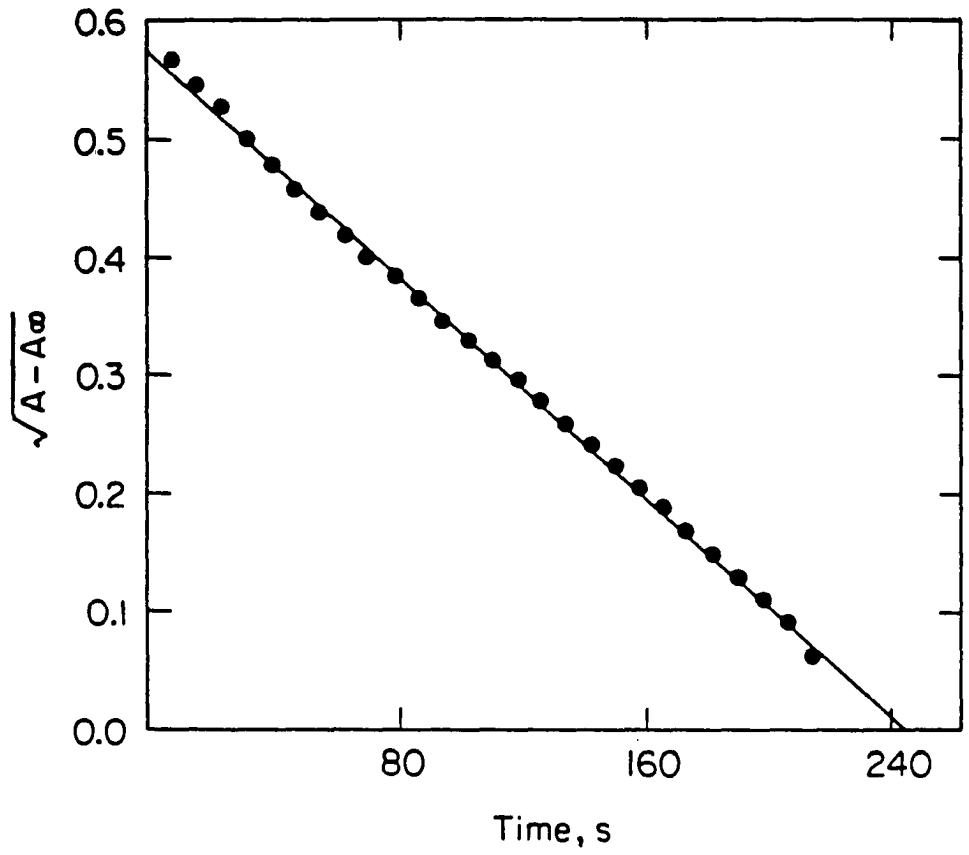

Figure II-6. Plot showing the fit to pseudo-half-order kinetics in a reaction between I_2 (2.0×10^{-5} M) and $4\text{-}BrC_6H_4CH_2CrL(H_2O)^{2+}$ (1.6×10^{-4} M) in the presence of I^- (4.0×10^{-3} M)

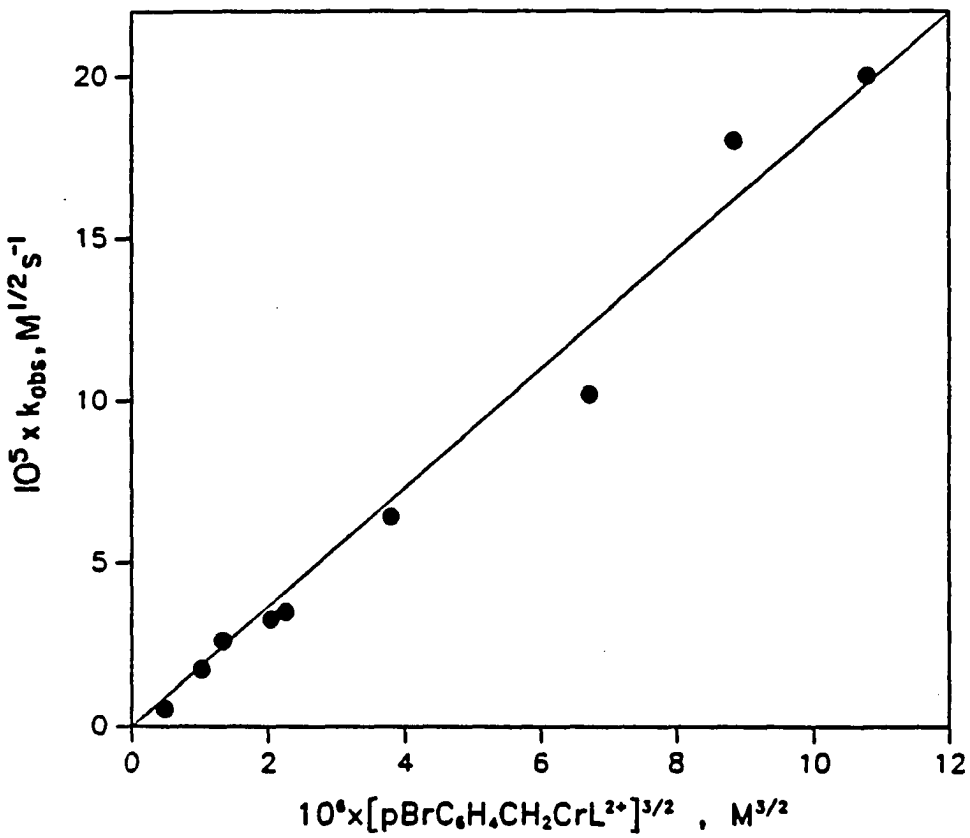

Figure II-7. Plot illustrating the variation of the half-order rate constant with the 3/2-power of the concentration of the bromobenzyl macrocycle. ($[I_2] = 2 \times 10^{-5}$ M, $[I^-] = 2 \times 10^{-3}$ M)

REFERENCES

(1) Kochi, J. K. "Organometallic Mechanisms and Catalysis", Academic Press, New York, 1978, Chapter 18.

(2) (a) Espenson, J. H.; Williams, D. A. J. Am. Chem. Soc. 1974, 96, 1008; (b) Chang, J. C.; Espenson, J. H. Chem. Commun. 1974, 233; (c) Espenson, J. H.; Samuels, G. J. J. Organomet. Chem. 1976, 113, 143.

(3) (a) Halpern, J.; Topich, J.; Zamaraev, K. I. Inorg. Chim. Acta 1976, 20, L21; (b) Topich, J.; Halpern, J. Inorg. Chem. 1979, 18, 1339.

(4) (a) Dreos, R.; Tauzher, G.; Marsich, N.; Costa, G. J. Organomet. Chem. 1975, 92, 227; (b) Dreos-Garlatti, R.; Tauzher, G.; Costa, G. J. Organomet. Chem. 1977, 139, 179; (c) Dreos-Garlatti, R.; Tauzher, G.; Costa, G. J. Organomet. Chem. 1979, 182, 409.

(5) (a) Okamoto, T.; Goto, M.; Oka, S. Inorg. Chem. 1981, 20, 899; (b) Fukuzumi, S.; Ishikawa, K.; Tanaka, T. Chem. Lett. 1986, 1801; (c) Fanchiang, Y.-T. Organometallics 1985, 4, 1515; (d) Fukuzumi, S.; Goto, T.; Ishikawa, K.; Tanaka, T. J. Chem. Soc. Chem. Commun. 1989, 260.

(6) Toscano, P. J.; Barren, E.; Seligson, A. L. Organometallics 1989, 8, 2085.

(7) Fukuzumi, S.; Nishizawa, N.; Tanaka, T. Bull. Chem. Soc. Jpn. 1983, 56, 709.

(8) Samuels, G. J.; Espenson, J. H. Inorg. Chem. 1979, 18, 2587. [15]aneN_4 = 1,4,8,12-tetraazacyclopentadecane.

(9) Samuels, G. J.; Espenson, J. H. Inorg. Chem. 1980, 19, 233.

(10) Holah, D. G.; Fackler, J. P., Jr.; Inorg. Synth. 1969, 10, 26.

(11) Awtry, A. D.; Connick, R. E. J. Am. Chem. Soc. 1965, 87, 5026.

(12) Shi, S.; Espenson, J. H.; Bakac, A. Inorg. Chem. 1990, 29, 4318.

(13) Ogino, H.; Shoji, M.; Abe, Y.; Shimura, M.; Shimoi, M. Inorg. Chem. 1987, 26, 2592.

(14) Abe, Y.; Ogino, H. Bull. Chem. Soc. Jpn. 1989, 62, 56.

(15) Daly, J. J.; Sanz, F.; Sneeden, R. P. A.; Zeiss, H. H. J. Chem. Soc. Dalton Trans. 1973, 1497. We appreciate a referee calling this paper to our attention.

(16) Samuels, G. J. Ph.D. Thesis, Iowa State University, 1979.

(17) Rabani, J.; Pick, M.; Simic, M. J. Phys. Chem. 1974, 78, 1049.

(18) (a) Buxton, G. V.; Green, J. C. J. Chem. Soc., Faraday Trans. I 1978, 74, 697; (b) Scaiano, J. C.; Leigh, W. J.; Ferraudi, G. Can. J. Chem. 1984, 62, 2355.

(19) Laurence, G. S.; Thornton, A. J. J. Chem. Soc., Dalton Trans. 1974, 1142.

(20) $ABTS^{2-}$ = 2,2'-azino-bis(3-ethylbenzthiazoline-6-sulfonate ion.

(21) Shi, S.; Bakac, A.; Espenson, J.H. (Submitted for publication), or see Part IV of this thesis.

PART III. REACTIVITY OF ORGANOCHROMIUM COMPLEXES TOWARD INORGANIC RADICALS. A PULSE RADIOLYSIS STUDY

INTRODUCTION

In a previous paper[1] of this series we discovered a chain reaction between organochromium(III) macrocyclic complexes $RCrL(H_2O)^{2+}$ and iodine where an oxidation step of $RCrL(H_2O)^{2+}$ by a diiodide radical anion $I_2^{\cdot -}$ served as one of the chain propagation steps.

$$RCrL(H_2O)^{2+} + I_2^{\cdot -} \longrightarrow RCrL(H_2O)^{3+} + 2I^- \qquad \text{(III-1)}$$

This study seeks independent evidence of the oxidation of $RCrL(H_2O)^{2+}$ by dihalogen radical anions. It concerns the rate of the oxidation as well as the reaction mechanism.

EXPERIMENTAL SECTION

Reagents. Organochromium(III) complexes were prepared according to the known methods.[2,3] The concentrations of various organochromium(III) complexes were measured spectrophotometrically.[1-3] Sodium halides and sodium thiocyanate solutions were prepared from commercial A.R. grade solids and triply distilled water. All solutions were deaerated and saturated with N_2O for the purpose of pulse radiolysis.

Pulse Radiolysis. The oxidizing reagents $X_2^{\cdot -}$ (X = I, Br, SCN) were generated from the O_2-free, N_2O-saturated aqueous solution of sodium halides or sodium thiocyanate.[4]

The pertinent reactions are as follows,

$$H_2O + e^- \text{ (pulse)} \longrightarrow e_{aq}^-,\ HO\cdot,\ H\cdot,\ H^+,\ H_2O_2 \qquad \text{(III-2)}$$

$$N_2O + e_{aq}^- + H^+ \longrightarrow HO\cdot + N_2 \qquad \text{(III-3)}$$

$$HO\cdot + 2X^- \longrightarrow OH^- + X_2^{\cdot -} \qquad \text{(III-4)}$$

$$X_2^{\cdot -} + RCrL(H_2O)^{2+} \longrightarrow 2X^- + RCrL(H_2O)^{3+} \qquad \text{(III-5)}$$

The acidity of 10^{-4} M was used so that e_{aq}^- reacts as in eq III-3, not with H_3O^+. An ionic strength of 0.1 M was realized by addition of $NaClO_4$. No thermal reaction was found between N_2O and organochromium(III) complexes. Pulse radiolysis experiments were performed at Argonne National Laboratory with an electron beam of 15-MeV and 4-ns pulse length. The reaction were followed by monitoring the disappearance of $X_2^{\cdot -}$ at various wave lengths (e.g., 340, 370, 400, 475

nm).[4-8] A 1-cm or a 2-cm cell was used depending on the concentration of radical anions and organochromium complexes to obtain a sizable change of optical density and at the same time minimize the background absorbance. Pseudo-first-order rate constants were calculated from the observed kinetic traces by using a nonlinear least-squares data fitting program.

RESULTS AND DISCUSSION

The reactions were conducted under conditions with concentrations of organochromium(III) complexes $RCrL(H_2O)^{2+}$ in large excess over those of oxidants $X_2^{\cdot -}$, so that the pseudo-first-order rate constant (k_{obs}) varied linearly with $[RCrL(H_2O)^{2+}]$. With the concentration of organochromium(III) complexes typically controlled at 10^{-4} ~ 10^{-3} M, the pseudo-first-order rate constants observed range from 9×10^3 to 8×10^4 s^{-1} consistent with the role $I_2^{\cdot -}$ played in the chain reaction with $RCrL(H_2O)^{2+}$.

The pseudo-first-order rate constants obtained are independent of the wavelength of observation. The influence of the second order radical self reaction is often significant only to the first several percent of kinetic data which were obtained immediately after the pulse. Generally speaking, the contribution of the radical self-reaction to the total optical absorbance change is normally small and constant and can be corrected by blank experiments conducted under identical conditions but in the absence of $RCrL(H_2O)^{2+}$. Good quality of data fitting was obtained in most of the cases. A typical plot is shown in **Figure III-1.**

A linear relationship between k_{obs} and $[RCrL(H_2O)^{2+}]$ was observed throughout the concentration range used, as depicted in **Figure III-2.** The second-order rate constants are listed in **Table III-1** along with other pertinent values.

The second-order rate constants increase as the oxidizing ability of the oxidants. But the change in rate constants for a given

$Br_2^{\cdot -}$ is much smaller than one would expect based on calculations according to Marcus theory.[9] Similarly, for a chosen radical anion, the change in the rate constants along the series of alkyl groups is also smaller than that observed with $IrCl_6^{2-}$ as an oxidant (Table III-1). When $IrCl_6^{2-}$ was used, the observed ratio of rate constant of $4\text{-}CH_3C_6H_4CH_2CrL(H_2O)^{2+}$ over that of $4\text{-}BrC_6H_4CH_2CrL(H_2O)^{2+}$ is ca. 40 whereas in $Br_2^{\cdot -}$ or $(SCN)_2^{\cdot -}$ series, the ratio is only ca. 2. More pronouncedly, in the $IrCl_6^{2-}$ series, the ratio of rate constant of $2\text{-}C_3H_7CrL(H_2O)^{2+}$ over that of $1\text{-}C_3H_7CrL(H_2O)^{2+}$ is ca. 8×10^3 whereas in the $Br_2^{\cdot -}$ and $(SCN)_2^{\cdot -}$ series is only ca. 6.

Apparently, an $X_2^{\cdot -}$ oxidant reacts quite differently with $RCrL(H_2O)^{2+}$, as compared to transition metal complexes. For example, $4\text{-}CH_3C_6H_4CH_2CrL(H_2O)^{2+}$ reacts with $IrCl_6^{2-}$ (E^o = 0.89 V[10]) and $Ru(bpy)_3^{3+}$ (E^o = 1.26 V[11]) at specific rates of 4.60×10^5 $M^{-1}s^{-1}$ [12] and 1.05×10^9 $M^{-1}s^{-1}$ [13] respectively. The observed 5×10^3 times difference in rate constants is quite consistent with what is predicted by Marcus theory based on a pure outer-sphere electron transfer mechanism. But the linearity and the typical slope of 0.5 are no longer obtainable in a plot of lnk vs. E^o (oxidants) with a series of oxidants including any $X_2^{\cdot -}$, even though the charge carried by $X_2^{\cdot -}$ is between those carried $IrCl_6^{2-}$ and $Ru(bpy)_3^{3+}$.

It is noticeable that the small changes of k along the series of alkyl group or along the series of $X_2^{\cdot -}$ can not be accounted for by the intrinsic modest response of rate constant to the driving force in the "plateau region" of a lnk vs. E^o plot, since bigger responses were observed with other oxidants (e.g., $IrCl_6^{2-}$).[12]

All these facts seem to suggest the formation of a loosely bound adduct $\{X_2\cdot^-, RCrL(H_2O)^{2+}\}$ prior to the electron transfer step.

$$X_2\cdot^- + RCrL(H_2O)^{2+} \text{ ==== } \{X_2\cdot^-, RCrL(H_2O)^{2+}\} \qquad k_6,\ k_{-6} \qquad \text{(III-6)}$$

$$\{X_2\cdot^-, RCrL(H_2O)^{2+}\} \longrightarrow 2X^- + RCrL(H_2O)^{3+} \qquad k_7 \qquad \text{(III-7)}$$

If

$$k = \frac{k_{obs}}{[RCrL(H_2O)^{2+}]} = \frac{k_6 k_7}{k_{-6} + k_7} \qquad \text{(III-8)}$$

and if k_7 is proportional to the driving force for the electron transfer step as predicted by Marcus equation,[9] the depressed response of the change in k values to the change of E^o values of X_2^- must indicate a very small ($k_6/(k_{-6} + k_7)$ value. This implies a very unstable adduct with respect to both dissociation and electron transfer.

While we can not exclude the possibility for the adduct to be an ion pairing complex, we are inclined to suggest that the adduct reflects an interaction between $X_2\cdot^-$ and the α-carbon of the alkyl group bound to chromium. This is because: (1) No indication of ion pairing was observed in the previous study when the charge of the oxidants changed from 2- ($IrCl_6^{2-}$) to 3+ (Fe^{3+}).[12] (2) As revealed in **Table III-1**, the depressed response of the change of k to the change of alkyl group in $RCrL(H_2O)^{2+}$ was observed with singly charged $X_2\cdot^-$ series whereas a much larger response was observed with doubly charged $IrCl_6^{2-}$. We believe that the interaction X_2^---$RCrL(H_2O)^{2+}$ bears an intrinsic connection with the polarizing ability of halogens. While a direct attack by $X_2\cdot^-$ at a α-carbon bound to a metal is not known, the same attack by X_2 is well

documented.[7] Perhaps the major difference between the attack by X_2 and that by $X_2^{\cdot -}$ is that the former is a two electron reagent thus the electrophilic substitution products (X^-, RX, $CrL(H_2O)^{3+}$) were formed[1] and the latter is an one electron reagent[6] hence the electron transfer products ($2X^-$, $RCrL(H_2O)^{3+}$) were formed.

Table III-1. Summary of Reduction Potentials and Rate Constants of the Oxidation of Organochromium(III) Complexes $RCrL(H_2O)^{2+}$ by Inorganic Radical Anions.

Oxidant	E^o / V	k / M^{-1} s^{-1}			
		R=4-$CH_3C_6H_4CH_2$	R=4-$BrC_6H_4CH_2$	R=2-C_3H_7	R=1-C_3H_7
$Br_2^{-\cdot}$	1.62[a]	9.8×10^7	4.8×10^7	1.8×10^8	2.7×10^7
$(SCN)_2^{-\cdot}$	1.32[b]	4.9×10^7	2.3×10^7	8.0×10^7	1.3×10^7
$I_2^{-\cdot}$	1.03[c]	8.4×10^6		3.7×10^7	
$IrCl_6^{2-}$ [e]	0.89[d]	4.60×10^5	1.29×10^4	8.54×10^4	1.01×10^1

[a]Ref.6; [b]Ref.4a, 7; [c]Ref.4a, 8; [d]Ref.10; [e]Ref.12;

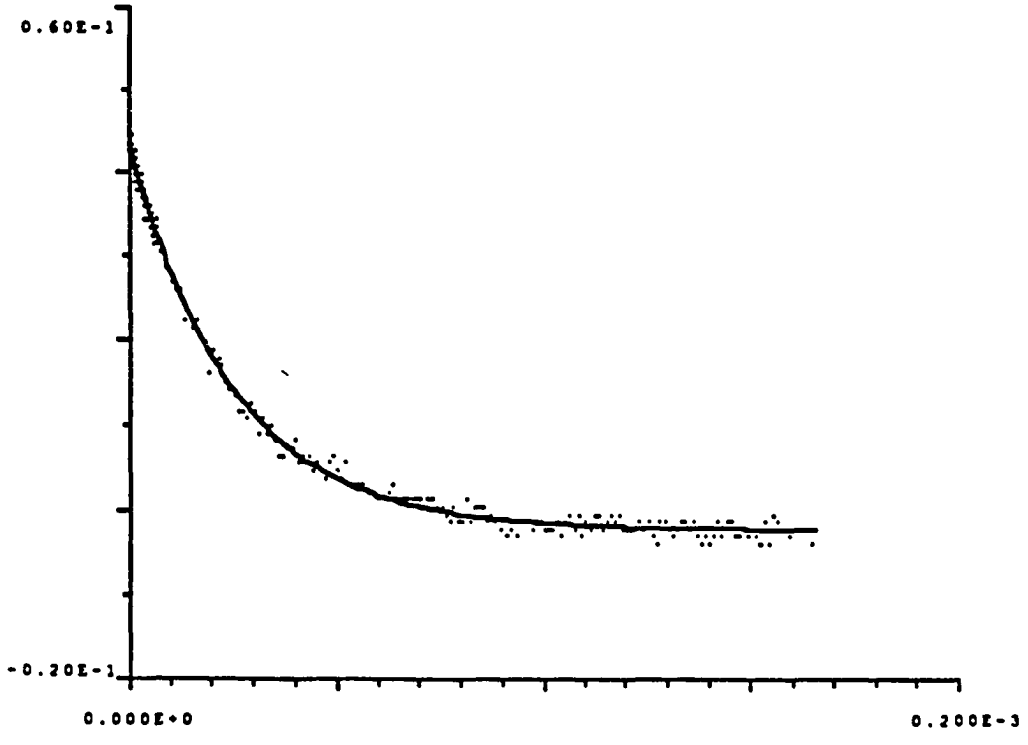

Figure III-1. An observed kinetic trace of the oxidation of $4\text{-}CH_3C_6H_4CH_2CrL(H_2O)^{2+}$ (2.5×10^{-4} M) by Br_2^- generated by pulse radiolysis. N_2O-saturated aqueous solution Monitored at λ = 400 nm. Room temperature. The solid curve was calculated from a pseudo-first-order data fitting program

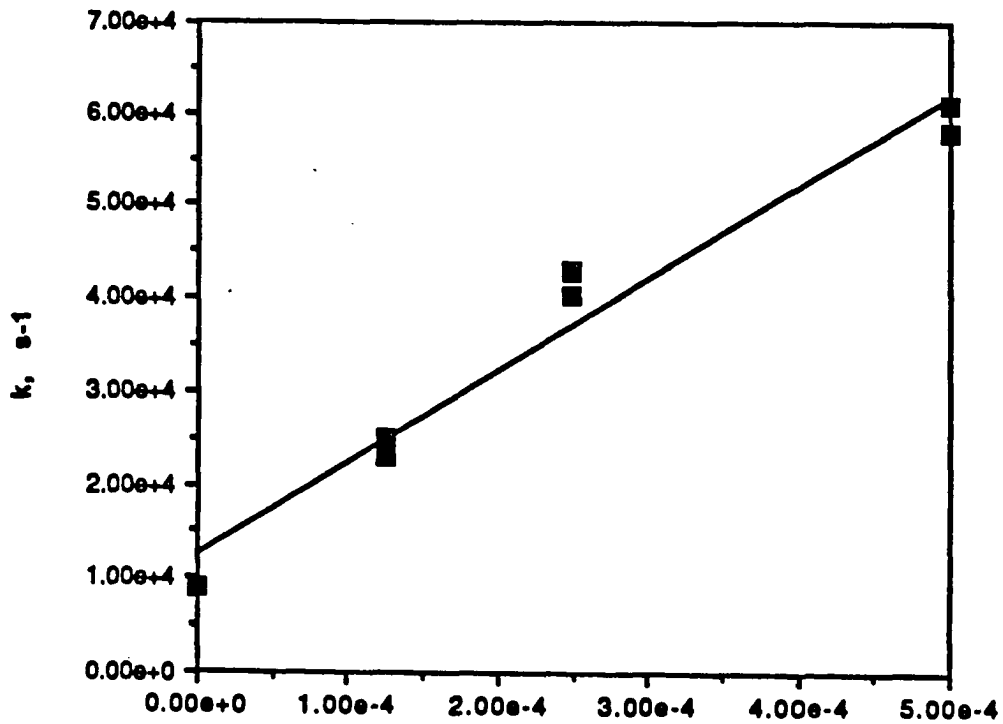

Figure III-2. A plot showing a linear relationship between the observed pseudo-first-order rate constant k_{obs} and the concentration of 4-$CH_3C_6H_4CH_2CrL(H_2O)^{2+}$ (excess) for the reaction between 4-$CH_3C_6H_4CH_2CrL(H_2O)^{2+}$ and $Br_2^{\cdot -}$

REFERENCES

(1) Shi, S.; Espenson, J. H.; Bakac, A. J. Am. Chem. Soc. 1990, 112, 1841.

(2) Samuels, G. J.; Espenson, J. H. Inorg. Chem. 1979, 18, 2587.

(3) Shi, S.; Espenson, J. H.; Bakac, A. Inorg. Chem. 1990, 29, 4318.

(4) For a review, see (a) Stanbury, D.M. Adv. Inorg. Chem. 1989, 33, 69. (b) Fornier de Violet Rev. Chem. Intermediates 1981, 4, 121.

(5) (a) Teinin, A.; Hayon, E.; J. Am. Chem. Soc. 1975, 97, 1716. (b) Fornier de Violet, P.; Bonneau, R.; Joussot-Dubien, J. Chem. Phys. Lett. 1973, 5, 61. (c) Fornier de Violet, P.; Bonneau, R.; Joussot-Dubien, J. J. Chim. Phys. 1973, 70, 1404.

(6) (a) Laurence, G. S.; Thornton, A. T. J. Chem. Soc., Dalton Trans. 1973, 1637. (b) Schwarz, H. A.; Dodson, R. W. J. Phys. Chem. 1984, 88, 3643.

(7) (a) Nord, C.; Pederson, B.; Farver, O. Inorg. Chem. 1978, 17, 2233. (b) Nord, C.; Pederson, B.; Floryan-lovberg, E.; Pagsberg, P. Inorg. Chem. 1982, 21, 2327.

(8) Haim, A.; Taube, H. J. Amer. Chem. Soc. 1963, 85, 495.

(9) Marcus, R. A. J. Chem. Phys. 1965, 43, 679, 2654.

(10) Margerum, D. W.; Chellappa, K. L.; Bossu, F. P.; Burce, G. L. J. Am. Chem. 1975, 97, 6894.

(11) Sutin, N.; Creutz, C. Adv. Chem. Ser. 1978, No. 168, 1.

(12) Shi, S.; Bakac, A.; Espenson, J. H. (to be published), or see Part IV of this thesis.

(13) Steffan, C. Ph.D. thesis, Iowa State University, 1990.

(14) (a) Espenson, J. H.; Williams, D. A. J. Am. Chem. Soc. 1974, 96, 1008. (b) Chang, J. C.; Espenson, J. H. J. Chem. Soc., Chem. Commun. 1974, 233. (c) Espenson, J. H.; Samuel, G. J. J. Organomet. Chem. 1976, 113, 143.

PART IV. REVERSIBLE ELECTRON TRANSFER REACTIONS OF ORGANOCHROMIUM(III) MACROCYCLIC COMPLEXES

INTRODUCTION

Transition metal complexes containing metal-carbon bonds are known to participate in various oxidation mechanisms.[1] Unlike inorganic complexes, where the metal may exist in two or more stable oxidation states (particularly with well-chosen ligand sets), an one electron oxidation of the organometal (RM) yields a species (RM^+) which often undergoes ready decomposition, usually by homolysis ($RM^+ \rightarrow R^\cdot + M^+$).

The series of complexes $(H_2O)_5CrR^{2+}$ is oxidized by strong one-electron acceptors such as $Ni(cyclam)^{3+}$, E^o 1.0 V;[2] $Ru(bpy)_3^{3+}$, E^o 1.27 V; and NO^+, E^o 1.51 V.[2-4] Each of these reactions yields $(H_2O)_5CrR^{3+}$ as a transient. Although not (yet) detected directly, the presence of this transient is indicated by the formation of $Cr(H_2O)_6^{3+}$, by products derived from $R^\cdot$, and by stoichiometric factors that become incorporated into some rate constants. Interestingly, the much milder[5,6] oxidant Br_2 reacts with $(H_2O)_5CrR^{2+}$ by a straightforward electrophilic mechanism (S_E2),[7] and not by an oxidative process.

The mechanism of chromium-carbon bond cleavage by halogens changes, however, when this organometal is incorporated into a macrocyclic ligand. Even with a mild acceptor like I_2,[8] the complexes SSRS-$RCrL(H_2O)^{2+}$ (R = $ArCH_2$, 2°-alkyl; L = 1,4,8,12-tetraazacyclopentadecane) react by a radical chain mechanism in which the initiating step is electron transfer (eq IV-1).[9] Presumably the macrocycle, a much more electron-donating ligand, lowers the potential such that its organochromium complexes are more readily oxidized.

$$RCrL(H_2O)^{2+} + I_2 \longrightarrow RCrL(H_2O)^{3+} + I_2^{\cdot -} \qquad (IV\text{-}1)$$

It thus became of interest to examine the reactions with other species capable of oxidizing the $RCrL(H_2O)^{2+}$ complexes. One problem in gaining a fundamental understanding of such reactions is the lack of information about the RM^+/RM reduction potential and self-exchange rate (SER). Kinetic studies can provide an approach to both issues by relating a given cross reaction to the reduction potential by means of the Marcus-Hush theory. The approach we suggest is to use two oxidants for a given $RCrL(H_2O)^{2+}$ complex, from which the E^o and SER of the $RCrL^{3+/2+}$ couple can be estimated.

We have first chosen to examine the oxidation of one organometal, $4\text{-}BrC_6H_4CH_2CrL(H_2O)^{2+}$, by a series of electron acceptors: $ABTS^{\cdot -}$ (A^-), $IrCl_6^{2-}$, and $Fe(H_2O)_6^{3+}$. This enables the electron-transfer mechanism to be considered in the absence of E^o and the SER for $RCrL(H_2O)^{2+}$. Then two oxidants were chosen such that one is weak ($ABTS^{\cdot -/2-}$, E^o = 0.43 V), the other strong ($E^o_{IrCl_6}$ = 0.89 V). With the weak oxidant, the retarding effect of $ABTS^{2-}$ can be tested experimentally, which can in turn provide an additional rate constant ratio from which a lower limit can be set for the kinetic lifetime of the purported product, $RCrL(H_2O)^{3+}$. An upper limit of the lifetime of $RCrL(H_2O)^{3+}$ can then be set by its reaction rate with the strong oxidant. A combination of these limits allows an estimate of the E^o value and SER constant of the $RCrL(H_2O)^{3+/2+}$ couple.

As far as the oxidation processes themselves are concerned, we ask the following questions. How are the $RCrL(H_2O)^{2+}$ species oxidized? What are the decomposition products of $RCrL(H_2O)^{3+}$? What is the rate of its decomposition, and how does it compare to that of its 2+ parent? What role do the R groups play? What is the structure of transition state of the electron-transfer process? We have focused with $ABTS^{\cdot -}$ primarily on $4\text{-}BrC_6H_4CH_2CrL(H_2O)^{2+}$, whose reaction with iodine was the one most carefully studied.[9] With $IrCl_6^{2-}$ as oxidant, an entire range of alkyl and aralkyl groups was explored.

EXPERIMENTAL SECTION

Materials. The organochromium macrocyclic complexes $RCrL(H_2O)^{2+}$ with R = C_2H_5, 1-C_3H_7, 2-C_4H_9, 4-$CH_3C_6H_4CH_2$, $C_6H_5CH_2$, and 4-$BrC_6H_4CH_2$ were obtained from the reaction of $(H_2O)_2CrL^{2+}$ and RX and purified by ion exchange on Sephadex C-25.[9,10] The following molar absorptivities were determined, which were then used to calculate the concentrations of the complexes for the kinetic studies. For R = 1-C_3H_7, λ_{max}/nm (ε/L mol^{-1} cm^{-1}) = 265(3.44×10^3) and 383(4.65×10^2); 2-C_3H_7, 287(3.28×10^3) and 396(5.50×10^2); 2-C_4H_9, 292(3.31×10^3) and 390(5.60×10^2); 4-$CH_3C_6H_4CH_2$, 243(6.72×10^3), 281(7.65×10^3), and 302(6.78×10^3); $C_6H_5CH_2$, 273(7.92×10^3), 297(7.47×10^3), and 353(2.17×10^3); 4-$BrC_6H_4CH_2$, 247(1.07×10^4), 281(9.82×10^3), 303(8.83×10^3),and 361(2.40×10^3).[9-11]

The compound $(NH_4)_2$ABTS (α,α'-azino-bis(3-ethylbenzthiazoline-6-sulfonic acid)diammonium salt, see structural formula) was purchased (Aldrich); it was converted to the radical ion ABTS$^{\cdot-}$ by oxidation with an equivalent amount of ceric ammonium sulfate. The radical ABTS$^{\cdot-}$

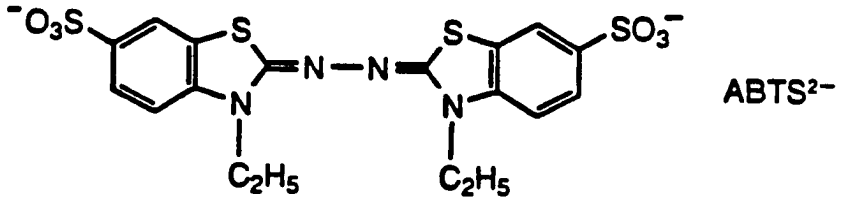

$ABTS^{2-}$

persists in solutions for several weeks; it is characterized by a number of UV-visible absorption bands of which the peak at 650 nm (ε 1.01×10^4 L mol^{-1} cm^{-1}) was used to follow its reactions. Other reagents were obtained from standard sources and used as received.

Techniques, Kinetics. Kinetic measurements were conducted at 25 °C with $[H^+] = 1.0 \times 10^{-2}$ M (perchloric acid) and ionic strength 0.20 M (maintained with sodium perchlorate). Air-free conditions were maintained in all experiments by a blanket of argon. Depending on the rate constant for a given reaction, kinetic data were collected with a Durrum-Dionex stopped flow spectrophotometer or a conventional spectrophotometer, a modified Cary 14. Both instruments are controlled by the On Line Instrument Systems data acquisition and analysis software. Kinetic data were fit to the equation $D_t = D_\infty + (D_0-D_\infty)\exp(-k_\psi t)$ by a nonlinear least-squares method.

RESULTS AND DISCUSSION

Reactions of $4\text{-BrC}_6\text{H}_4\text{CH}_2\text{CrL}(\text{H}_2\text{O})^{2+}$ with $\text{ABTS}^{\cdot-}$. The $\text{ABTS}^{\cdot-}$ radical functions as an oxidizing agent with $E^o = 0.43$ V.[12] We suggest that, following the electron transfer step, the species $\text{RCrL}(\text{H}_2\text{O})^{3+}$ undergoes homolysis, with the resulting radical forming an adduct with $\text{ABTS}^{\cdot-}$ in a known reaction.[13] These reactions are shown as follows:

$$\text{RCrL}(\text{H}_2\text{O})^{2+} + \text{ABTS}^{\cdot-} \rightleftharpoons \text{RCrL}(\text{H}_2\text{O})^{3+} + \text{ABTS}^{2-} \qquad (k_2, k_{-2}) \qquad \text{(IV-2)}$$

$$\text{RCrL}(\text{H}_2\text{O})^{3+} + \text{H}_2\text{O} \longrightarrow \text{R}^{\cdot} + (\text{H}_2\text{O})_2\text{CrL}^{3+} \qquad (k_3) \qquad \text{(IV-3)}$$

$$\text{R}^{\cdot} + \text{ABTS}^{\cdot-} \longrightarrow \text{R-ABTS}^{-} \qquad (k_4)^{13} \qquad \text{(IV-4)}$$

According to this scheme, the reactions should show a stoichiometry of 2 $\text{ABTS}^{\cdot-}$: 1 $\text{RCrL}(\text{H}_2\text{O})^{2+}$. This ratio is indeed found by spectrophotometric titration as shown in **Figure IV-1.** The rate equation derived on the basis of eq IV-2 to IV-4, with the steady-state approximation for $[\text{RCrL}(\text{H}_2\text{O})^{3+}]$, is

$$\frac{-d[\text{RCrL}(\text{H}_2\text{O})^{2+}]}{dt} = \frac{k_2 k_3 [\text{ABTS}^{\cdot-}][\text{RCrL}(\text{H}_2\text{O})^{2+}]}{k_3 + k_{-2}[\text{ABTS}^{2-}]} = k_\psi [\text{RCrL}(\text{H}_2\text{O})^{2+}] \qquad \text{(IV-5)}$$

With $ABTS^{\cdot -}$ (1.2-12.0 x 10^{-5} M average conc.) in excess over $4\text{-}BrC_6H_4CrL(H_2O)^{2+}$ (2.1-5.9 x 10^{-6} M), and with no added $ABTS^{2-}$, the expression reduces to $k_\psi = k_2[ABTS^{\cdot -}]$. This is illustrated in Figure IV-2. The average value of k_2 is (1.51 ± 0.11) x 10^2 L mol^{-1} s^{-1} in six determinations. A series of seven experiments was then done with added $ABTS^{2-}$ (range of average concentrations 7.0 x 10^{-6} - 3.39 x 10^{-4} M). Values of k_ψ become smaller with increasing $[ABTS^{2-}]$, as expected from eq IV-5. A nonlinear least-squares fit to eq IV-5 affords an independent estimate of k_2 = (1.51 ± 0.10) x 10^2 L mol^{-1} s^{-1}, and the ratio k_{-2}/k_3 = (6.7 ± 0.7) x 10^3 L mol^{-1}. The effect can be displayed graphically by a rearrangement to eq IV-6, which is useful since all these experiments had $[ABTS^{\cdot -}]_{av}$ = 9.32 x 10^{-5} M. The data are shown according to eq IV-6 in Figure IV-3.

$$k_\psi = k_2[ABTS^{\cdot -}]_{av} - (k_{-2}/k_3)k_\psi[ABTS^{2-}]_{av} \qquad \text{(IV-6)}$$

Oxidations of $4\text{-}BrC_6H_4CH_2CrL(H_2O)^{2+}$ by $IrCl_6^{2-}$ and $Fe(H_2O)_6^{3+}$. The reaction with $IrCl_6^{2-}$ also proceeds with a 1:2 stoichiometry (Figure IV-1). The scheme is analogous to eq IV-2 to IV-4, except that the fate of the radical is oxidation to a mixture of alcohol and halide:[14]

$$R^{\cdot} + IrCl_6^{2-} + H_2O \longrightarrow ROH + IrCl_6^{3-} + H^+ \qquad \text{(IV-7)}$$

$$R^{\cdot} + IrCl_6^{2-} + H_2O \longrightarrow RCl + IrCl_5(H_2O)^{2-} \qquad \text{(IV-8)}$$

Kinetics experiments were done both with $[RCrL(H_2O)^{2+}] > 10\ [IrCl_6^{2-}]_o$ and with $[IrCl_6^{2-}] > 10[RCoL(H_2O)]_o$. In all, the concentration variations were $[RCrL(H_2O)^{2+}]_o = 1.55 \times 10^{-5} - 2.44 \times 10^{-4}$ M and $[IrCl_6^{2-}]_o = 5 \times 10^{-6} - 4.5 \times 10^{-3}$ M in eleven experiments. The reaction follows mixed second-order kinetics with $k = (1.29 \pm 0.18) \times 10^4$ L mol^{-1} s^{-1}, where k is defined by the rate law, $-d[RCrL(H_2O)^{2+}]/dt = -d[IrCl_6^{2-}]/2dt = k[RCrL(H_2O)^{2+}][IrCl_6^{2-}]$.

The reaction with the mild oxidant Fe^{3+} ($E^o_{Fe} = 0.745$ V)[15] has a 1:1 stoichiometry, and produces Fe^{2+} according to a test of the products with 1,10-phenanthroline. Kinetic data were obtained in 7 experiments with concentrations of $(1.6 - 8.0) \times 10^{-5}$ M Fe^{3+} and $(1.0 - 6.8) \times 10^{-4}$ M $RCrL(H_2O)^{2+}$. The second-order rate constant is 3.09 ± 0.28 L mol^{-1} s^{-1}. The reaction stoichiometry deserves a comment, in that in the sequence eq IV-2 to IV-4 (modified to include Fe^{3+} in place of $ABTS^{\bullet-}$), one expects[16] the final step to be oxidation of the benzyl radical by Fe^{3+} ($ArCH_2^{\bullet} + Fe^{3+} + H_2O \rightarrow ArCH_2OH + Fe^{2+} + H^+$). The stoichiometry indicates this does not occur. We suggest that the oxidation at these very low $[Fe^{3+}]$ is too slow to compete with radical dimerization.

Analysis of Oxidation Rates on the Basis of the Marcus Equation. Given that each oxidizing agent has a known reduction potential (E^o_{ox}) [12,15,17] and some have known self-exchange rate constant (k_{11}) [17-19], it is possible to consider the data further. First, the self-exchange rate of $ABTS^{2-/\bullet-}$ (k_{AA}) was calculated here from the cross-reaction rate constants for the reactions of $RCrL(H_2O)^{2+}$ with $ABTS^{\bullet-}$

(k_{ACr}) and $IrCl_6^{2-}$ (k_{IrCr}) and their known reduction potentials according to

$$k_{AA} = \{k_{IrIr}\exp[(F/RT)(E^{o}_{Ir}-E^{o}_{A})]\}\ (k_{ACr}/k_{IrCr})^{2} \qquad \text{(IV-9)}$$

This yields a value $k_{AA} = 2.2 \times 10^{9}$ L mol^{-1} s^{-1}, a quantity not previously reported. That this is a diffusion-controlled value, or nearly so, is consistent with there being very little molecular reorganization accompanying the redox change. With k_{AA} known we can then consider all of the cross reactions according to the simplified Marcus cross relation, $k_{12} = (k_{11}k_{22}K_{12})^{1/2}$; rearrangement yields

$$2\ln k_{12} = \ln k_{11} + \ln k_{22} + (F/RT)(E^{o}_{ox}-E^{o}_{RCr}) \qquad \text{(IV-10)}$$

This predicts that a plot of $\ln k_{12}$ versus $[\ln k_{11} + (F/RT)E^{o}_{ox}]$ will be a straight line with a slope of 0.5. In this series where a given 4-$BrC_6H_4CH_2CrL(H_2O)^{2+}$ complex was used, even though neither k_{22} nor E^{o}_{RCr} is known, it is still possible to consider the mechanism of the oxidation. The experimental data are summarized in **Table IV-1** and plotted according to eq IV-10 in **Figure IV-4**. The slope of 0.49 indicates that this family of reactions proceeds by an outer-sphere electron transfer mechanism. The intercept is -27.1, which will be considered later.

The Reduction Potential, Lifetime and Self-Exchange Rate of $RCrL(H_2O)^{3+}$. The reaction with $IrCl_6^{2-}$ was conducted with either reagent in excess. A single exponential kinetic trace was obtained throughout. The absence of a second stage, even under the concentration conditions where k_ψ was the highest observed value (57 s^{-1}), allows us to set a rough lower limit $k_3 > 60\ s^{-1}$. The same limit of k_3 should hold for the oxidation by $ABTS^{\cdot-}$ as well. Since the ratio k_{-2}/k_3 is known (6.7 x 10^3 L mol^{-1}) for $ABTS^{\cdot-}$, we can set broad limits on k_{-2}: 4 x 10^5 - 1 x 10^{10} L mol^{-1} s^{-1}, which combined with k_2 = 1.5 x 10^2 L mol^{-1} s^{-1} and E^o_A = 0.43 V affords a limit for the reduction potential of $4\text{-}BrC_6H_4CH_2CrL(H_2O)^{3+/2+}$: $0.89 > E^o_{RCr} > 0.63$ V. We therefore adopt the value $E^o_{RCr} = 0.76 \pm 0.13$ V.

With this potential, a cross-reaction rate constant k_{12} = 1.15 x 10^4 L mol^{-1} s^{-1} for $RCrL(H_2O)^{2+}$ with $IrCl_6^{2-}$, k_{IrIr} = 2.0 x 10^5 L mol^{-1} s^{-1}, and E^o_{Ir} = 0.89 V,[17] we calculate a self-exchange rate constant of ca. 4 L mol^{-1} s^{-1} for $RCrL(H_2O)^{3+/2+}$. With the range of E^o_{RCr} values, the self-exchange rate constant may be better expressed as a range: 5 x 10^{-2} < k < 7 x 10^2 L mol^{-1} s^{-1}.

The intercept in **Figure IV-4**, (-27.1) represents an experimentally measured value of $\ln k_{22} - (F/RT)E^o_{RCr}$ based on eq IV-10. The value of $\ln k_{22} - (F/RT)E^o_{RCr}$ calculated from the adopted E^o = 0.76 and k = 4 L mol^{-1} s^{-1} is ln(4)-(F/RT)(0.76) = -28.2. The two values are in reasonable agreement with each other.

Oxidation of Various $RCrL(H_2O)^{2+}$ Complexes by $IrCl_6^{2-}$. These reactions also proceed with a stoichiometry of 1 $RCrL(H_2O)^{2+}$:2 $IrCl_6^{2-}$ and a mixed second-order rate law. Kinetic data are summarized in Table IV-2. The rate constants span a factor of 2×10^6, from Me($k = 0.22$ L mol^{-1} s^{-1}) to p-xylyl (4.6×10^5 L mol^{-1} s^{-1}). Among the aralkyl complexes, there is a clear trend in reactivity in which electron-donating substituents on the benzene ring facilitate the reaction. The data are fit by a Hammett correlation, $\log k_x = \log k_H + \sigma_p \rho$. The reaction constant so derived is $\rho = -4.3$. This substantial and negative value implies a transition state at which the (formal) benzylic carbanion has become substantially more radical-like in character. That is, electron transfer to $IrCl_6^{2-}$ is substantially advanced at the transition state. We conclude from the magnitude of ρ that the site of oxidation is indeed the benzylic carbon and not the more distant chromium center.

This conclusion is consistent with the kinetic trends within the series of alkyl complexes, where the rate progression is $CH_3 \ll C_2H_5 \tilde{=} 1\text{-}C_3H_7 = 1\text{-}C_4H_9 < 2\text{-}C_3H_7 \sim 2\text{-}C_4H_9$. That is, the reaction is clearly not hindered by steric bulk of the group R. This again signals a mechanism in which electron transfer is rate controlling.

An interesting comparison can be made about the rate constant k_3($k_3 > k_1[IrCl_6^{2-}]_{max} \sim$ (57 s^{-1} for R = 4-$BrC_6H_4CH_2$ to 92 s^{-1} for R = 2-C_3H_7)) of $RCrL(H_2O)^{3+}$ and the homolysis rate constant k_3' of $RCrL(H_2O)^{2+}$ ($k_{hom} \sim 10^{-4}$ s^{-1}),[11] where R = aralkyl and 2°-alkyl. We believe that it is the different charge distribution in the transition state that causes $k_3 \gg k_{hom}$.

According to the rules usually used for metal alkyls, the transient species $RCr([15]aneN_4)(H_2O)^{3+}$ are "assigned" as containing chromium in oxidation state +4. We note the $PhCH_2Co(dmgH)_2^+$ analogues certainly <u>are</u> complexes of cobalt(IV), because their kinetic lifetimes are sufficiently long to allow an assignment from EPR data.[20-23] The reactivities of the two series are very different. The one undergoes unimolecular homolysis, eq IV-11, while the other is subject to nucleophilic attack, e.g., eq IV-12.[23-26] It is therefore not at all unreasonable to suggest that the entities $RCr([15]aneN_4)(H_2O)^{3+}$ are more reasonably formulated as Cr(III) complexes of $R^{\cdot}$, rather than Cr(IV) complexes of R^-. Further experiments on the oxidized organochromium species are in progress.

$$RCrL(H_2O)^{3+} + H_2O \longrightarrow R^{\cdot} + (H_2O)_2CrL^{3+} \qquad \text{(IV-11)}$$

$$PhCH_2Co(dmgH)_2OH_2^{+} + Cl^- + H_2O \longrightarrow PhCH_2Cl + (H_2O)_2Co(dmgH)_2 \qquad \text{(IV-12)}$$

Table IV-1. Reduction Potentials, Self-Exchange Rate Constants and Cross-Reaction Rate Constants[a] Pertaining to the Oxidation of $4\text{-}BrC_6H_4CH_2Cr([15]aneN_4)(H_2O)^{2+}$

Oxidant	k_{12}/L mol^{-1} s^{-1}	k_{11}/L mol^{-1} s^{-1}	E^o_{ox}/V
$IrCl_6^{2-}$	$(1.29 \pm 0.18)\times10^4$	2.0×10^5 [b]	0.892[c]
$ABTS^{\bullet-}$	$(1.55 \pm 0.11)\times10^2$	2.2×10^9 [d]	0.43[e]
$Fe(H_2O)_6^{3+}$	3.09 ± 0.28	4.0[f]	0.745[g]

[a]At 25 °C, $[H^+] = 1.0 \times 10^{-2}$ M, and $\mu = 0.20$ M maintained with sodium perchlorate; [b]Ref. 18; [c]Ref. 17; [d]This work; [e]Ref. 12; [f]Ref. 19; [g]Ref. 15.

Table IV-2. Rate Constants[a] for the Oxidation of a Series of $RCr([15]aneN_4)(H_2O)^{2+}$ Complexes by $IrCl_6^{2-}$

R	k/L mol^{-1} s^{-1}
CH_3	2.20×10^{-1}
C_2H_5	7.88×10^{1}
$1\text{-}C_3H_7$	1.01×10^{1}
$1\text{-}C_4H_9$	0.96×10^{1}
$2\text{-}C_3H_7$	8.54×10^{4}
$2\text{-}C_4H_9$	4.87×10^{4}
$4\text{-}BrC_6H_4CH_2$	1.29×10^{4}
$C_6H_5CH_2$	3.86×10^{4}
$4\text{-}CH_3C_6H_4CH_2$	4.60×10^{5}

[a]At 25 °C, $[H^+] = 1.0 \times 10^{-2}$ M and $\mu = 0.20$ M, maintained with $NaClO_4$.

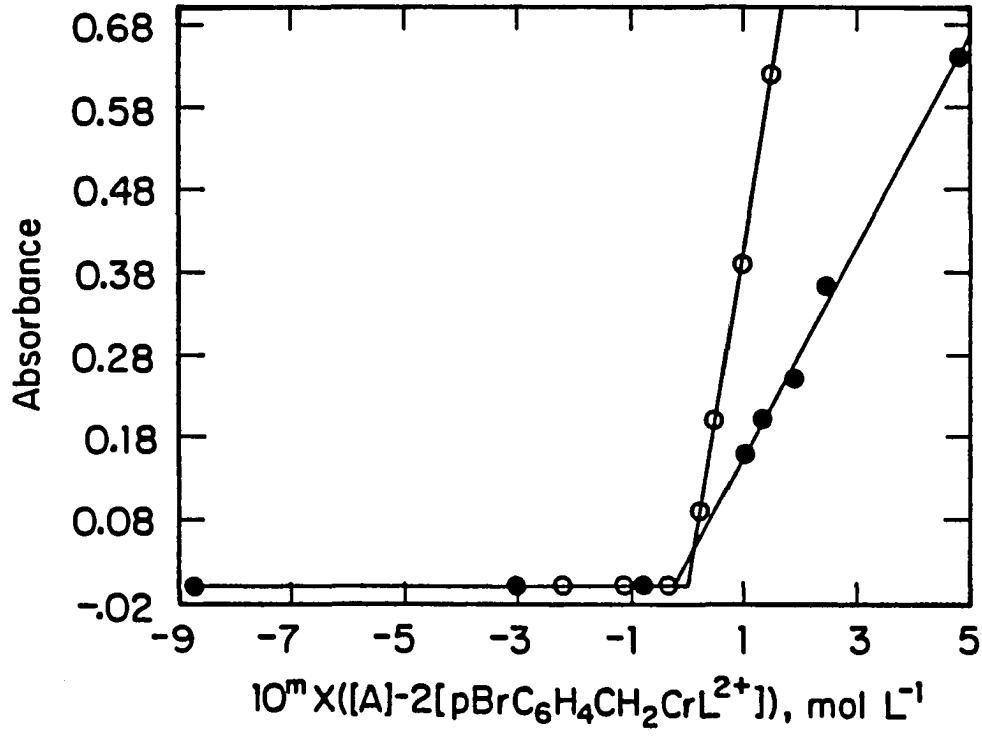

Figure IV-1. Spectrophotometric titrations of $4\text{-}BrC_6H_4CH_2CrL(H_2O)^{2+}$ by $ABTS^{\bullet-}$ (A) (filled circles, m = -4) and $IrCl_6^{2-}$ (open circles, m = -5) showing 1:2 stoichiometry as in eq IV-2 to IV-4

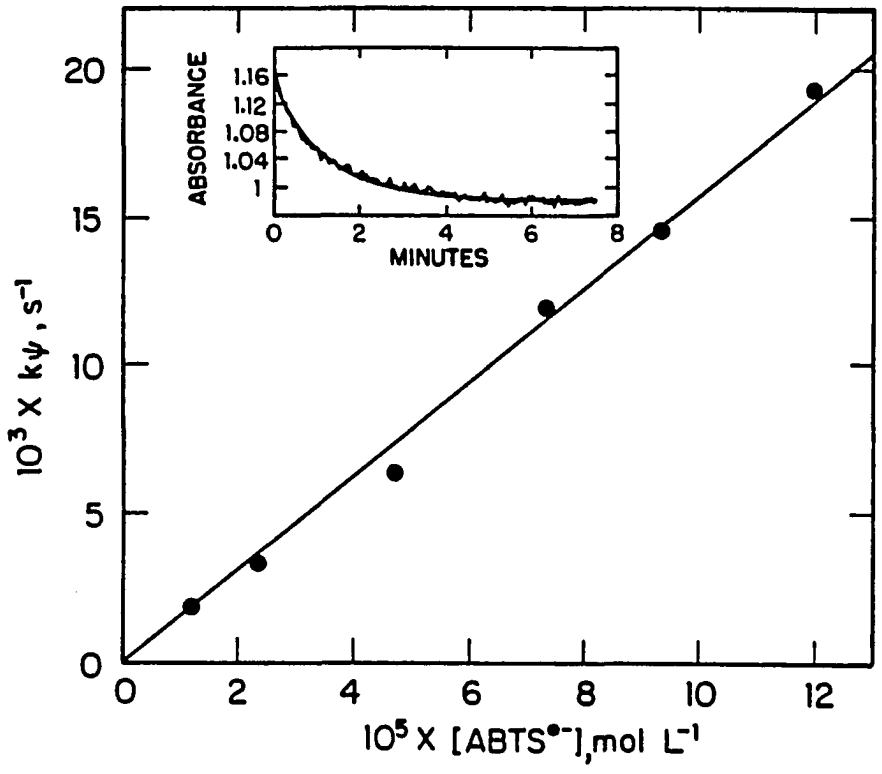

Figure IV-2. A plot showing the linear variation of k_{obsd} with $[ABTS^{\bullet-}]$ in experiments without added $ABTS^{2-}$. The inset shows the kinetic trace and the least-squares fit to it, for an experiment with $[ABTS^{\bullet-}]_o = 1.05 \times 10^{-4}$ M, $[4\text{-}BrC_6H_4CH_2CrL(H_2O)^{2+}]_o = 6.0 \times 10^{-6}$ M, $[H^+] = 1.0 \times 10^{-2}$ M at $\mu = 0.20$ M and 25 °C

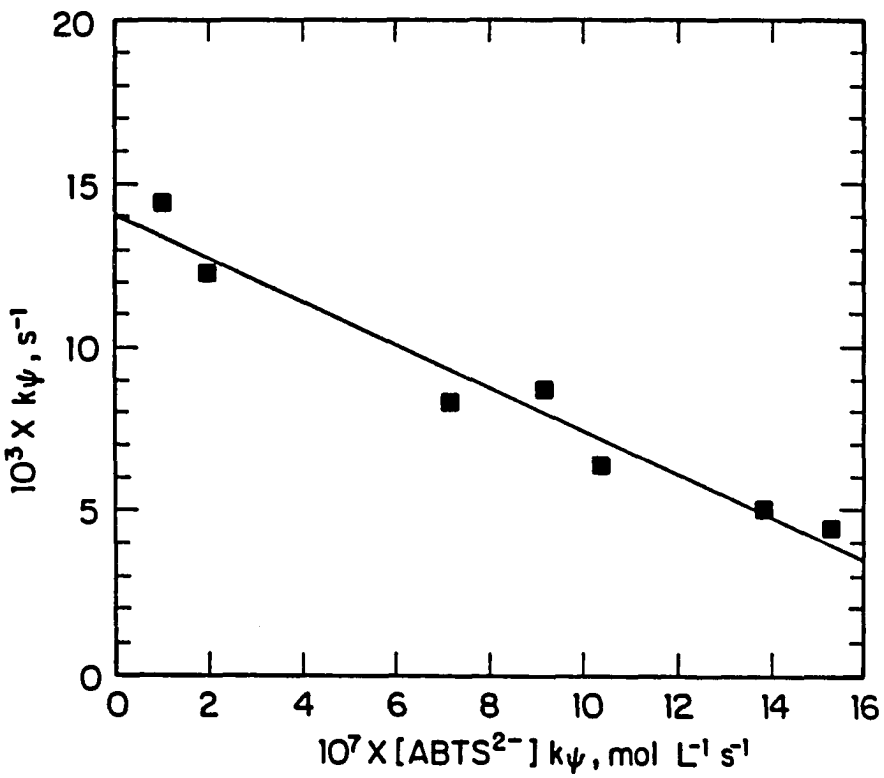

Figure IV-3. The inhibiting effect of added $ABTS^{2-}$ is illustrated in a plot according to eq IV-6

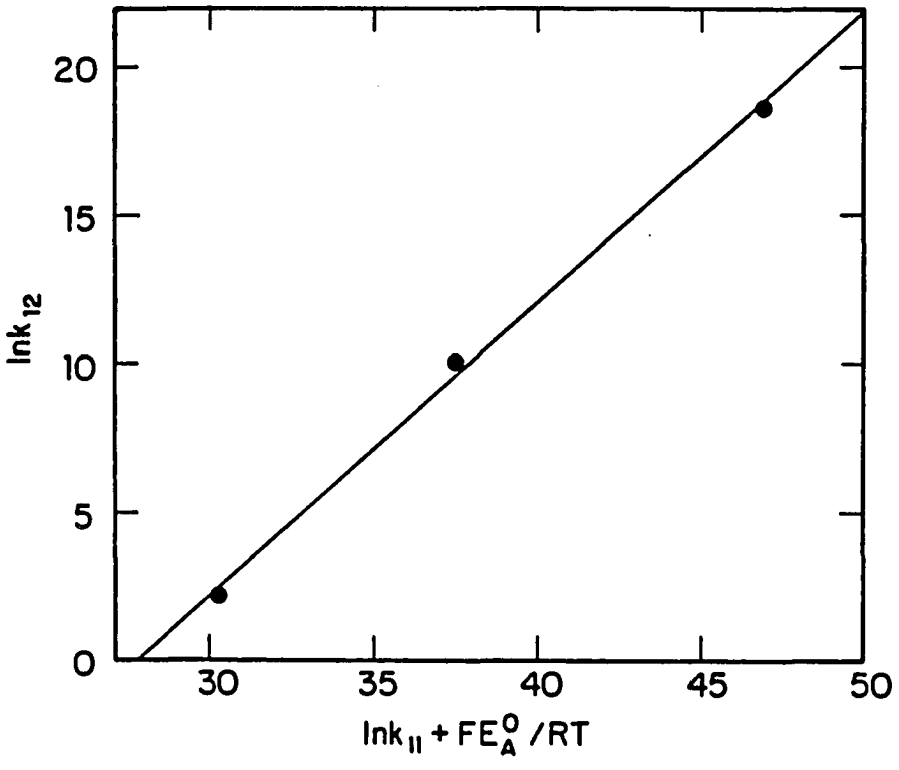

Figure IV-4. A plot showing the analysis of the rate constant for oxidation of $4\text{-}BrC_6H_4CH_2CrL(H_2O)^{2+}$ by $IrCl_6^{2-}$ according to the Marcus cross relation, eq IV-10. The ordinate is derived from the second-order rate constants (Table IV-2), and the abscissa scales the oxidizing ability of the oxidants (Table IV-1)

REFERENCES

(1) Kochi, J. K. "Organometallic Mechanisms and Catalysis"; Academic Press:New York, 1978; Chapters 15-16.

(2) Katsuyama, T.; Bakac, A.; Espenson, J. H. Inorg. Chem. 1989, 28, 339.

(3) Melton, J. D.; Espenson, J. H.; Bakac, A. Inorg. Chem. 1986, 25, 4104.

(4) Melton, J. D.; Bakac, A.; Espenson, J. H. Inorg. Chem. 1986, 25, 3360.

(5) The relevant potential is the one-electron potential of $Br_2(aq)/Br_2^{\cdot -}$, 0.58 V (see ref. 6).

(6) Stanbury, D. M. Adv. Inorg. Chem. 1989, 33, 69-138.

(7) (a) Espenson, J. H.; Williams, D. A. J. Am. Chem. Soc. 1974, 96, 1008; (b) Chang, J. C.; Espenson, J. H. J. Chem. Soc. Commun. 1974, 233; (c) Espenson, J. H.; Samuels, G. J. J. Organomet. Chem. 1976, 113, 143.

(8) E^o = 0.21 V for $I_2(aq) + e^- = I_2^{\cdot -}$.[6]

(9) Shi, S.; Espenson, J. H.; Bakac, A. J. Am. Chem. Soc. 1990, 112, 1346.

(10) Samuels, G. J.; Espenson, J. H. Inorg. Chem. 1979, 18, 2587.

(11) Shi, S.; Espenson, J. H.; Bakac, A., Inorg. Chem. 1990, 29, 4318.

(12) Maruthamuthu, P.; Venkatasubramanian, L.; Dharmalingam, P. Bull. Chem. Soc. Jpn. 1987, 60, 113.

(13) (a) Kelley, D. G.; Espenson, J. H.; Bakac, A. Inorg. Chem. 1990, 29, 0000; (b) Wolfenden, B. S.; Willson, R. L. J. Chem. Soc. Perkin Trans II 1982, 805; (c) Rush, J. D.; Koppenol, W. H. J. Am. Chem. Soc. 1988, 110, 4957; (d) Lindsay Smith, J. R.; Balasubramanian, P. N.; Bruice, T. C. J. Am. Chem. Soc. 1988 110, 7411; (e) Majkic-Singh, N.; Bogavac, L.; Kalimanovska, V.; Jelic, Z.; Spasic, S. Clinica Chimica Acta 1987, 162, 29; (f) Erben-Russ, M.; Michel, C.; Bors, W.; Saran, M. J. Phys. Chem. 1987, 91, 2362.

(14) Steenken, S.; Neta, P. J. Am. Chem. Soc. 1982, 104, 1244.

(15) (a) Yee, E. L.; Cave, R. J.; Guyer, K. L.; Tyma, P. D.; Weaver, M. J. J. Am. Chem. Soc. 1979, 101, 1131; (b) Weaver, M. J.; Yee, E. L. Inorg. Chem. 1980, 19, 1936.

(16) Nohr, R. S.; Espenson, J. H. J. Am. Chem. Soc. 1975, 97, 3392.

(17) Margerum, D. W.; Chellappa, K. L.; Bossu, F. P.; Burce, G. L. J. Am. Chem. Soc. 1975, 97, 6894.

(18) Hurwitz, P.; Kustin, K. Trans. Faraday Soc. 1966, 62, 427.

(19) Silverman, J.; Dodson, R. W. J. Phys. Chem. 1952, 56, 816.

(20) Halpern, J.; Chan, M. S.; Hanson, J.; Roche, T. S.; Topich, J. A. J. Am. Chem. Soc. 1975, 97, 1606.

(21) Halpern, J.; Topich, J.; Zamaraev, K. I. Inorg. Chim. Acta 1976, 20, L21.

(22) Topich, J.; Halpern, J. Inorg. Chem. 1979, 18, 1339.

(23) Halpern, J.; Chan, M. S.; Roche, T. S.; Tom, G. M. Acta Chem. Scand. A 1979, 33, 141.

(24) Anderson, S. N.; Ballard, D. H.; Chrzastowski, J. Z.; Dodd, D.; Johnson, M. D. J. Chem. Soc. Chem. Commun. 1972, 685.

(25) Anderson, S. N.; Ballard, D. H.; Johnson, M. D. J. Chem. Soc. Perkin Trans. 2 1972, 311.

(26) Jensen, F. R.; Madan, V.; Buchanan, D. H. J. Am. Chem. Soc. 1971, 93, 5283.

PART V. REDUCTION INDUCED COBALT-CARBON BOND CLEAVAGE IN ORGANOCOBALT MACROCYCLIC COMPLEXES

INTRODUCTION

Reduction induced cleavage of cobalt-carbon bond in organocobalt macrocyclic complexes presents challenging questions. Detailed mechanistic and kinetic information is still insufficient to understand fully the roles of vitamin B_{12} in the catalysis of reactions such as skeletal 1,2-rearrangements,[1,2] reduction of ribonucleoside triphosphates,[3-5] and biosynthesis of methionine,[6,7] methane,[8-11] and acetate.[10,12-14] A new domain of chemistry studying reactivities of "partial-strength" M-C σ-bonds, namely the reactivities of M-C bonds in complexes containing one or more electrons in antibonding orbitals, begins to emerge.[15]

The electrochemical reduction of alkylcobalt(III) compounds generally gives unstable alkylcobalt anions which decompose by the cleavage of the Co-C bond. Both homolytic and heterolytic decomposition pathways were reported to be operative after one electron reduction.[16-21] For example, in the case of $RCo^{II}(salen)^-$, when R = C_6H_5[16-18] or fluoroalkyl,[19] the decomposition yields R^- and $Co^{II}(salen)$. For R = CH_3 or C_2H_5, $R\cdot$ and $Co^{I}(Salen)^-$ are produced.[17,20] These two decomposition mechanisms were also observed for the bond cleavage induced by chemical reduction.[22-27]

It has been noticed in some cases that the equatorial ligand may play an active part in the reduction induced cleavage of the Co-C bond. A reversible trapping of the alkyl group by the equatorial ligands was proposed to account for the c.a. 60-80% recovery of the starting organocobalt(III) complexes and for the retention of configuration of the alkyl group after one-electron reduction followed by re-oxidation.[28] The

electrochemical reductive cleavage of a steroidal cobalt porphyrin complex proceeds with retention of configuration.[29,30]

Notwithstanding the wealth of information about the reduction potentials,[21] little is known about the reduction and decomposition kinetics,[15] about the electron configuration of the reduced organocobalt intermediates and about the mechanisms by which the equatorial ligands participate in the reduction induced cleavage of the Co-C bond.

We wish to present here the results of our investigation on a series of organocobalt macrocyclic complexes, $RCo^{III}(dmgBF_2)_2A$, where R = CH_3, C_2H_5, 1-C_3H_7, 4-$BrC_6H_4CH_2$, $C_6H_5CH_2$, 4-$CH_3C_6H_4CH_2$ and A = py, H_2O and OH^-. We will focus on the following issues: (1) The mechanisms of reduction induced decompositions of organocobalt complexes. (2) The electron configuration of $RCo^{II}(dmgBF_2)_2^-$ and the reason that the Co-C bond in these reduced species does not decompose immediately after reduction. (3) Participation of the equatorial ligand, especially the possibility of the alkyl group transfer and hydrogen atom transfer to the equatorial ligand. (4) Reaction kinetics.

EXPERIMENTAL SECTION

Materials. Organocobalt(III) macrocyclic complexes, $RCo(dmgBF_2)_2A$ (A = py, H_2O) were synthesized from $RCo(dmgH)_2A$ and BF_3 according to the known methods,[31] and recrystallized from acetone. All the complexes had satisfactory elemental analysis, UV-vis spectra,[32] and ^1H-NMR.[32] Inorganic cobalt(II) macrocyclic complexes, $Co(dmgH)_2A_2$, were prepared by a literature method.[33] Nickel tetramethylcyclam, R,S,R,S-$Ni(tmc)^{2+}$ (tmc = 1,4,8,11-tetramethyl-1,4,8,11-tetraazacyclotetradecane), was prepared by a known procedure.[34] Other reactants and solvents were obtained commercially and often used without further purification.

Electrochemical Reduction. Voltammetric experiments were conducted at room temperature in acetonitrile with 0.06 M Me_4NBF_4 (Aldrich) as the supporting electrolyte. It was performed on a BAS-100 electrochemical analysis system with a glassy-carbon working electrode, a platinum wire auxiliary electrode, and a Ag/AgCl (3 M NaCl) reference electrode. Controlled potential electrolysis of $RCo(dmgBF_2)_2A$ for product analysis was conducted in 0.06 M Me_4NBF_4 of either dry acetonitrile or acetonitrile-water solution and performed on a BAS CV-27 voltammograph with a Hg-pool working electrode, a platinum plate auxiliary electrode, and a Ag/AgCl (3 M NaCl) reference electrode. Electrochemical preparation of $Ni(tmc)^+$ was achieved by controlled potential reduction of $Ni(tmc)^{2+}$ in aqueous solution containing 0.08M $LiClO_4$ and 0.02M NaOH.[35] Oxygen free conditions were maintained by Ar atmosphere.

Product Analysis. The organic decomposition products were detected by GC and GC-mass spectroscopic techniques. The GC detection was performed on a Hewlett-Packard Model 5790 gas chromatograph with 6′ columns packed either with VZ-10 or OV-101 as stationary phases. The instrument was calibrated by use of commercial organic compounds. The GC-mass spectra of the decomposition products of $C_3H_7Co(dmgBF_2)_2^-$ were obtained on a Finnigan 4500 GC-mass spectrometer interfaced to the Incos data system. Cooling with liquid N_2 (for 1.5 min) was employed to separate the organic molecules to be detected from gaseous impurities. A 30m DB 624 capillary column was used for chromatographic separation before mass detection. In addition, the different relative abundance of mass = 41 peak over mass = 42 peak could be taken advantage of to detect cyclopropane in the presence of propene. For propene, abundance of mass = 41 > abundance of mass = 42; for cyclopropane, the opposite is true.[36] Therefore the decomposition products, propane, propene, and cyclic propane, can be detected individually from reaction mixture by a GC-mass spectrometer. The inorganic decomposition products were detected by their electronic spectra,[37] and reduction potentials.

Spectroscopic Studies. The ^1H-NMR and ^{13}C-NMR studies were conducted in DMSO-d_6 solution at room temperature on Nicolet-300 MHz and Bruker WM-200 MHz nuclear magnetic resonance spectrometers. The ESR spectra were collected on an IBM/Brucker ER-200 electron paramagnetic resonance spectrometer at 100 K. The electronic spectra were obtained on a Cary-219 and a Perkin-Elmer Lambda Array UV-vis spectrometer.

Kinetics. The kinetics of the reaction between $RCo(dmgBF_2)_2OH^-$ and $Ni(tmc)^+$ was studied at 25.0 ± 0.1 °C in 0.7% acetone aqueous solution with ionic strength of 0.1 M controlled by $NaClO_4$, and pH 12 controlled by NaOH. The reaction process was monitored at λ = 610 nm by a Durrum-Dionex stopped-flow spectrometer. The same instrument was used for fast repetitive scans of the electronic spectra. All the experiments were conducted under an argon atmosphere owing to the sensitivity of $Ni(tmc)^+$ and reduced cobalt species towards oxygen. Concentrations of reactants were determined spectrophotometrically.[32,35]

RESULTS

Reduction Induced Decompositions. The cyclic voltammogram for the one electron reduction of the trans aquaorganocobalt(III) macrocyclic complexes, $RCo(dmgBF_2)_2A$, (R = CH_3, C_2H_5, 1-C_3H_7, 4-$BrC_6H_4CH_2$, $C_6H_5CH_2$, 4-$CH_3C_6H_4CH_2$; A = py, H_2O) exhibits one cathodic wave and two anodic waves in the first scan and two cathodic waves and two anodic waves in the following scans in the range 0 to -1.2 V (vs Ag/AgCl), yielding $E_{1/2}$ -0.5 V and $E_{1/2}(1)$ ca. -1.0 V, as shown in **Figure V-1a.** A control experiment under identical conditions but with $Co^{II}(dmgBF_2)_2(H_2O)_2$ replacing $RCo^{III}(dmgBF_2)_2(H_2O)$ afforded a cyclic voltammogram containing only one reduction wave and one oxidation wave, at $E_{1/2}$ -0.5 V, as shown in **Figure V-1b.** A blank experiment under identical conditions but in the absence of cobalt species showed no redox wave in this region.

Changing the trans group from H_2O to py introduces no additional feature except for a slight shift of the reduction wave (0.01 to 0.03 V) towards more negative value. An increase of scan rate makes the oxidation wave at ca. -1.0 V better developed, but the overall voltammogram was less reversible.

The fate of the one electron reduction product $RCo(dmgBF_2)_2^-$ [38] was studied by analyzing its decomposition products. For R = CH_3, only CH_4 was detected after one electron reduction. For R = C_2H_5 and 1-C_3H_7, both RH and R(-H) were detected. No R_2 was found in any circumstances. In the case of primary alkylcobalt complexes, the RH/R(-H) ratio increases with the water content in the solvent, **Table V-1.** Reduction of $RCo(dmgBF_2)_2A$

could also be accomplished chemically over Zn(Hg) ($E_{1/2}$ = -0.76 V[39]) and with $Ni(tmc)^+$ ($E_{1/2}$ = -0.87 V[35]).

About 1% cyclopropane was detected in the head gas on an aqueous solution of $1\text{-}C_3H_7Co(dmgBF_2)_2py$ reduced by Zn(Hg). Propane and propene constitute 99% of the organic decomposition products.

The short-lived $RCo(dmgBF_2)_2^-$ can be captured by quenching its decomposition in liquid N_2 immediately after its formation as signaled by visible color change of the solution from bright yellow (parent $RCo^{III}(dmgBF_2)_2A$) to dark green upon one electron reduction. The low temperature (100 K) ESR spectrum of this frozen dark green solution shows an unprecedented d^7 cobalt electron resonance pattern with $g_{\parallel}$ = 2.23, $g_{\perp}$ = 2.07, $A_{\parallel}$ = 106.4 G, and $A_{\perp}$ = 56 G, as shown in **Figure V-2.** This ESR spectrum disappears and replaced by that of $Co^{II}(dmgBF_2)_2(H_2O)_2$[37] if the dark green solution is allowed to warm to room temperature and then cooled to 100 K again. No room temperature ESR was observed.

Participation of the Equatorial Ligand. Reduction of $1\text{-}C_3H_7Co(dmgBF_2)_2py$ by excess $NaBH_4$ in DMSO-d_6 yielded a deep blue solution. Both C_3H_8 and C_3H_6 were detected in the head gas with C_3H_8/C_3H_6 = 0.25. Reduction of $CH_3Co(dmgBF_2)_2py$ by excess $NaBH_4$ afforded a similar deep blue solution with CH_4 detected as the only gaseous product. The deep blue solutions of reduced organocobalt complexes so obtained (R = CH_3, C_3H_7, $C_6H_5CH_2$) are diamagnetic exhibiting no ESR signal but well define ^1H-, and ^{13}C-NMR spectra.

The ^1H-NMR spectrum in DMSO-d_6 of such a solution of $CH_3Co(dmgBF_2)_2py$ / $NaBH_4$ (excess) shows a set of four new resonance peaks at 1.90 ppm (3H,

broad), 2.01 ppm (3H), 2.04 ppm (3H), 2.10 ppm (10H) as compared to the ^{1}H-NMR spectrum of $Co(dmgBF_2)_2(py)_2$ reduced by excess $NaBH_4$ in DMSO-d_6 (a singlet at 1.75 ppm), as depicted in **Figure V-3a.** The borohydride resonances centered at ca. -0.35 ppm as a quartet (from ^{11}B-H) accompanied by a set of seven peaks of much less total intensity (from ^{10}B-H) as well as the resonance of the pyridine hydrogen at lower field (ca. 7.50 ppm) are well separated from the methyl hydrogen resonances and do not interfere. Peaks at 2.04, 2.01, and 1.90 ppm are of comparable intensity and were assigned to the methyl group of the reduction product. The peaks at 2.10 and 1.75 ppm correspond to the one electron reduction products of $Co(dmgBF_2)_2(H_2O)_2$ and $Co(dmgBF_2)_2(py)_2$ in DMSO respectively. Variation of magnetic field strength from 200 MHz to 300 MHz did not change the chemical shifts of these peaks, indicating that they are independent resonance peaks rather than components of a multiplet.

The ^{13}C-NMR spectrum of the $CH_3Co(dmgBF_2)_2py$ / $NaBH_4$(excess) solution exhibits a set of peaks at 10.9 ppm to 23.8 ppm, which are due to the methyl and imine carbons, **Figure V-3b.** The resonances of pyridine carbons centered at ca. 140 ppm do not interfere with those.

Kinetics of the Reduction of $RCo(dmgBF_2)_2A$ by $Ni(tmc)^+$. The reaction between $RCo(dmgBF_2)_2py$ and $Ni(tmc)^+$ generates the blue cobalt(I), as shown by the repetitive scans of **Figure V-4.** Both ethane and ethylene were detected in the head gas after the reaction between $C_2H_5Co(dmgBF_2)_2py$ and $Ni(tmc)^+$ was complete. The C_2H_6 / C_2H_4 ratio decreases as the proportion of CH_3CN as co-solvent increases. This ratio also decreases as the $Ni(tmc)^+$ / $C_2H_5Co(dmgBF_2)_2py$ ratio decreases. When

R = primary alkyl, the reaction proceeds according to a simple mixed second order rate law, eq V-1,

$$\frac{d[Co^{I}(dmgBF_2)_2py]}{dt} = \frac{-d[RCo^{III}(dmgBF_2)_2py]}{dt}$$

$$= k_{e,1}[RCo(dmgBF_2)_2][Ni(tmc)^{+}] \qquad (V-1)$$

The reaction rate constant, $k_{e,1}$, as defined by eq V-1 and evaluated with excess $Ni(tmc)^{+}$, is independent of acetone concentration (0% to 3.8%), independent of pH (pH 11-12) and independent of $[Ni(tmc)^{2+}]$. A kinetic trace and a plot of k_{obs} vs. $[Ni(tmc)^{+}]$ are shown in **Figure V-5**. The $k_{e,1}$ values are listed in **Table V-2**.

When R = aralkyl, the reaction proceeds in two steps with a biphasic kinetic trace, implying accumulation of a reduction intermediate, **Figure V-6**. The fast phase is well separated from the slow one and both follow a pseudo-first order rate law and both show a first order dependence on $[Ni(tmc)^{+}]$, **Figure V-7a,b**. The second order rate constants, $k_{e,1}$ and $k_{e,2}$ were obtained by plotting k'_{obs} and k''_{obs} against $[Ni(tmc)^{+}]$; here k'_{obs} and k''_{obs} were obtained from traces of the fast and the slow phase respectively.

DISCUSSIONS

Reduction Induced Decompositions. The cyclic voltammagram of the one electron redox process measured at room temperature shows a quasi-reversible character, $I_a < I_c$ (**Figure V-1a**), indicating that follow-up chemical reactions destroy the electrochemically generated $RCo(dmgBF_2)_2^-$.[21] This EC mechanism is illustrated by eq V-2, to V-4.

$$RCo(dmgBF_2)_2A + e^- \rightarrow [RCo(dmgBF_2)_2A^-] \qquad (V\text{-}2)$$

$$[RCo(dmgBF_2)_2A^-] + 2H_2O \rightarrow RH + Co(dmgBF_2)_2A(H_2O) + OH^- \qquad (V\text{-}3)$$

$$[RCo(dmgBF_2)_2A^-] \rightarrow R(-H) + Co(dmgBF_2)_2(H_2O)A^- \qquad (V\text{-}4)$$

We believe that hydrolysis (eq V-3) and β-hydrogen elimination (eq V-4) as opposed to the simple C-Co(II) bond homolysis[21] constitute of the major pathways of the reduction induced decomposition of these organocobalt complexes. This is because the detected RH/R(-H) ratio deviates significantly from unity and varies with water content of the solvent. This is also because that no radical coupling product R_2 is detected in head gas.

Slow hydrolysis of a C-Co(III) bond was observed before.[40-42] Detection of alkanes soon after one electron reduction of $RCo(dmgBF_2)_2A$ signals a more ready hydrolysis of a C-Co(II) bond in $RCo(dmgBF_2)_2A^-$. One could speculate that the alkyl group in $RCo(dmgBF_2)_2^-$ possesses higher electron density and hence renders the C-Co bond more subject to hydrolysis. Theoratically, since the homolysis can be viewed as an intramolecular electron transfer from carbanion to cobalt, any factor

that lowers the LUMO level on cobalt will increase the homolysis rate and vice versa. Thus it is easily understood why reduction promotes heterolysis and oxidation promotes homolysis. It is known experimentally that oxidation of organocobalt(III) complexes does accelerate homolysis of the C-Co bond.[43,44]

Rather unexpectedly, an oxidized organic compound, R(-H), is formed upon reduction of $RCo(dmgBF_2)_2A$. Since R(-H) is not formed from an alkyl radical, the formation of R(-H) could only be realized by further reduction of the cobalt macrocycle fragment. β-H elimination is a plausible pathway leading to R(-H) from $RCo(dmgBF_2)_2^-$. It seems quite unlikely for cobalt center to serve as the hydrogen acceptor in the β-H elimination, since no adjacent coordination vacancy is available. In addition, no precedent of cobalt(II) hydride is known.

Participation of the Equatorial Ligand. We propose the following scheme to accommodate our observations.

Scheme 1

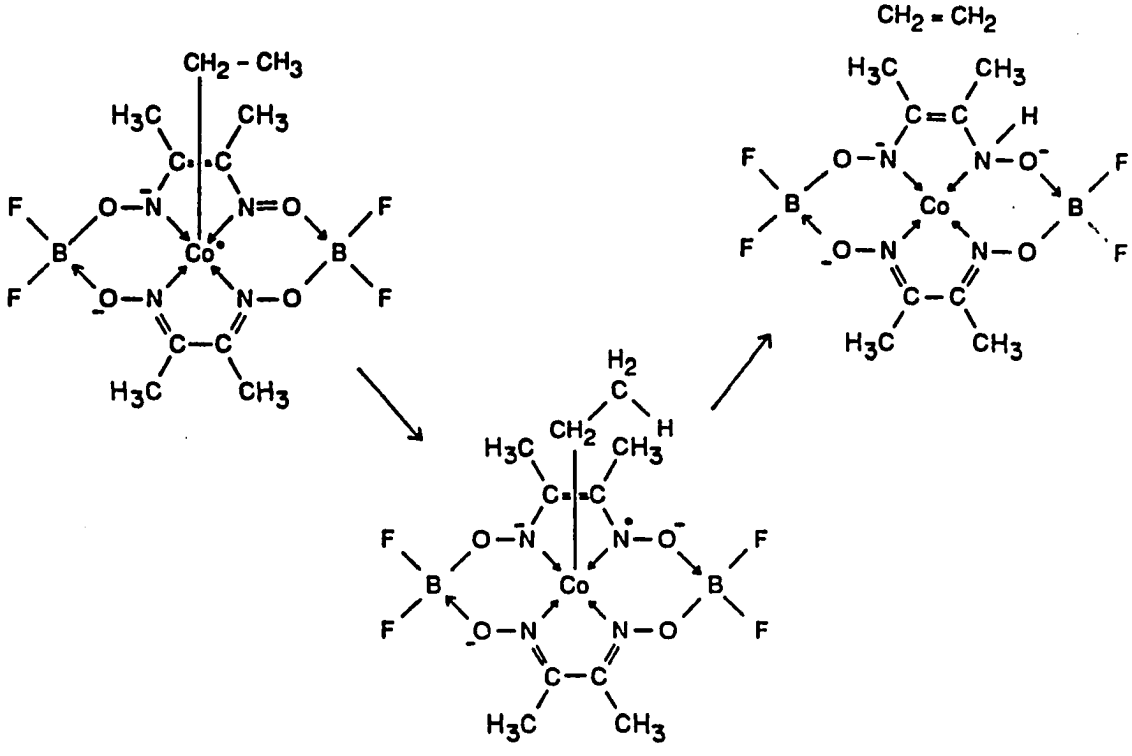

Scheme 1 suggests that the oxidation of the alkyl group to alkene is accomplished by reduction of the equatorial ligand. The cobalt center plays a role to mediate the intramolecular hydrogen atom transfer. Participation of conjugated macrocyclic ligand in the formation and cleavage of C-Co(II) bond was proposed before,[28-30,45] and observed in the decomposition of a CH_3-Co(III) bond.[46]

The γ-H elimination product of $C_3H_7Co(dmgBF_2)_2py^-$, c-C_3H_6, was also detected (ca. 1%) in the head gas. It seems likely that both β-H and γ-H eliminations operate by the same mechanism, i.e., hydrogen transfer from

the axial alkyl to the equatorial ligand. Steric factors favor β-H elimination over γ-H elimination.

In the absence of β- and γ-hydrogens, migration of alkyl group to the equatorial ligand is expected. The ^{1}H-NMR and ^{13}C-NMR spectra of the reduced product of $CH_3Co(dmgBF_2)_2py$ (Figure V-3) suggest the formation of a new complex of structure 1.

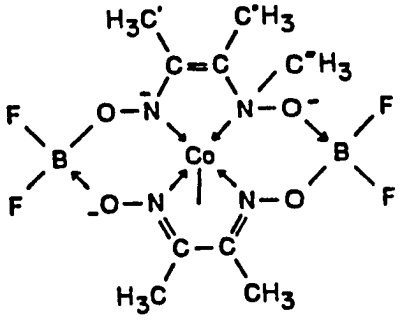

Structure 1

In the ^{1}H-NMR the broad 1.90 ppm broad peak is assigned to the resonance of $C'''H_3$ protons and the 2.01 ppm and 2.04 ppm peaks are assigned to $C''H_3$ and $C'H_3$ groups respectively. A penta-coordination geometry in solution is assumed based on crystal structure of $Co(dmgBF_2)_2py^-$.[47]

It is interesting to question why is the unpaired electron not directed to the C-Co antibonding orbital. If the latter happened, an immediate homolysis of the C-Co bond and detection of radical self-reaction products would be expected. This question is answered experimentally by an ESR study of the reduction intermediate trapped at liquid N_2 temperature.

The one electron reduction product of $RCo(dmgBF_2)_2A$ exhibits an unique ESR spectrum (Figure V-2) with $g_{\parallel} > g_{\perp}$ which is clearly

distinguishable from d^7 inorganic cobalt(II) complexes where $g_{\parallel}$ is most commonly found smaller than $g_{\perp}$.[37,48-50]

According to eq V-5 and V-6,[51]

$$g_{\parallel} = g_e[1 + (4\zeta/\Delta)] \qquad \text{(V-5)}$$

$$g_{\perp} = g_e[1 - (4\zeta/\Delta')] \qquad \text{(V-6)}$$

where ζ is the spin-orbital coupling constant for a single electron and it is always a positive value, $\zeta = Z_{eff}e^2\langle r^{-3}\rangle/(2m^2c^2)$. Whereas Δ and Δ' are the absolute values of the energy differences between the ground state and the symmetry allowed lowest excited states.[51] Regardless of the numerical details, the odd electron must reside in the $d_{x^2-y^2}$ orbital instead of in d_{z^2} orbital in order to maintain the relationship of $g_{\parallel} > g_{\perp}$. In other words, the ESR spectrum demands an orbital energy order of $E(d_{z^2}) > E(d_{x^2-y^2})$. Qualitatively, a strong C-Co bond existing along the z-axis in conjunction with the upward displacement of cobalt from the equatorial base plane could render the orbital energy of d_{z^2} higher than that of $d_{x^2-y^2}$. This is because the overlap between $d_{x^2-y^2}$ orbital of cobalt and σ-orbitals of nitrogens may decrease significantly and also because the π-overlap between the d_{z^2} orbital of cobalt and the p-orbitals of the equatorial nitrogen atoms becomes no longer negligible once cobalt atom moves above the basal plane as evidenced by a significant N-Co bond shortening in $Co^{I}(dmgBF_2)_2^-$.[47]

It is noticeable that the $g_{\parallel}$ resonances are significantly broadened, which is consistent with the notion that the unpaired electron in $d_{x^2-y^2}$

interacts with the nuclear spin of the four nitrogen atoms of the equatorial ligand.

The residence of the unpaired electron in $d_{x^2-y^2}$ orbital rather than in the C-Co antibonding orbital, d_{z^2}, explains why the homolysis of the C-Co bond does not occur immediately after the reduction. It also provides a hint as to how the equatorial ligand is directed to participate in the decomposition reactions, **Scheme 1**. The electron density could move from the $d_{x^2-y^2}$ orbital of cobalt into the equatorial ligand generating a transient nitrogen centered radical which in turn functions as a radical acceptor to facilitate the cleavage of the C-Co bond, and hence triggers the alkyl group transfer from cobalt to the equatorial ligand or hydrogen atom migration from alkyl to the nitrogen affording alkenes.

We summarize the reduction induced decomposition reactions of $RCo(dmgBF_2)_2A$ into **Scheme 2**.

Scheme 2

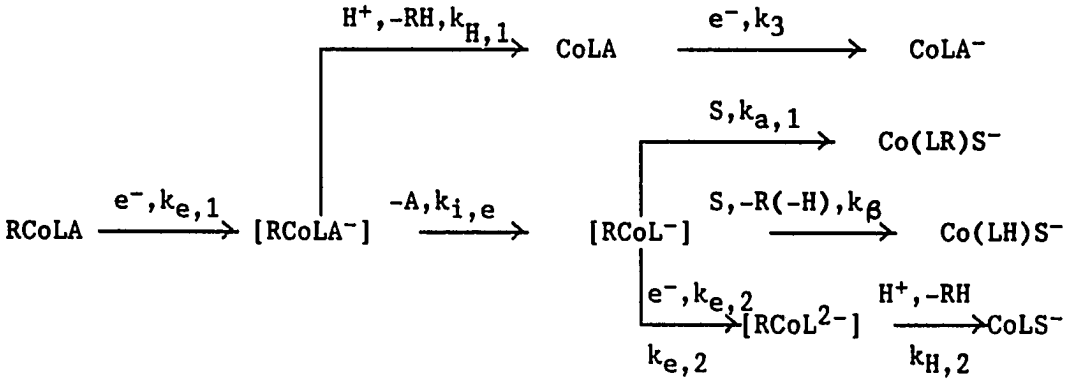

Kinetics. The reduction of primary alkyl cobalt(III) macrocyclic complexes, $RCo(dmgBF_2)_2A$, by $Ni(tmc)^+$ obeys monophasic pseudo-first order rate law, eq V-1. The first order dependence on $[Ni(tmc)^+]$ in conjunction with the lack of $[Ni(tmc)^{2+}]$ effect (over 10^{-4} to 10^{-3} M) on k_{obs} values as well as pH independence between pH 11-12 ruled out the possibilities for $k_{H,1}$, $k_{e,2}$, $k_{i,e}$ or k_β steps to be rate limiting. Also the reduction of $Co(dmgBF_2)_2(py)_2$ to $Co(dmgBF_2)_2py^-$ proceeds very fast (> 10^6 M^{-1},s^{-1}), therefore the rate determine step is the initial electron transfer of eq V-7.

$$RCo(dmgBF_2)_2A + Ni(tmc)^+ \rightarrow RCo(dmgBF_2)_2A^- + Ni(tmc)^{2+} \qquad (V\text{-}7)$$

Reduction of aralkylcobalt(III) macrocyclic complexes, $ArCH_2Co(dmgBF_2)_2A$, by $Ni(tmc)^+$ proceeded in a biphasic fashion, signaling an accumulation of reduction intermediate, $ArCH_2Co(dmgBF_2)_2^-$. The second order rate constants deduced from the fast phase are close to those obtained for alkylcobalt(III) analogues, and assigned to $k_{e,1}$ step. An electron withdrawing substituent in the aralkyl group causes an increase of the reduction rate whereas an electron donating substituent causes a decrease in the reduction rate. We assign the second order rate constant of the slow phase to $k_{e,2}$ step for the following reasons. (1) The pseudo-first-order rate constant, k_{obs}, shows a first order dependence on $[Ni(tmc)^+]$ and yet is independent of $[Ni(tmc)^{2+}]$. (2) Optical absorbance changes of the two phases add up to the total absorbance change expected for a 100% conversion of aralkylcobalt(III) macrocycles to inorganic

cobalt(I) macrocycles. (3) Biphasic kinetic profiles were observed only for aralkylcobalt complexes.

It is interesting to note that the biphasic behavior is not observed in the reduction of primary alkylcobalt(III) macrocycles by $Ni(tmc)^+$. In another word, $k_{e,2}$-$k_{H,2}$ sequence of reaction does not contribute much there. This phenomenon can be explained by the structural and electronic difference between primary-alkylcobalt(III) complexes and their aralkyl analogues. The decomposition reactions probably operate much better in the alkyl series than in the aralkyl series. With much better electron delocalization ability of aralkyl group, the α-carbon in the aralkylcobalt complexes should be much less carbanion in character as compared to that of alkylcobalt analogues, hence much less subject to hydrolysis ($k_{H,1}$). This renders the relative importance of $k_{i,e}$ pathway higher in aralkylcobalt series over that in alkyl cobalt series. Yet, the lack of β-hydrogen shuts off the k_β pathway. Therefore the reaction is forced to proceed along $k_{e,2}$ pathway. Obviously, the $k_{H,2}$ step also helps to pull the second electron transfer step $k_{e,2}$ to completion. Apparently there is no need for the reduction of alkylcobalt complexes by $Ni(tmc)^+$ to proceed along the $k_{e,2}$ pathway. In the alkylcobalt series, both hydrolysis ($k_{H,1}$) and β-hydrogen elimination (k_β) operate in a facile manner, and thus no intermediate accumulation is observed.

Generally speaking, $k_{e,1}$ values for aralkylcobalt macrocyclic complexes are higher than those for their alkyl analogues, consistent with the differences among their first electron reduction potentials[21] and the notion that aralkyl groups stablize reduced cobalt better by electron delocalization than alkyl groups do. The higher $k_{e,1}$ values of

aralkylcobalt complexes are probably also partly responsible for the observed accumulation of the reduction intermediate.

CONCLUSIONS

Our observations about reductions and subsequent decompositions of various $RCo^{III}(dmgBF_2)_2A^{n-}$ are accommodated in Scheme 2. (1) The first electron reduction of $RCo^{III}(dmgBF_2)_2py$ generates a d^7 cobalt species with $(t)^6(d_{x^2-y^2})^1$ electron configuration. The existence of a C-Co bond in this d^7 cobalt species is strongly suggested by the observed ESR spectrum. (2) Two reactions may occur after the first electron reduction. They are hydrolysis and intramolecular electron transfer. The later reaction further branches into three follow-up reactions, β-H elimination, alkyl group migration, and the second electron reduction. The hydrolysis and β-H elimination produce alkanes and alkenes respectively. (3) The relative importance of hydrolysis over β-H elimination is influenced by water content of the solvent, and controlled by the probability of the intramolecular electron transfer (from cobalt(I) to a π^*-orbital of the equatorial ligand) and by the availability of β-hydrogen. (4) The first electron reduction by $Ni(tmc)^+$ occurs at high speeds ($6x10^4$-10^6 $M^{-1}s^{-1}$), whereas the second electron reduction proceeds more slowly (10^4 $M^{-1}s^{-1}$). (5) The life times of the first electron reduction products, as reflected by their kinetic behaviors (monophasic vs. biphasic), are determined by both the electron delocalization ability of the axial organic groups and the availability of β-hydrogen.

Table V-1. Distribution of the Decomposition Products, RH/R(-H) Formed by Reduction of $RCo(dmgBF_2)_2py$ in CH_3CN/H_2O Solutions[a]

Complex	RH / R(-H)	
	0 % H_2O	33 % H_2O
$CH_3Co(dmgBF_2)_2py$	1.0 / 0.0	1.0 / 0.0
$C_6H_5CH_2Co(dmgBF_2)_2py$	1.0 / 0.0	1.0 / 0.0
$C_2H_5Co(dmgBF_2)_2py$	0.38 / 0.62	0.55 /0.45
$1\text{-}C_3H_7Co(dmgBF_2)_2py$	0.22 / 0.78	0.68 /0.32

[a]Reduction was conducted at -1.0 V (vs. Ag/AgCl) with 0.06 M Me_4NBF_4 as supporting electrolyte, at 25 °C. $[RCo(dmgBF_2)_2py] = 2.0 \times 10^{-3}$ M.

Table V-2. Second Order Rate Constants for Reductions of $RCo(dmgBF_2)_2A$ by $Ni(tmc)^+$ in Aqueous Solution[a]

Complex	$k_{e,1}$ / $M^{-1}s^{-1}$	$k_{e,2}$ / $M^{-1}s^{-1}$
$CH_3Co(dmgBF_2)_2py$	5.95×10^4	
$C_2H_5Co(dmgBF_2)_2py$	1.28×10^5	
$1\text{-}C_3H_7Co(dmgBF_2)_2py$	1.57×10^5	
$1\text{-}C_3H_7Co(dmgBF_2)_2OH^-$	1.14×10^5	
$4\text{-}CH_3C_6H_4CH_2Co(dmgBF_2)_2py$	7.78×10^5	3.06×10^4
$C_6H_5CH_2Co(dmgBF_2)_2py$	8.00×10^5	1.70×10^4
$4\text{-}BrC_6H_4CH_2Co(dmgBF_2)_2py$	1.14×10^6	2.91×10^4
$4\text{-}BrC_6H_5CH_2Co(dmgBF_2)_2OH^-$	1.75×10^6	2.70×10^4

[a]At 25 °C with [NaOH] = 0.02 M, ionic strength μ = 0.10 M.

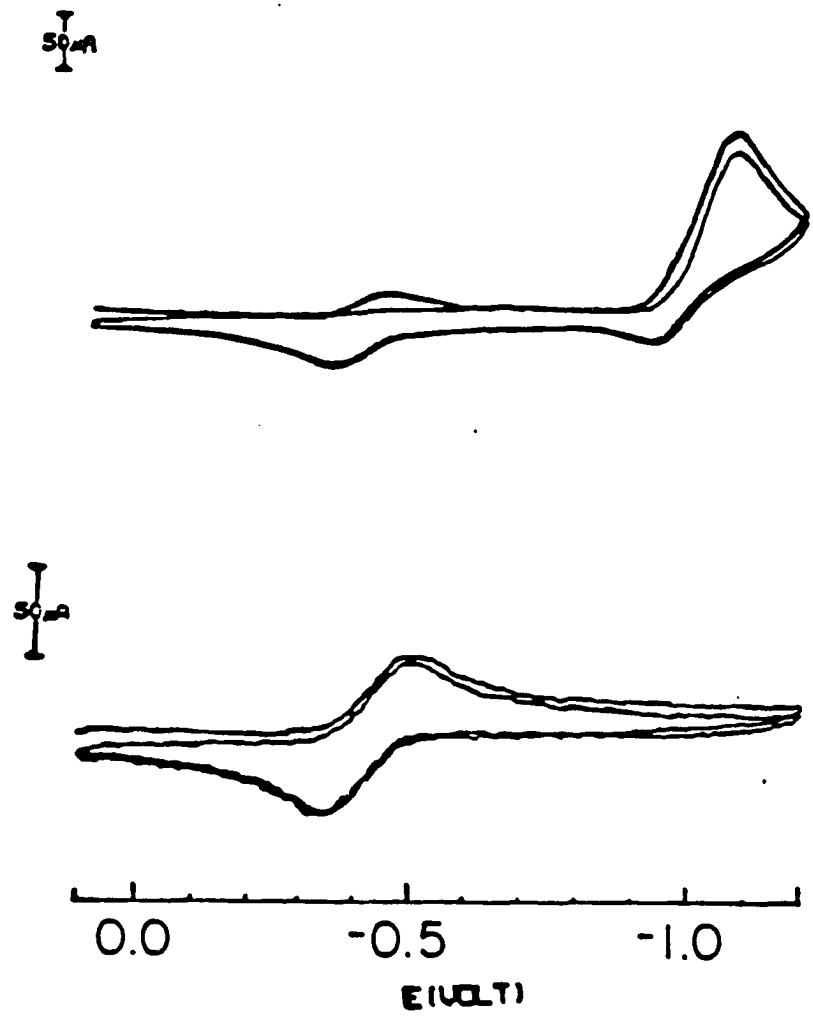

Figure V-1. Cyclic voltammograms at 25 °C in air-free 0.06 M Me_4NBF_4 CH_3CN solutions of (a) 2.0×10^{-3} M $1\text{-}C_3H_7Co_3Co(dmgBF_2)_2H_2O$, scan rate 1.2 V/s; (b) 2.0×10^{-3} M $Co(dmgBF_2)_2(H_2O)_2$, scan rate 1.3 V/s

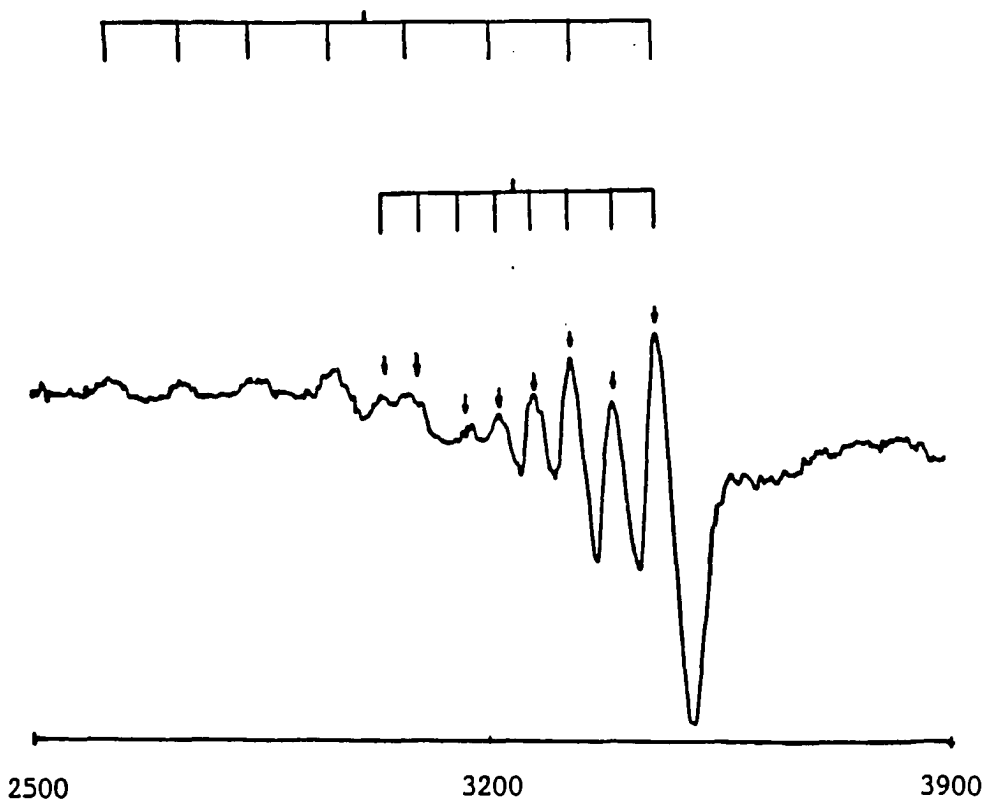

Figure V-2. ESR spectrum of a frozen solution (100 K) obtained after a 2.0×10^{-3} M solution of $4\text{-}BrC_6H_4CH_2Co(dmgBF_2)_2(H_2O)$ was partly reduced electrochemically at -1.0 V in 0.06 M Me_4NBF_4 in acetonitrile. ν = 9.4582 GHz, CF = 3200 G, SW = 1400 G, PW = 12 dB, Gain = 1.25×10^6, Mod = 4.0 Gpp, ST = 500 s, TC = 2.0×10^3 ms

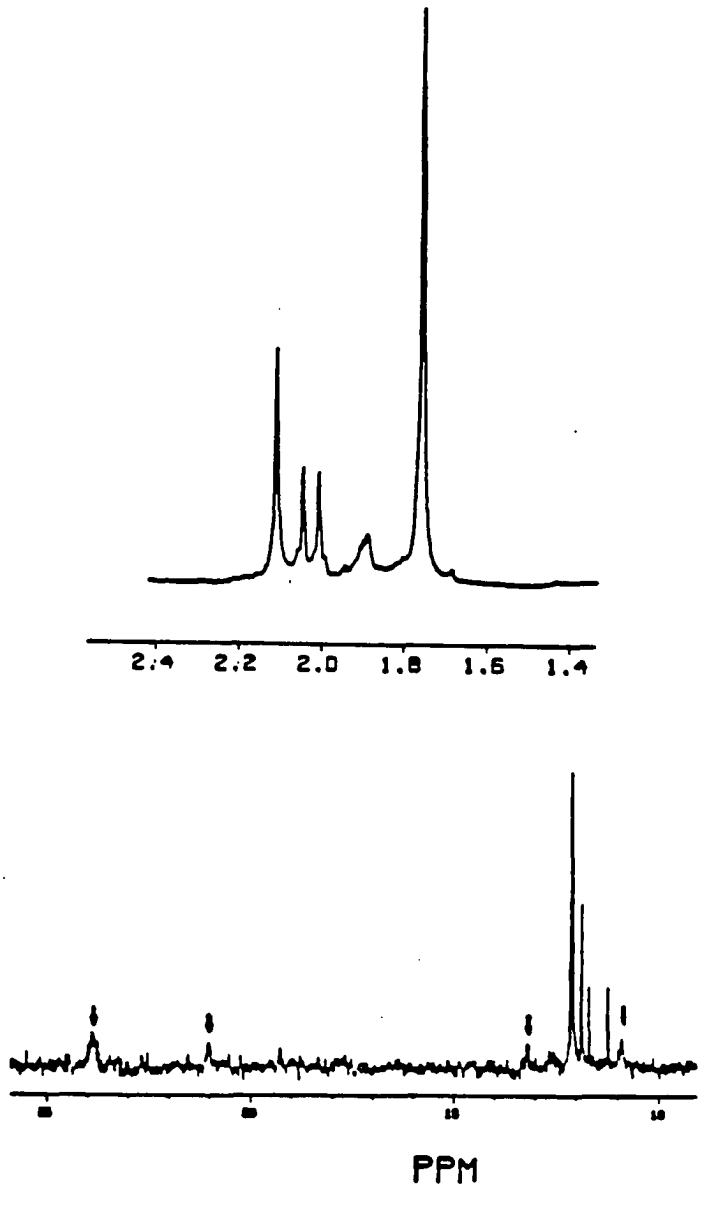

Figure V-3. ^{1}H-NMR (a), and ^{13}C-NMR (b) of 1.0×10^{-2} M $CH_3Co(dmgBF_2)_2py$ reduced by excess $NaBH_4$ in air-free DMSO-d_6 solution at 25 °C. Arrows in (b) show four kinds of different carbons attached to nitrogens

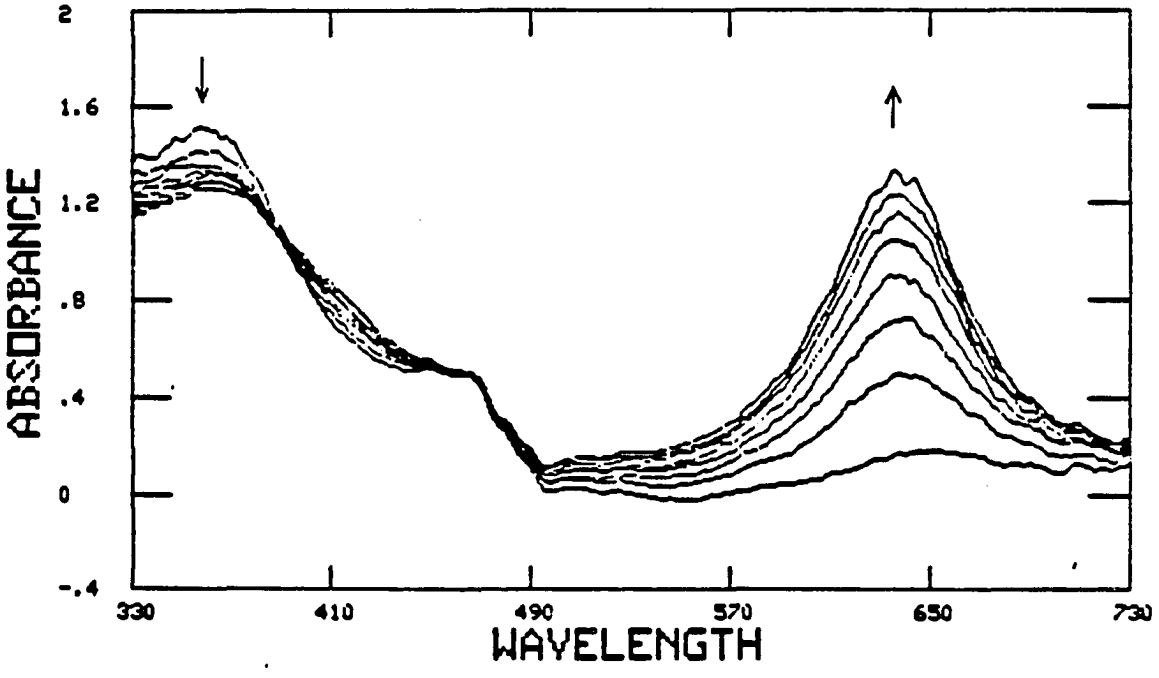

Figure V-4. Fast repetitive scans at 25 °C, following the reaction between 1.7 x 10^{-4} M $CH_3Co(dmgBF_2)_2py$ and 4.1 x 10^{-4} M $Ni(tmc)^+$ in 1:1 CH_3COCH_3 / H_2O air-free solution. Ionic strength μ = 0.06 M ($LiClO_4$); pH = 12 (NaOH)

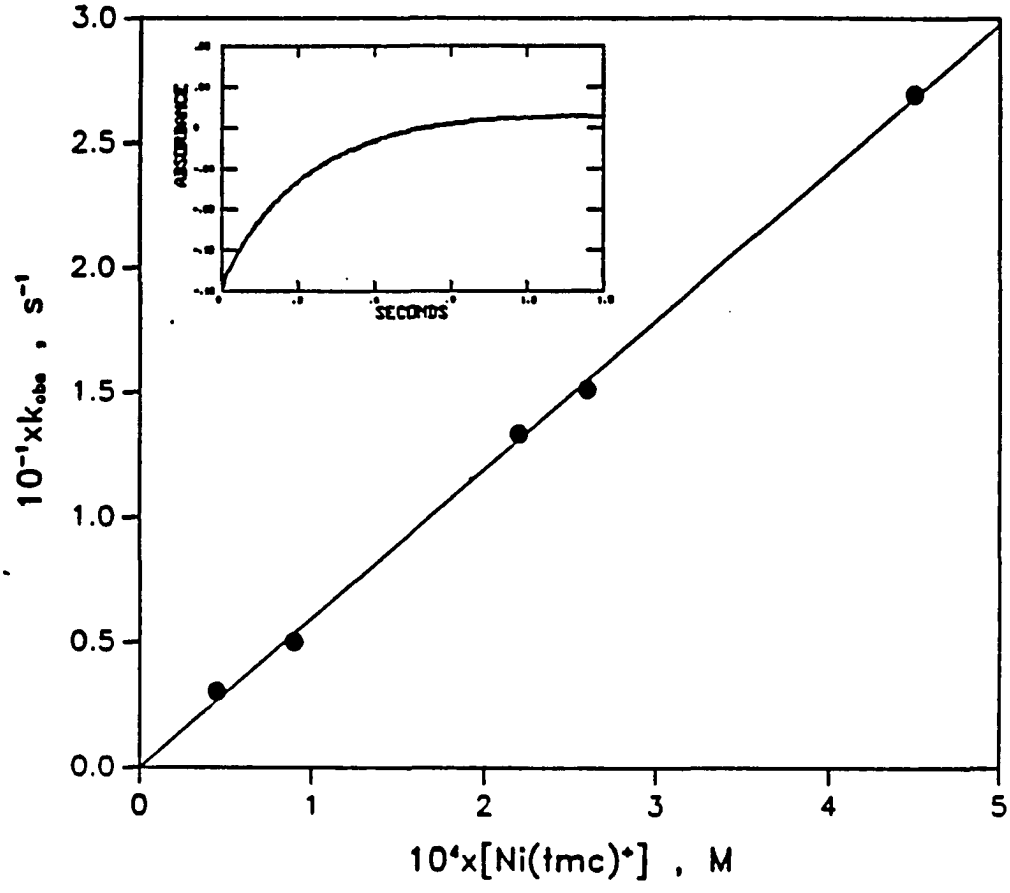

Figure V-5. A plot showing the variation of the pseudo-first-order rate constant k_{obs} with concentration of $Ni(tmc)^+$ at 25 °C for the reaction between $CH_3Co(dmgBF_2)_2py$ and $Ni(tmc)^+$ in an air-free aqueous solution of pH 12 (NaOH) and 0.10 M ionic strength ($LiClO_4$). The inset shows a stopped-flow kinetic trace monitored at 610 nm for a run with $[Ni(tmc)^+]_{av} = 2.7 \times 10^{-4}$ M and $[CH_3Co(dmgBF_2)_2py]_0 = 3.7 \times 10^{-5}$ M

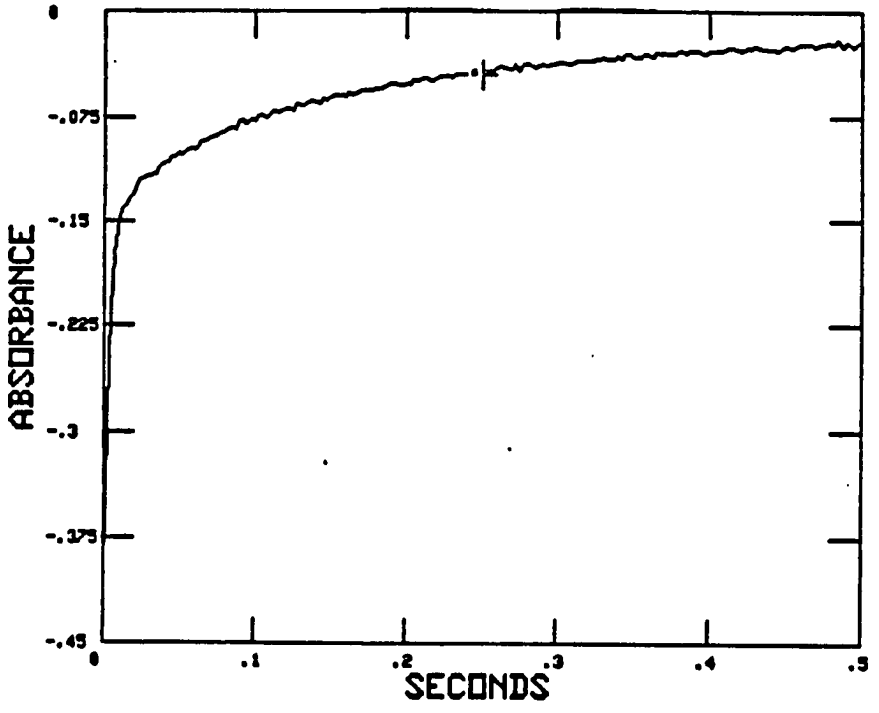

Figure V-6. A typical bi-exponential kinetic trace recorded at 25 °C in an air-free aqueous solution of pH 12 (NaOH) and 0.10 M ionic strength ($LiClO_4$), showing a two-step reaction process. The reaction was monitored at 610 nm with $[4\text{-}BrC_6H_4CH_2Co(dmgBF_2)_2(H_2O)]_0 = 2.5 \times 10^{-5}$ M, and $[Ni(tmc)^+]_0 = 2.64 \times 10^{-4}$ M

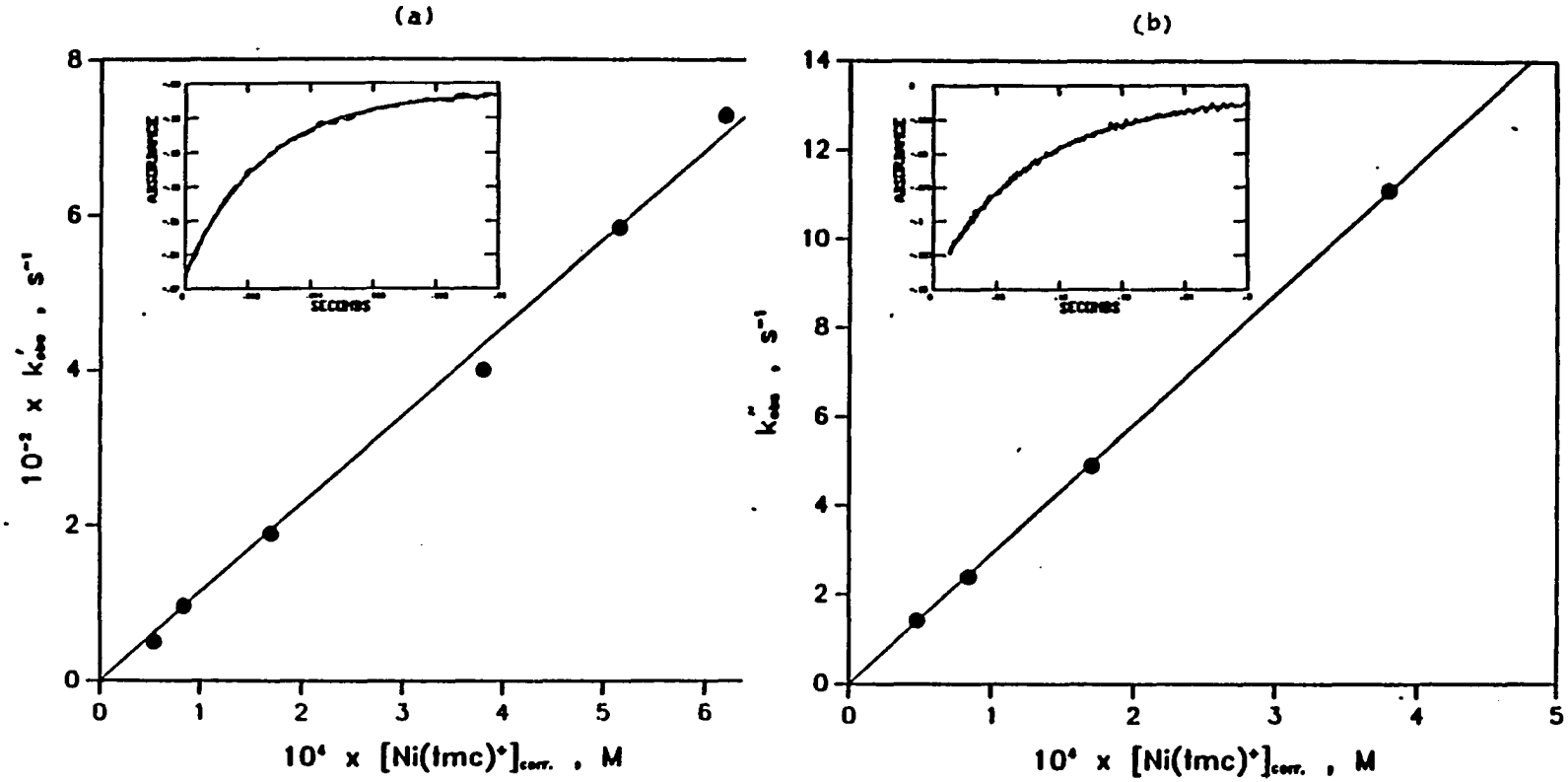

Figure V-7. Dependence of k_{obs} on $[Ni(tmc)^+]$ in the fast (a) and slow (b) phase of the reaction between $4\text{-}BrC_6H_4CH_2Co(dmgBF_2)_2py$ and $Ni(tmc)^+$ in a pH 12 aqueous solution with μ = 0.10 M. The insets show the kinetic traces in the fast and slow phases with $[Ni(tmc)^+]_{av} = 3.8 \times 10^{-4}$ M, and $[4\text{-}BrC_6H_4CH_2Co(dmgBF_2)_2py]_0 = 2.5 \times 10^{-5}$ M

REFERENCES

(1) Iodice, A. A.; Barker, H. J. Biol. Chem. 1963, 238, 2094.

(2) Eagar, R. G.; Baltimore, B. G.; Herbst, M. M.; Barker, H.A.; Richards, J. H. Biochemistry 1972, 11, 253.

(3) Blakley, R. L. J. Biol. Chem. 1965, 240, 2173.

(4) Goulian, M.; Beck, W. S. J. Biol. Chem. 1966, 241, 4233.

(5) Beck, W. S. Vitam. Horm. 1968, 26, 413.

(6) Blakley, R. L. "The Biochemistry of Folic Acid and Related Pteridines" Wiley, New York, 1969, Chapter 9.

(7) Weissbach, H.; Tayler, R. T. Vitam. Horm. 1968, 26, 395.

(8) Lezius, A. G.; Barker, H. A. Biochemistry 1965, 4, 510.

(9) Stadtman, T. C.; Blaylock, B. A. Fed. Proc. 1966, 25, 1657.

(10) Ljungdahl, L.; Irion, E.; Wood, H. G. Fed. Proc. 1966, 25, 1642.

(11) Wood, J. M.; Wolfe, R. S.; Biochemistry 1966, 5, 3598.

(12) Lentz, K.; Wood, H. G. J. Biol. Chem. 1955, 215, 645.

(13) Ljungdahl, L.; Irion, E.; Wood, H. G. Biochemistry 1965, 4, 2771.

(14) Schrauzer, G. N.; Sibert, J. W. J. Am. Chem. Soc. 1970, 92, 3509.

(15) Martin, B. D.; Finke, R. G. J. Am. Chem. Soc. 1990, 12, 2419.

(16) Costa, G.; Puxeddu, A.; Reisenhofer, E. Bioelectrochem. Bioenerg. 1974, 1, 29.

(17) Costa, G.; Puxeddu, A.; Reisenhofer, E. Experientia Suppl. 1971, 18, 235.

(18) Costa, G.; Puxeddu, A.; Reisenhofer, E. J. Chem. Soc. Commun. 1971, 993.

(19) Brockway, D. J.; West, B. O.; Bond, A. M. J. Chem. Soc., Dalton Trans. 1979, 1891.

(20) Costa, G.; Puxeddu, A.; Rersenhofer, E. J. Chem. Soc., Dalton Trans. 1972, 1519.

(21) Costa, G.; Puxeddu, A.; Tavagnacco, C.; Balducci, G.; Kumar, R. Gazzetta Chim. Ital. 1986, 116, 735.

(22) Dolphin, D.; Johnson, A. W.; Rodrigo, R. Ann. N.Y. Acad. Sci. 1964, 112, 590.

(23) Schrauzer, G. N.; Acc. Chem. Res. 1968, 1, 97.

(24) (a)Schrauzer, G. N.; Pure Appl. Chem. 1973, 33, 545. (b)Schrauzer, G. N.; Grate, J. H.; Katz, R. H. Bioinorg. Chem. 1978, 8, 1. (c)Schrauzer, G. N.: Deutsch, E.; Windgassen, R. J. J. Amer. Chem. Soc. 1968, 90, 2441.

(25) Schrauzer, G. N.; Sock, J. A.; Holland, R. J.; Beckham, T. M.; Rubin, E. M.; Sibert, J. W. Bioinorg. Chem. 1972, 2, 93.

(26) Schrauzer, G.N.; Sibert, J.W. J. Am. Chem. Soc. 1970, 92, 3509.

(27) Atkins, M. P.; Golding, B. T.; Burg, A.; Johnson, M. D.; Sellars, P. J. J. Am. Chem. Soc. 1980, 102, 3630.

(28) LeHoang, M.; Robin, Y.; Devynck, J.; Bied-Charreton, C.; Gaudemer, A.; J. Organomet. Chem. 1981, 222, 311.

(29) Rytz, G.; Walder, L.; Scheffold, R. In "Vitamin B_{12}: Proceedings of the Third European Symposium". Zagalak, B.; Friedrich, W. Eds., Walter de Gruyter, New York, 1979, p 173.

(30) Walder, L.; Rytz, G.; Meier, K.; Scheffold, R. Helv. Chim. Acta 1978, 61, 3013.

(31) Schrauzer, G. N.; Windgassen, R.J. J. Am. Chem. Soc. 1966, 88, 3738.

(32) Bakac, A.; Espenson, J. H. J. Am. Chem. Soc. 1984, 106, 5197.

(33) Tovrog, B. S.; Kitko, D. J.; Drago, R. S. J. Am. Chem. Soc. 1976, 98, 5144.

(34) Barefield, E. K.; Wagner, F. Inorg. Chem. 1973, 12, 2435.

(35) Ram, M. S.; Bakac, A.; Espenson, J. H. Inorg. Chem. 1986, 25, 3267.

(36) Heller, S. R. "EPA/NIH Mass Spectral Data Base" Vol. 1. Washington, 1978.

(37) Bakac, A.; Brynildson, M. E.; Espenson, J. H. Inorg. Chem. 1986, 25, 4108.

(38) The configuration of the singly reduced organochromium(II) species is assumed to be penta coordinated because of its expected ligand substitutional lability (17 e^-, Co(II) species). Experimentally, the distribution of the decomposition products shows no observable difference wether one started with $RCo(dmgBF_2)_2py$ or with $RCo(dmgBF_2)_2H_2O$.

(39) "Lange's Handbook of Chemistry" 13th Ed. Edt. by Dean, J.A., McGraw-Hill Book Company, New York, 1985.

(40) Brown, K. L.; Syeverenyi, Z. Inorg. Chem. Acta 1986, 119, 149.

(41) Brown, K. L.; Hessley, R. K. Inorg. Chem. 1980, 19, 2410.

(42) Espenson, J. H.; Wang, D. M. Inorg. Chem. 1979, 18, 2853.

(43) Samsel, E. G.; Kochi, J. K. J. Am. Chem. Soc. 1986, 108, 4790.

(44) Tamblyn, W. H.; Klingler, R. J.; Hwang, W. S.; Kochi, J. K. J. Am. Chem. Soc. 1981, 103, 3161.

(45) Sorek, Y.; Cohen, H.; Meyerstein, D. J. Chem. Soc. Faraday Trans. 1, 1989, 85, 1169.

(46) Brown, K. L. J. Am. Chem. Soc. 1979, 101, 6600.

(47) Shi, S.; Daniels, L.M.; Espenson, J. H. Inorg. Chem. (submitted).

(48) Endicott, J. F.; Lilie, J.; Kuszaj, J. M.; Ramaswamy, B. S.; Schmonsees, W. G.; Simic, M. S.; Glick, M. D.; Rillema, J. A. J. Am. Chem. Soc. 1977, 99, 429.

(49) Walker, F. A. J. Am. Chem. Soc. 1970, 92, 4235.

(50) Nishida, Y.; Kida, S.; Coord. Chem. Rev. 1979, 27, 275.

(51) Lin, W. C.; McDowell, C. A.; Ward, D.J. J. Chem. Phys. 1968, 49, 2883.

PART VI. MOLECULAR STRUCTURE OF A COBALT(I) COMPLEX LACKING A CARBONYL LIGAND. A UNIQUE EXAMPLE OF Co-N BOND SHORTENING

INTRODUCTION

It is well known that Vitamin B_{12} (= cyanocobalamin) and its derivative B_{12a} (aquocobalamin) can be reduced by one electron to B_{12r} (= cobalt(II)cobalamin) and by two electrons to B_{12s}.[1] The crystal structure of B_{12r} was also determined recently.[2] Vitamin B_{12s} exists in solution as the cobalt(I) complex, although at higher acidities it is in equilibrium with its conjugate acid, HCo^{III}(corrin), with pK_a 1.[3-5] The B_{12} model complexes $Co^{I}(dmgH)_2py^-$ and $HCo^{III}(dmgH)_2py$ are also known; here the acidity is lower (pK_a 9)[6-9] and the rate of acid-base interconversion sufficiently low that the two forms undergo separate and not always identical chemical reactions.[9-12]

We have now succeeded in isolating single crystals of a closely related model complex which is an example of a nonporphyrin cobalt(I) macrocycle, and which lacks a carbonyl or phosphine ligand. The compound studied is $[(CH_3)_4N][Co(dmgBF_2)_2py]CH_3CN$. It contains the anion $Co(dmgBF_2)_2py^-$ (py = C_5H_5N; $(dmgBF_2)_2^{2-}$ = bis[(difluoroboryl)dimethylglyoximato]), which was first prepared by Schrauzer.[13] This is of interest not only because of the biological role B_{12}, but also because, aside from species containing carbonyl, phosphine, or porphyrin ligands,[14-20] this is the first cobalt(I) macrocyclic complex to be so characterized. Moreover, the structure is of interest in its own right because of the considerable variations in distances, angles, and displacements that are found in it, compared to those in the cobalt(II) analogue. Cobalt(I) macrocycle complexes are often short lived owing to high reactivity with protic solvents or to internal metal-

ligand decompositions. The species examined here is moderately stable, even more so than the cobaloxime parent, $Co(dmgH)_2py^-$. In general cobalt(I) complexes are strong nucleophiles[2,12,13,21-24] and Bronsted (as well as Lewis) bases.[6-9,24] Several catalytic reactions of cobalt(I) macrocycles are known.[23-25]

RESULTS AND DISCUSSION

The pentacoordinated structure of the cobalt(I) monoanion $Co(dmgBF_2)_2py^-$ is depicted in the ORTEP diagram given in **Figure VI-1.** The structure is square pyramidal. The closest analogues are cobalt(I) porphyrins.[26,27] Most often cobalt(I) needs to be stabilized by CO (or phosphine) coordination,[25-30] as in the trigonal bipyramidal 18e cobalt(I) compound $Co(BiPh_2)(CO)_3(PPh_3)$.[16]

The structural refinement of $Co(dmgBF_2)_2^-$ establishes that the imine nitrogens, methylene carbons, and oxygens of the $(dmgBF_2)_2^{2-}$ macrocycle constitute a base planar (χ^2 = 4105) entity made rigid by the sp^2 C=N hybridization. The cobalt atom is displaced 0.257 Å toward pyridine above the macrocyclic plane. The aromatic plane of pyridine bisects the equatorial plane through the two boron atoms; the two BF_2 units are displaced below the equatorial plane, away from the coordinated pyridine. Crystallographic data are summarized in **Tables VI-1** and **VI-2.**

Selected bond lengths and angles are given in **Tables VI-3, VI-4** And **VI-5. Table VI-5** also contains data for analogous compounds. The bond distance between cobalt(I) to a nitrogen atom of the equatorial ligands 1.839(4) Å is significantly shorter than other Co(I)-N_{eq} single bonds (ca. 2.1 Å, **Table VI-5**). Moreover the distance is unmistakably shorter than the average Co(II)-N_{eq} distance of 1.878(4) in the cobalt(II) complex, $Co(dmgBF_2)_2(CH_3OH)_2$. In fact, the Co(I)-N_{eq} distance in the anion is the shortest distance so far reported.

The short Co(I)-N_{eq} bond distance relative to Co(II)-N_{eq} contradicts what one might have presumed: a considerable bond lengthening should

attend reduction of cobalt(II) to cobalt(I). The displacement of cobalt(I) above the N_4 equatorial plane is therefore not to be attributed to the larger size of the low-valent cobalt ion. Correspondingly, to accommodate the change of the Co-N bond distance, the O-N-C(methylene) and N-C(methylene)-C(methylene) bond angles in the cobalt(I) anion are smaller (av. 116.3(3) and 111.0(4)°, respectively) than those in the cobalt(II) compound (av. 119.76(39) and 112.72(42)°, respectively).[31]

It is interesting to note that the addition of one extra electron to the d_{z^2} orbital in the cobalt(II) complex is not only accompanied by a reduction in coordination number but also by a decrease in the $Co-N_{eq}$ bond distances. Strengthening of an M-CO bond attending an increase of electron density at the metal center is well known, as it is often reflected by the decrease of ν_{CO}.[32] Similar shortening of the $Co-N_{eq}$ bond in macrocycles is rare, the only example being the carbonyl containing species $[Co(CO)(C_{10}H_{17}N_8)]$[28] where π-backbonding to the equatorial ligand was invoked to account for short Co-N bonds. Our data clearly support a similar explanation. We feel this is a particularly clear example since no carbonyl group is involved and since the same $Co(dmgBF_2)_2$ unit has been structurally characterized in both cobalt(I) and (II) oxidation states.

The diamagnetism of the low spin d^8 $Co(dmgBF_2)_2py^-$ is consistent with our finding that it has a normal ^1H nmr spectrum and no ESR signal. The diamagnetism of similar cobalt(I), rhodium(I), and iridium(I) compounds is well documented.[33-36] There is no evidence of axial hydrogen coordination from the difference Fourier map and refinement. The electron configuration at cobalt should be $(d_{xz})^2(d_{yz})^2(d_{xy})^2(d_z)^2$

because of the short $Co^{I}-N_{eq}$ bonds, the absence of a sixth axial ligand, and the diamagnetism of the complex.

The axial displacement of cobalt may significantly decrease the repulsion between the electron lone pairs of nitrogen atoms in $(dmgBF_2)_2$ ligand and the filled d_z2 orbital of the cobalt as the upward displacement of the cobalt from the basal plane results in the nitrogen lone pairs approaching the nodal plane of the d_z2 orbital of cobalt. This diminishing antibonding repulsion may contribute to the shortening of the $Co^{I}-N_{eq}$ bonds.

It is also very important to note that the axial displacement of cobalt in $Co(dmgBF_2)_2py^-$ removes the symmetry forbiddeness of the overlap of the cobalt d_z2 orbital with the π_1^* orbital of $(dmgBF_2)_2$ [37] which is otherwise present in the cobalt(II) complex. This allows charge transfer (backbonding) to occur in the sense $Co(d_z2) \rightarrow (dmgBF_2)_2(\pi_1^*)$. The doubly populated d_z2 orbital in the cobalt(I) form not only increases the electron density available for back donation but also increases the energy of the d_z2 orbital making back bonding more energetically favorable.

An extreme of such back donation is an intramolecular electron transfer resulting $[Co^{III}(dmgBF_2)_2{}^{4-}py]^-$ or $[Co^{III}(dmgBF_2)_2{}^{2-}py^{2-}]^-$. But we do not believe the assignment of Co(III) oxidation state to $[Co(dmgBF_2)_2]^-$ to be appropriate. This is because: (1)The deep blue color of $[Co(dmgBF_2)_2]^-$ is known to be associated with Co(I) oxidation state. Relavent inorganic Co(III) macrocyclic complexes are known to be yellow (e.g., $ClCo(dmgBF_2)_2P(C_4H_9)_3$) or brown (e.g., $ClCo(dmgBF_2)_2py$).[38] (2)All the known inorganic Co(III) complexes of bis(dimethylglyoximato)

and bis[(difluoroboryl)dimethylglyoximato] are hexacoordinated to satisfy the 18e rule.[38-41] No precedent is found in these groups of Co(III) complexes where cobalt is only pentacoordinated.

Displacement of cobalt above the N_4 equatorial plane seems necessary to make such a short Co^I-N_{eq} bond. Such a displacement is also noticed in $Co(CO)(C_{10}H_{17}N_8)$,[28] where a short Co-N bond was observed. On the other hand, consider the case of Co^I(HDP) (HDP = 2,2,3,3,7,7,8,8,12,12,13,13,17,17,18,18-hexadecamethyl-10,20-diaza-octahydroporphinato)[27] where such a displacement is absent and cobalt is coplanar with the four nitrogen atoms of the equatorial ligand. Even though the ligand contains a more highly conjugated π-system (and is therefore a better electron acceptor) the Co^I-N bond is still relatively long, 1.91 Å.[27] This comparison suggests that the metal donor orbital needs to be displaced from the coordination plane in order to function, recommending the notion of the cobalt d_z2 orbital being the electron donating orbital.

As shown in Table VI-5, the bond distances between imine nitrogens and adjacent carbons, and those between the pair of adjacent methylene carbons change with oxidation state, such that: N-C(Co^I) > N-C(Co^{II}) and C-C(Co^I) < C-C(Co^{II}). This bond length alternation is indicative of increased electron density in the π*(LUMO) orbital of $(dmgBF_2)_2$, apparently as a result of the Co(d_{z^2}) → $(dmgBF_2)_2(\pi_1^*)$ backbonding.

Obviously the bond length change within the equatorial ligand cannot be attributed to axial coordination. Moreover the bond parameters of the axial pyridine are normal.[42] The BF_2 units certainly serve to stabilize

the cobalt(I) oxidation state via an inductive effect, but no unambiguous comparison can be made based on the structural data.

EXPERIMENTAL SECTION

Crystal Growth. The formation of the macrocyclic monoanion $Co(dmgBF_2)_2py^-$ is recognized by the intense blue coloration[43,44] that develops. It can be generated either by controlled potential reduction of its parent neutral compound $Co(dmgBF_2)_2(H_2O)_2$ in acetonitrile in the presence of one equivalent of pyridine at -0.44 V (vs NHE) or by decomposition of alkyl-$Co(dmgBF_2)_2py^{2-}$ in acetonitrile. Formation of n-$C_3H_7Co(dmgBF_2)_2py^{2-}$ can be achieved by controlled potential electrolysis of n-$C_3H_7Co(dmgBF_2)_2py$ at -1.90 V (vs NHE) in 0.06 M $(CH_3)_4NBF_4$ acetonitrile solution. An air-free electrocell with a mercury pool working electrode, a platinum plate auxiliary electrode, and an Ag/AgCl reference electrode was used to conduct the electrolysis. Owing to much the higher solubility of n-$C_3H_7Co(dmgBF_2)_2py$ over $Co(dmgBF_2)_2(H_2O)_2$ in acetonitrile, the second method was adopted to obtain a crystal for this study. A three layer solution system in a test tube was employed for the crystal to grow. Diethyl ether was allowed to diffuse slowly from the top layer through a C_5H_{12} middle layer into the bottom layer of the dark blue acetonitrile solution containing the title compound, all at 0 °C. The middle layer, which is immiscible with the blue acetonitrile solution on the bottom, functions as a spacer to slow the diffusion of diethyl ether into the acetonitrile solution and ensure the quality of crystals for the diffraction study. Anaerobic conditions are required owing to the extreme sensitivity of $Co(dmgBF_2)_2py^-$ solution toward oxygen. The deep blue crystal of $[(CH_3)_4N][Co(dmgBF_2)_2py]\cdot CH_3CN$ is less air sensitive.

X-Ray Data Collection. A dark blue crystal of the title compound was taken from a nitrogen-filled test tube and attached to the tip of a glass fiber. The crystal was then moved into the cold stream of the low-temperature device on the diffractometer, and slowly cooled to -75 °C. The cell constants were determined from a list of reflections found by an automated search routine. Pertinent data collection and reduction information are given in **Table VI-1.**

A total of 4741 reflections were collected in the ±h, k, ±l hemisphere. Lorentz and polarization corrections were applied. An absorption correction based on a series of psi-scans was applied, and equivalent reflections were averaged.

Determination and Refinement of the Structure. The choice of the centric triclinic group was indicated initially by intensity statistics, and later confirmed by the successful refinement of the structure. the positions of all of the non-hydrogen atoms of the complex and the associated counter ion were found by an automatic Patterson interpretation method.[45] One molecule of acetonitrile was later located in a difference Fourier map. In the final stages of refinement, the non-hydrogen atoms were refined with anisotropic temperature factors, and hydrogen atoms were added in idealized positions. A common isotropic temperature factor was refined for each of these groups of hydrogen atoms: one for the methyl hydrogens of the complex, one for the pyridinyl hydrogens, and one for the methyl hydrogen atoms on the $[(CH_3)_4N]^+$ and CH_3CN moieties.

X-ray data collection and structure solution were carried out at the Iowa State Molecular Structure Laboratory. Refinement calculations were

performed on a Digital Equipment Corp. Micro VAX-II computer using the SHELX-76 programs.[46]

Table VI-1. Crystallographic Data for $[(CH_3)_4N][Co(dmgBF_2)_2py]\cdot CH_3CN$.

Formula	$C_{18}H_{29}B_2N_6O_4F_4Co\cdot CH_3CN$
Formula weight	579.02
Space Group	$P\bar{1}$
a, Å	12.492(4)
b, Å	12.883(3)
c, Å	8.996(3)
α, deg	99.39(2)
β, deg	109.25(2)
γ, deg	103.72(2)
V, Å^3	1280.9(7)
Z	2
d_{calc}, g/cm^3	1.501
Crystal size, mm	0.4 x 0.3 x 0.2
$\mu(MoK_\alpha)$, cm^{-1}	7.338
Data collection instrument	Enraf-Nonius CAD4
Radiation (monochromated in incident beam)	$MoK_\alpha(\lambda = 0.71073Å)$
Orientation reflections, number, range (2θ)	19, $18.2 < 2\theta < 34.7$
Temperature, °C.	-75(1)
Scan method	ω–scans
Data col. range, 2θ, deg	4.0–50.0
No. data collected:	4741
No. unique data, total:	4513
with $F_o^2 > 3\sigma(F_o^2)$:	3341
Number of parameters refined	337
R[a]	0.045
R_w[b]	0.061
Quality-of-fit indicator	1.01
Largest shift/esd, final cycle	<0.01
Largest peak, e/Å^3	0.62(8)

[a] $R = \Sigma||F_o| - |F_c||/\Sigma|F_o|$ [b] $R_w = [\Sigma w(|F_o| - |F_c|)^2/\Sigma w|F_o|^2]^{1/2}$; $w = 1/\sigma^2(|F_o|)$

Table VI-2. Positional Parameters of $[(CH_3)_4N][Co(dmgBF_2)_2py]\cdot CH_3CN$

Atom	x	y	z	B(Å²)
Co(1)	0.21545(4)	0.27016(4)	0.00770(6)	1.61(1)
F(1)	0.0133(2)	0.1333(2)	-0.3952(3)	3.04(7)
F(2)	-0.0705(2)	0.2693(2)	-0.4501(3)	3.70(8)
F(3)	0.3714(2)	0.0810(2)	0.1245(3)	2.80(6)
F(4)	0.4863(2)	0.1802(2)	0.3886(3)	3.06(7)
O(1)	0.1290(2)	0.3214(2)	-0.3003(3)	2.41(7)
O(2)	-0.0258(2)	0.2426(2)	-0.1963(3)	2.29(7)
O(3)	0.2955(2)	0.1829(2)	0.2852(3)	2.30(7)
O(4)	0.4527(2)	0.2749(2)	0.1923(3)	2.31(7)
N(1)	0.0515(3)	0.2176(2)	-0.0673(4)	1.78(8)
N(2)	0.2002(3)	0.1897(3)	0.1554(4)	1.85(8)
N(3)	0.3732(3)	0.2853(2)	0.0492(4)	1.95(8)
N(4)	0.2232(3)	0.3081(3)	-0.1772(4)	2.01(8)
N(5)	0.2407(3)	0.4225(3)	0.1407(4)	2.04(9)
C(1)	0.0036(3)	0.1653(3)	0.0208(5)	2.0(1)
C(2)	0.0939(3)	0.1493(3)	0.1560(4)	2.0(1)
C(3)	0.4198(4)	0.3299(3)	-0.0478(5)	2.2(1)
C(4)	0.3286(4)	0.3424(3)	-0.1843(5)	2.2(1)
C(5)	-0.1269(4)	0.1254(4)	-0.0178(5)	3.1(1)
C(6)	0.0686(4)	0.0932(4)	0.2772(6)	3.5(1)
C(7)	0.5496(4)	0.3617(4)	-0.0176(6)	3.1(1)

Table VI-2. (continued)

Atom	x	y	z	B(Å²)
C(8)	0.3494(4)	0.3843(4)	-0.3207(5)	3.4(1)
C(11)	0.1794(4)	0.4875(3)	0.0770(5)	2.8(1)
C(12)	0.1921(4)	0.5909(4)	0.1644(6)	3.7(1)
C(13)	0.2732(5)	0.6304(4)	0.3261(6)	3.7(1)
C(14)	0.3386(4)	0.5654(4)	0.3915(5)	3.3(1)
C(15)	0.3200(4)	0.4621(3)	0.2966(5)	2.6(1)
B(1)	0.0136(4)	0.2400(4)	-0.3348(5)	2.4(1)
B(2)	0.3993(4)	0.1795(4)	0.2435(5)	2.2(1)
N(6)	0.3308(3)	-0.0035(3)	-0.3228(4)	2.34(9)
C(21)	0.2385(4)	0.0515(4)	-0.3199(6)	3.3(1)
C(22)	0.3144(4)	-0.1002(4)	-0.2514(5)	3.0(1)
C(23)	0.4528(4)	0.0766(4)	-0.2291(6)	3.5(1)
C(24)	0.3165(4)	-0.0436(4)	-0.4972(5)	3.0(1)
N(7)	0.8121(6)	0.3497(6)	0.2190(9)	9.0(3)
C(31)	0.9116(6)	0.3823(6)	0.2816(8)	5.8(2)
C(32)	1.0392(6)	0.4204(6)	0.3562(9)	6.7(2)

Anisotropically refined atoms are given in the form of the isotropic equivalent displacement parameter defined as:
(4/3) * [a²*B(1,1) + b²*B(2,2) + c²*B(3,3) + ab(cos gamma)*B(1,2) + ac(cos beta)*B(1,3) + bc(cos alpha)*B(2,3)]

Table VI-3. Bond Distances ($d/10^{-10}$ m) and their Standard Deviations of $[(CH_3)_4N][Co(dmgBF_2)_2py]\cdot CH_3CN$.

Atom 1	Atom 2	Distance	Atom 1	Atom 2	Distance
Co(1)	N(1)	1.842(3)	N(4)	C(4)	1.312(6)
Co(1)	N(2)	1.844(4)	N(5)	C(11)	1.337(6)
Co(1)	N(3)	1.836(3)	N(5)	C(15)	1.349(4)
Co(1)	N(4)	1.834(4)	C(1)	C(2)	1.443(5)
Co(1)	N(5)	2.019(3)	C(1)	C(5)	1.488(6)
F(1)	B(1)	1.393(6)	C(2)	C(6)	1.479(7)
F(2)	B(1)	1.385(6)	C(3)	C(4)	1.436(5)
F(3)	B(2)	1.407(5)	C(3)	C(7)	1.494(6)
F(4)	B(2)	1.393(5)	C(4)	C(8)	1.491(7)
O(1)	N(4)	1.392(4)	C(11)	C(12)	1.375(6)
O(1)	B(1)	1.468(5)	C(12)	C(13)	1.394(6)
O(2)	N(1)	1.384(4)	C(13)	C(14)	1.373(7)
O(2)	B(1)	1.481(6)	C(14)	C(15)	1.380(6)
O(3)	N(2)	1.398(4)	N(6)	C(21)	1.495(7)
O(3)	B(2)	1.472(6)	N(6)	C(22)	1.495(6)
O(4)	N(3)	1.392(4)	N(6)	C(23)	1.490(5)
O(4)	B(2)	1.472(6)	N(6)	C(24)	1.506(6)
N(1)	C(1)	1.317(6)	N(7)	C(31)	1.12(1)
N(2)	C(2)	1.309(5)	C(31)	C(32)	1.43(1)
N(3)	C(3)	1.330(6)			

Numbers in parentheses are estimated standard deviations in the least significant digits.

Table VI-4. Bond Angles (degrees) and their Standard Deviations of $[(CH_3)_4N][Co(dmgBF_2)_2py]\cdot CH_3CN$

Atom 1	Atom 2	Atom 3	Angle	Atom 1	Atom 2	Atom 3	Angle
N(1)	Co(1)	N(2)	80.7(1)	O(1)	N(4)	C(4)	115.8(3)
N(1)	Co(1)	N(3)	164.4(1)	Co(1)	N(5)	C(11)	121.1(2)
N(1)	Co(1)	N(4)	96.6(1)	Co(1)	N(5)	C(15)	121.1(3)
N(1)	Co(1)	N(5)	98.5(1)	C(11)	N(5)	C(15)	117.8(3)
N(2)	Co(1)	N(3)	96.9(2)	N(1)	C(1)	C(2)	111.1(4)
N(2)	Co(1)	N(4)	162.4(1)	N(1)	C(1)	C(5)	124.1(4)
N(2)	Co(1)	N(5)	99.7(1)	C(2)	C(1)	C(5)	124.7(4)
N(3)	Co(1)	N(4)	81.0(2)	N(2)	C(2)	C(1)	111.0(4)
N(3)	Co(1)	N(5)	97.0(1)	N(2)	C(2)	C(6)	124.9(4)
N(4)	Co(1)	N(5)	97.9(1)	C(1)	C(2)	C(6)	124.2(4)
N(4)	O(1)	B(1)	113.0(3)	N(3)	C(3)	C(4)	110.9(4)
N(1)	O(2)	B(1)	111.9(3)	N(3)	C(3)	C(7)	124.1(4)
N(2)	O(3)	B(2)	112.8(3)	C(4)	C(3)	C(7)	125.1(4)
N(3)	O(4)	B(2)	111.9(2)	N(4)	C(4)	C(3)	111.2(4)
Co(1)	N(1)	O(2)	124.7(3)	N(4)	C(4)	C(8)	124.1(4)
Co(1)	N(1)	C(1)	118.0(2)	C(3)	C(4)	C(8)	124.7(4)
O(2)	N(1)	C(1)	116.5(3)	N(5)	C(11)	C(12)	122.9(4)
Co(1)	N(2)	O(3)	124.9(2)	C(11)	C(12)	C(13)	118.8(5)
Co(1)	N(2)	C(2)	118.3(3)	C(12)	C(13)	C(14)	118.7(4)
O(3)	N(2)	C(2)	116.0(3)	C(13)	C(14)	C(15)	119.1(4)
Co(1)	N(3)	O(4)	124.2(3)	N(5)	C(15)	C(14)	122.6(4)
Co(1)	N(3)	C(3)	117.5(3)	F(1)	B(1)	F(2)	110.7(3)

Table VI-4. (continued)

Atom 1	Atom 2	Atom 3	Angle	Atom 1	Atom 2	Atom 3	Angle
O(4)	N(3)	C(3)	117.0(3)	F(1)	B(1)	O(1)	110.7(4)
Co(1)	N(4)	O(1)	125.1(3)	F(1)	B(1)	O(2)	109.5(4)
Co(1)	N(4)	C(4)	118.2(3)	F(2)	B(1)	O(1)	105.6(4)
F(2)	B(1)	O(2)	104.7(4)	C(21)	N(6)	C(22)	109.9(4)
O(1)	B(1)	O(2)	115.4(3)	C(21)	N(6)	C(23)	110.3(3)
F(3)	B(2)	F(4)	109.5(4)	C(21)	N(6)	C(24)	108.8(3)
F(3)	B(2)	O(3)	110.4(3)	C(22)	N(6)	C(23)	109.9(3)
F(3)	B(2)	O(4)	109.6(4)	C(22)	N(6)	C(24)	109.2(3)
F(4)	B(2)	O(3)	104.5(4)	C(23)	N(6)	C(24)	108.8(4)
F(4)	B(2)	O(4)	106.0(3)	N(7)	C(31)	C(32)	177.5(9)
O(3)	B(2)	O(4)	116.5(4)				

Numbers in parentheses are estimated standard deviations in the least significant digits.

Table VI-5. A Comparison of Selected Bond Distances ($d/10^{-10}$ m).

Complex	Coord. No.	Co-N_{eq}	NC(methylene)	C-C	Co-N_4 plane	Ref.
$Co^{II}(dmgBF_2)_2(CH_3OH)_2$	6	1.878(4)	1.270(7)	1.473(7)	0	31
$Co^{I}(dmgBF_2)_2py^-$	5	1.839(4)	1.317(6)	1.443(5)	0.257(1)	This work
$Co^{II}[Me_6[14]dieneN_4]Cl_2$	6	1.976(6)	1.282(9)		0	29
$Co^{I}(CO)(Me_6[14]dieneN_4)^+$	5	2.158(5)	1.271(8)		0.57	29
$Co^{II}(bpy)_3^{2+}$	6	2.128(8)				47
$Co^{I}(bpy)_3^+$	6	2.11(2)				47
$Co^{I}(CO)(C_{10}H_{17}N_8)$	5	1.873(5)	1.335(3)			28
$Co^{I}(HDP)$	4	1.91				27

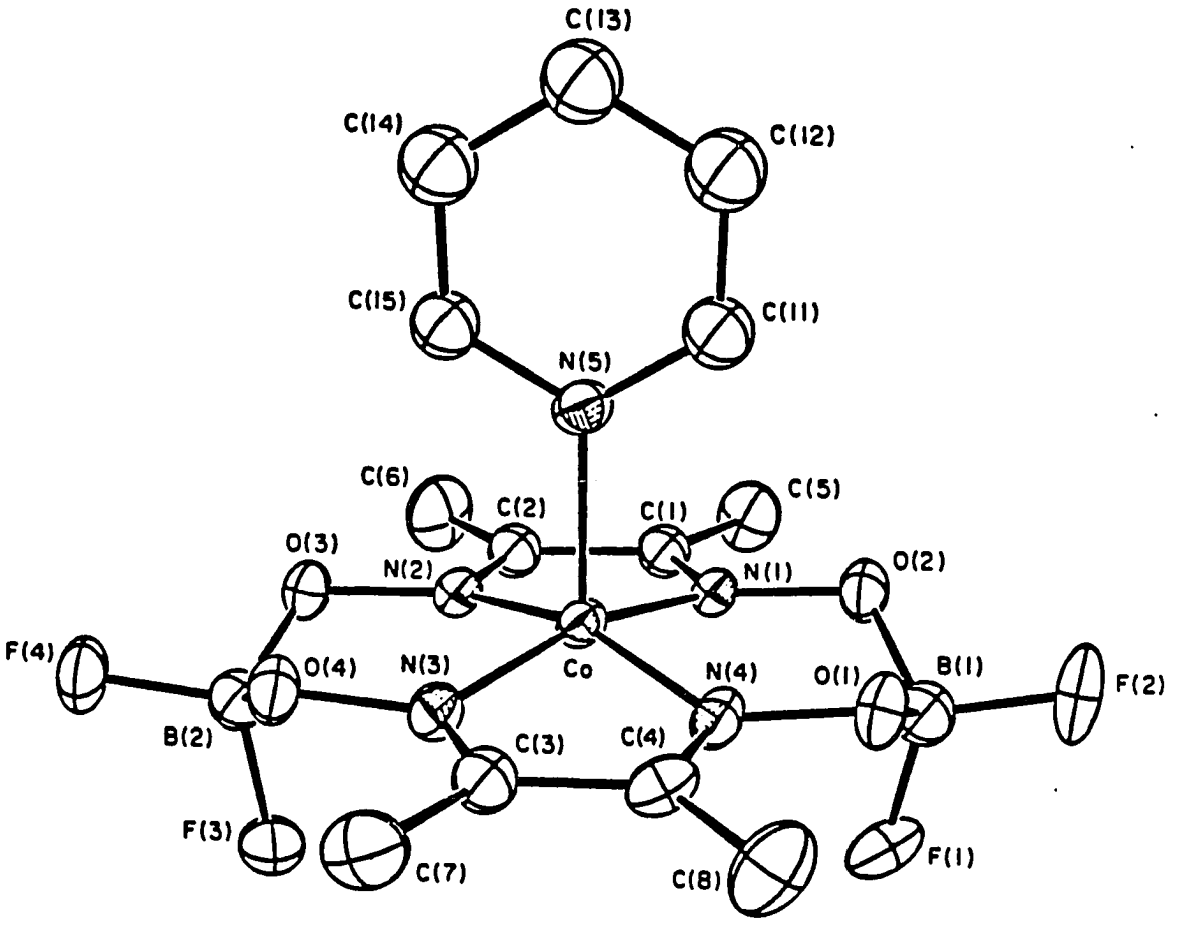

Figure VI-1. An ORTEP view of the monoanion, $Co^{I}(dmgBF_2)_2py^-$

REFERENCES

(1) (a) Schrauzer, G.N. Acc. Chem. Res. 1968, 1, 97. (b) Schrauzer, G.N. Pure Appl. Chem. 1973, 33, 545. (c) Jaselskis, B.; Diehl, H. J. Am. Chem. Soc. 1954, 76, 4345; For reviews see: (d) Pratt, J. M. "Inorganic Chemistry of Vitamin B_{12}", Academic Press, New York, 1972; (e) Smith, E. L. "Vitamin B_{12}", Third Edition, Methuen & Co., London, 1965.

(2) Krautler, B.; Keller, W.; Kratky, C. J. Am. Chem. Soc. 1989, 111, 8936.

(3) Lexa, D.; Savéant, J. M. J. Am. Chem. Soc. 1976, 98, 2652.

(4) Lexa, D.; Savéant, J. M. J. Chem. Soc. Chem. Commun. 1975, 872.

(5) Lexa, D.; Savéant, J. M. Acc. Chem. Res. 1983, 16, 235.

(6) Schrauzer, G. N.; Holland, R. J. J. Am. Chem. Soc. 1971, 93, 4060.

(7) Schrauzer, G. N.; Windgassen, R. J.; Kohnle, Chem. Ber. 1965, 98, 3324.

(8) Schrauzer, G. N.; Holland, R. J. J. Am. Chem. Soc. 1972, 93, 1505.

(9) Chao, T-H.; Espenson, J. H. J. Am. Chem. Soc. 1978, 100, 129.

(10) Johnson, M. D.; Meeks, B. S. J. Chem. Soc. B, 1971, 185.

(11) Naumberg, M.; Duong, K. N. V.; Gaudemer, A. J. Organometal. Chem. 1970, 2, 231.

(12) Dodd, D.; Johnson, M. D. J. Organometal. Chem. 1973, 52, 1-232.

(13) Schrauzer, G. N. Ann. N. Y. Acad. Sci. 1969, 158, 526.

(14) Ananias de Carvalho, L. C.; Dartiguenave, M.; Dartiguenave, Y.; J. Organomet. Chem. 1989, 367, 187.

(15) Hohman, W. H.; Kountz, D. J.; Meek, D. W. Inorg. Chem. 1986, 25, 616.

(16) Calderazzo, F.; Poli, R.; Pelizzi, G. J. Chem. Soc., Dalton Trans. 1984, 2535.

(17) Loghry, R.; Simonsen, S. H. Inorg. Chem. 1978, 17, 1986.

(18) Whitfield, J. M.; Watkins, S. F.; Tupper, G. B.; Baddley, W. H. J. Chem. Soc., Dalton Trans. 1977, 407.

(19) Zhang, Z. Z.; Wang, H. K.; Xi, Z.; Yao, X. K.; Wang, R. J. J. Organomet. Chem. 1989, 376, 123.

(20) Habadie, N.; Dartiguenave, M.; Dartiguenave, Y. Organometallics 1989, 8, 2564.

(21) Ochiai,E.; Long, K. M.; Sperati, C. R.; Busch, D. H. J. Am. Chem. Soc. 1969, 91, 3201.

(22) Farmery, K.; Busch, D. H. Inorg. Chem. 1972, 11, 2901.

(23) Costa, G.; Puxeddu, A.; Reisenhofer, E. J. Chem. Soc., Dalton Trans. 1973, 2034.

(24) Connolly, P.; Espenson, J. H. Inorg. Chem. 1986, 25, 2684.

(25) Fleischer, E. B.; Krishnamurthy, M. J. Am. Chem. Soc. 1972, 94, 1382.

(26) Doppelt, P.; Fischer, J.; Weiss, R. Inorg. Chem. 1984, 23, 2958.

(27) Walder, L.; Rytj, G.; Vogeli, U.; Scheffold, R. Helv. Chim. Acta 1984, 67, 1801.

(28) Goedken, V. L.; Peng, S.-M. J. Chem. Soc., Chem Comm. 1974, 914.

(29) Szalda, D. D. J.; Fujita, E.; Creutz, C. Inorg. Chem. 1989, 28, 1446.

(30) The structurally characterized compound $CoPC_{25}H_{45}N_5O_4$ was reported as a cobalt(I) complex; Adams, W. W.; Lenhart, P. G. Acta Cryst. 1973, B24, 2412, but it is actually a cobalt(III) derivative.

(31) Bakac, A.; Brynildson, M. E.; Espenson, J. H. Inorg. Chem. 1986, 25, 408.

(32) For example, see Lukehart, C. M.; "Fundamental Transition Metal Organometallic Chemistry" p. 40, Brocks/Cole Publishing Company, Monterey, 1985 and Lisic, E. C.; Hanson, B. E. Organometallics 1987, 6, 512.

(33) Rigo, P.; Bressan, M. J. Inorg. Nucl. Chem. 1975, 37, 1812.

(34) Rigo, P.; Bressan, M. Inorg. Nucl. Chem. Lett. 1973, 9, 527.

(35) Schrauzer, G. N. Chem. Ber. 1962, 95, 1438; Also see ref. 1(a).

(36) Slephens, F. S.; Vagg, R. S. Acta Cryst. 1977, B33, 3159.

(37) The conjugated π-bond $-N=C(CH_3)C(CH_3)=N-$ is viewed as similar to that of butadiene. π_1^* refers to the LUMO orbital of this π-system.

(38) Ramasami, T.; Espenson, J. H. Inorg. Chem. 1980, 19, 1523.

(39) Tyrlik, S. K.; Lenstra, A. T. H.; VanLoock, J. F. J.; Geise, H. J. Acta Cryst. 1986, C42, 553.

(40) Attia, M. W.; Zangrando, E.; Randaccio, L.; Lopez, C. Acta Cryst. 1987, C43, 1521.

(41) Lopez, C.; Alvarez, S.; Aguilo, M.; Solans, X.; Font-Altaba, M.; Inorg. Chim. Acta 1987, 127, 153.

(42) cf. data in Adams, W. W.; Lenhert, P. G. Acta Cryst. 1973, B29, 2412.

(43) Schrauzer, G. N.; Weber, J. H.; Beckham, T. M. J. Am. Chem. Soc. 1970, 92, 7078.

(44) Ramasami, T.; Espenson, J. H. Inorg. Chem. 1980, 19, 1523.

(45) SHELXS-86, Sheldrick, G. M. Institut für Anorganische Chemie der Universität, Göttingen, Germany.

(46) SHELX-76, Sheldrick, G. M., in "Computing in Crystallography", Schenk, H.; Olthof-Hazekamp, R.; Van Keningsveld, H.; Bassi, G. C., Eds., Delft University, Delft, 1978.

(47) Szalda, D. J.; Creutz, C.; Mahajan, D.; Sutin, N. Inorg. Chem. 1983, 22, 2372.

GENERAL SUMMARY

In Part I, kinetics studies were done of the homolytic and heterolytic cleavage reactions of the chromium-carbon bonds in the complexes $RCr(L)A^{n+}$ (where L = [15]aneN$_4$ = 1,4,8,12-tetraazacyclopentadecane; A = H_2O, and OH^-). Activation parameters ($\Delta H^{\ddagger}$/kJ mol^{-1}, $\Delta S^{\ddagger}$/J mol^{-1} K^{-1}) for homolysis of $RCrL(H_2O)^{2+}$ are: 111 ± 2, 54 ± 6 (R = p-$CH_3C_6H_4CH_2$); 103 ± 2, 28 ± 5 ($C_6H_5CH_2$); 101 ± 3, 22 ± 9 (p-$BrC_6H_4CH_2$); and 110 ± 3, 62 ± 6 (R = i-C_3H_7). The $\Delta H^{\ddagger}$ and $\Delta S^{\ddagger}$ parameters are considerably smaller than those for homolysis of $(H_2O)_5CrR^{2+}$ analogues. Primary alkyl macrocyclic complexes do not undergo homolysis. The complexes $RCrL(OH)^+$ slowly hydrolyze for R = n-Pr and i-Pr, whereas those for which R = $ArCH_2$ do not. The activation parameters for heterolysis are 78 ± 1, -53 ± 2 (R = i-C_3H_7) and 83 ± 3, -46 ± 9 (n-Pr). This pathway shows no solvent deuterium isotope effect. The complexes $RCrL(H_2O)^{2+}$ are not subject to acidolysis by H_3O^+ or H_2O, unlike their $(H_2O)_5CrR^{2+}$ analogues.

In Part II, the kinetic studies on the reaction of $[RCr([15]aneN_4)(H_2O)]^{2+}$ hereafter $RCrL(H_2O)^{2+}$ (R = CH_3, C_2H_5, 1-C_3H_7, 1-C_4H_9, 4-$BrC_6H_4CH_2$) macrocycles with iodine show that the reactivity changes as a function of the nature of the organic group bound to chromium(III). In the case of primary alkylchromium(III) macrocycles, the reaction proceeds strictly by bimolecular electrophilic substitution. The specific rates are 4.7 x 10^3 M^{-1} s^{-1} (R = CH_3), 81 (C_2H_5), 12 (1-C_3H_7), 8.9 (1-C_4H_9), and 9.5 (4-$BrC_6H_4CH_2$). In the case of aralkyl-

and secondary alkylchromium(III) macrocycles, however, both the normal electrophilic substitution and an oxidatively-induced chain reaction mechanism are operative. Details of the chain reaction for R = $BrC_6H_4CH_2$ are reported. The rate constant for the formation of $4\text{-}BrC_6H_4CH_2CrL(H_2O)^{2+}$ from $CrL(H_2O)^{2+}$ and $4\text{-}BrC_6H_4CH_2Br$ was also determined, $k = 3.7 \times 10^4\ M^{-1}\ s^{-1}$. The crystal and molecular structure of $[4\text{-}BrC_6H_4CH_2CrL(H_2O)]^{2+}(ClO_4)_2 \cdot THF$ was determined. The molecule crystallizes in the space group $P2_1/c$. Cell parameters are a = 11.683(3) Å, b = 8.816(3) Å, c = 29.959(8) Å, β = 96.29(11)°. The chromium is octahedrally coordinated by four N atoms of the macrocyclic ligand at the equatorial positions and by the $4\text{-}BrC_6H_4CH_2$ and a water molecule at the axial positions.

Part III concerns the oxidation of organochromium(III) complexes by dihalide and pseudo-dihalide radical anions generated by pulse radiolysis.

Pulse radiolysis	$e^-(aq.) + N_2O + H_2O \longrightarrow HO\cdot + HO^- + N_2$
Conversion	$HO\cdot + 2X^- \longrightarrow HO^- + X_2^-$
Reaction	$X_2^- + RCrL(H_2O)^{2+} \longrightarrow 2X^- + RCrL(H_2O)^{3+}$

Results suggest an ion pairing process prior to the electron transfer step. The reactivity trend is discussed on the basis of the oxidation of a series of organochromium complexes by three radical anions.

In Part IV the complex SSRS-[4-$BrC_6H_4CH_2Cr$(1,4,8,12-tetrazacyclopentadecane)(H_2O)]$^{2+}$, abbreviated [$RCrL(H_2O)^{2+}$], is oxidized to [$RCrL(H_2O)^{3+}$], a species which then rapidly homolyzes. Rate constants were determined in aqueous solution at 25.0 °C for oxidation by $ABTS^{\cdot-}$, $Fe(H_2O)_6^{3+}$, and $IrCl_6^{2-}$; values are (1.55 ± 0.11) x 10^2, 3.09 ± 0.28, and (1.29 ± 0.11) x 10^4 L mol^{-1} s^{-1}. From these data the following estimates were made for the couple $RCrL(H_2O)^{3+/2+}$: E^o = 0.76 ± 0.13 V, 5 x 10^{-2} < k_{SER} < 7 x 10^2 L mol^{-1} s^{-1}. Oxidations of a series of $RCrL(H_2O)^{2+}$ complexes by $IrCl_6^{2-}$ were examined, with rate constants between 2.20 x 10^{-1} L mol^{-1} s^{-1} (R = CH_3) and 4.60 x 10^5 (R = 4-$CH_3C_6H_4CH_2$). Rate constants for the aralkyl series fit a Hammett correlation with ρ = -4.3. A lower limit was set on the rate constant for homolysis of 4-$BrC_6H_4CH_2CrL(H_2O)^{3+}$ of k > 60 s^{-1}.

In Part V, the study is extended to organocobalt complexes with attention turned to reduction induced cleavages of a transition metal-carbon bond. A series of organocobalt complexes were synthesized by a nucleophilic substitution, $Co^{I}L'^{-}$ + RX ⟶ $RCo^{III}L'$ + X^-. Electrochemical methods in conjunction with ESR, NMR, and GC-MASS are used to reveal evidence of novel reactions —— reduction induced hydrogen atom transfer from the cobalt bound alkyl group to the equatorial ligand, L', and reduction induced alkyl group migration from cobalt to the equatorial ligand.

$$RCoL' + e^- \longrightarrow RCoL'^- \longrightarrow R(-H) + Co(HL')^-$$
$$\quad\quad\quad\quad\quad\quad\quad \llcorner\!\!\longrightarrow Co(RL')^-$$

In Part VI, the following compound, $[(CH_3)_4N][Co(dmgBF_2)_2py]$, where py = C_5H_5N and $(dmgBF_2)_2^{2-}$ = bis[(difluoroboryl)dimethylglyoximato], was crystallized, and its molecular structure determined by X-ray diffraction. The distances between Co(I) and the nitrogen of the macrocycle are unusually short (1.839 Å), even shorter than the corresponding bond (1.878 Å) in the cobalt(II) analogue. The cobalt atom is displaced 0.257 Å above the axial plane toward pyridine. Reasons of this unusual Co-N bond shortening is discussed along with the electronic structure of the d^8 cobalt(I) anion.

ACKNOWLEDGEMENTS

Many thanks go to professor James H. Espenson for his guidance, encouragement, great patience and understanding during the author's graduate career. The author owes a lot to his parents, and his wife S.H. Zeng for their love and constant support. Many thanks also go to Dr. Andreja Bakac and all the other members of Dr. Espenson's group for their friendship and assistance.

The author is grateful to the excellent instrument services of the Department of Chemistry, Iowa State University.

This work was performed at Ames Laboratory under contract no. W-7405-eng-82 with the U.S. Department of Energy. The United States government has assigned the DOE Report number IS-T 1493 to this thesis.